

STUDY OF SUN'S LONG PERIOD OSCILLATIONS

A Thesis

Submitted for the Degree of

DOCTOR OF PHILOSOPHY

In the Faculty of Science

BANGALORE UNIVERSITY

by

K. M. HIREMATH

INDIAN INSTITUTE OF ASTROPHYSICS

BANGALORE-560 034

INDIA

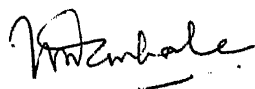
JULY 1994

DECLARATION

I hereby declare that the matter embodied in this thesis is the result of the investigations carried out by me in the Indian Institute of Astrophysics, Bangalore, under the supervision of Prof M.H.Gokhale . This work has not been submitted for the award of any degree , diploma, associateship, fellowship etc. of any university or institute.


[K.M. HIREMATH]

Candidate



M. H. GOKHALE

Supervisor

Bangalore 560034

Date : Jul 1994

Acknowledgements

I am greatly indebted to Prof M.H.Gokhale who introduced me this research problem, and took keen interest in all aspects of the work presented in this thesis. Without his great patience in going through the manuscript, this thesis would not have been in readable form.

I am grateful to the director Prof R.Cowsik for providing me excellent research facilities. I also wish to thank Prof J.C.Bhattacharya who encouraged me to pursue this study. I thankfully acknowledge Prof B.C.Chandrasekhara and Prof M.N.Anandaram of Bangalore University, for showing keen interest in my study.

I sincerely thank Mr B.S. Nagabhushana for carefully going through the entire manuscript and giving me useful suggestions. I also thank my brother Panchaxari Hiremath for carefully checking the references in the thesis.

Many colleagues, especially Dr R.T.Gangadhara, J. Javaraiah and Baba Verghese encouraged me during this study. I thankfully acknowledge them.

I am thankful to library staff, especially, Mrs. A.Vagiswari, Ms. Christina Louis and Mr. H.N.Manjunath for providing me all the required facilities and help in the library. Special thanks to Mr S.Muthukrishnan for making fine drawings.

I also thank Mr P.N.Prabhakara for making xerox copies and Mr D.Kanagaraj for making the bound volume of the thesis.

My acknowledgement, beyond words, are due to my family members : son Prashanth, wife Asha, and my parents who gave me love, affection and cooperation.

LIST OF PUBLICATIONS

- (1) " Variations in the Rotational Velocity of Sunspot groups ",
Gokhale, M.H. & Hiremath, K.M. 1984, Bull.Astron.Soc.
India, 12, 398
- (2) " Longitudinal Flows in Stellar Magnetic Flux Tubes ",
Gokhale, M.H. & Hiremath, K.M. 1986, Adv.Space.Res.
Vol 6, No. 8, 47
- (3) "Study Of Sun's Hydromagnetic Oscillations Using Sunspot Data"
, Gokhale, M.H., Javaraiah, J. & Hiremath, K.M. 1990, IAU
Symp.No.138, 375
- (4) " Steady and Fluctuating parts of Sun's Internal Magnetic
Field ", Gokhale, M.H. & Hiremath, K.M. 1993, in " Inside
the Stars ", eds. Weiss, W.W. & Annie Baglin, ASP Conf
Series, vol 40, p.66
- (5) " A model of the 'steady' and 'fluctuating' parts of the Sun's
internal magnetic fields ", Gokhale, M.H. & Hiremath, K.M.
1993, ApJ, 407, 359
- (6) "A model of the 'steady' and 'fluctuating' parts of the Sun's
internal magnetic fields ", Hiremath, K.M. & Gokhale, M.H.
1994, Submitted to Astrophysical Journal

ABSTRACT

Nearly 400 years ago sunspots were discovered as solar phenomena by Galileo. Schwabe (1843) detected the variability of sunspot occurrences with a 'cycle' of 11 years. Hale(1908) discovered strong bipolar magnetic fields associated with the sunspots. Hale *et.al.*(1913) showed that sunspot groups flip-flop their polarity every 22 years. Variations in many solar activity phenomena such as flares, coronal mass ejections, and also in luminosity of the sun, etc., are associated with the sunspot cycle. Manifestations of the sunspot activity can also be seen in the arorae, the cosmic ray events, geomagnetic phenomena, etc. Even, the variation in the rains of monsoon and the occurrences of draughts are believed to be associated with the sunspot activity phenomena. Thus, study of the solar cycle and the magnetic activity phenomena is crucial for understanding not only solar structure and evolution , but also terrestrial effects. It is also quite important for understanding the stellar magnetic fields and stellar activity.

The magnetic activity and the solar cycle phenomena have been modeled either in terms of *turbulent dynamo models* or in terms of *MHD oscillatory dynamo models*. The turbulent dynamo models explain qualitatively many of the observed solar magnetic cycle

phenomena. However, there are several difficulties and limitations in these models in their application to the solar cycle (Piddington 191,1972,1973; Cowling 1981; Levy 1992; Vainstein and Cattaneo 1992). The oscillatory theories also appear to have some theoretical difficulties (Schussler 1982) and lack of observational evidence for existence of steady field which is needed as background for oscillations.

In the present study, we use analysis of observational data and theoretical modeling to show that solar magnetic cycle can possibly be the effect of oscillations , especially ' long period ' torsional oscillations in the Sun's internal magnetic field. The properties of the 'Long Period Global Oscillations ' that may constitute the solar magnetic cycle are derived from Legendre-Fourier (LF) analysis of the Sun's magnetic field as inferred from sunspot data. For sustenance of such global oscillations , a 'steady' part of the internal magnetic field is required. The steady part of the magnetic field is modeled in two steps. In the 'preliminary' model, the steady part of the field is calculated assuming it to be current-free, using the condition of isorotation and the structure of Sun's internal rotation as given by helioseismology. In order to remove the central singularity and to obtain better isorotation in the radiative core, an improved

model is proposed. In the improved model reasonable assumptions and approximations are used to show that the steady part of the magnetic field can be expressed as analytical solution of magnetic diffusion equation. For testing the admissibility of global oscillations, Alfvén wave travel times are computed along the field lines in these two models of the steady field, along with three other arbitrary models. The steady part of the internal rotation is determined from the steady part of the magnetic field. The large-scale systematic patterns are detected in the remaining part of the rotation ('residual rotation'). From these patterns, the radial and the latitudinal structure of the dominant oscillation mode is estimated.

The thesis has been planned and presented in six chapters.

After giving a brief account of historical introduction to the present study, I review in chapter I the observational and theoretical knowledge of the Sun's global magnetic field and rotation.

In chapter II, I present the results obtained from the LF analysis of the Sun's magnetic field as inferred from the sunspot data during 1874-1976 (Gokhale, Javaraiah and Hiremath 1990).

From this analysis one sees that the sunspot activity can be considered as originating in superposition of the Sun's axisymmetric global oscillations of odd degrees up to $\ell = 29$ and period ~ 22 year. The main modes ($\ell < 11$) seem to represent approximately standing oscillations. The spectrum of these '22 year' modes with respect to ℓ is fitted to the mathematical forms for spectra of trapped waves. In the same chapter, I present the latest results obtained by Gokhale et.al. (1992) and, Gokhale and Javaraiah (1992). These authors have shown that the superposition of the first few odd degree modes reproduce not only the butterfly diagrams, but also the behavior of the field in the middle ($35^\circ - 70^\circ$) and high ($\geq 70^\circ$) latitudes, though the data used is only from low ($\leq 35^\circ$) latitudes. This supports the belief that the LF expansion represents a superposition of a set of real global oscillations of the Sun.

The MHD oscillations need a framework of a 'steady' poloidal field. Therefore in chapter III, I present a preliminary model of the structure of the 'steady' (slowest varying) part of the Sun's internal poloidal field. In this, the 'steady' part of the field is assumed to be current free and its field lines to be isorotating according to the Sun's internal rotation derived from helioseismology (Dziembowski et.al. 1989). The

resulting field model can be described as that of a central dipole and a central hexapole , both parallel to the rotation axis and embedded in a uniform external field B_0 . From the best fit of the model, we determine the field strengths of the dipole and hexapole to be $(0.61 \pm 0.10) B_0 R_0^3$ and $(0.16 \pm 0.05) B_0 R_0^5$ respectively.

Though the aforementioned model gives a satisfactory fit in the convective envelope (CE) , the fit is unsatisfactory in the outer radiative core (ORC) taken alone. Moreover, owing to the singularity at the center, it will not be possible to extend this model inwards when the rotation data in the inner radiative core is available in future. For these reasons, we have modified and improved the model (chapter IV). It is shown that the poloidal component of the 'steady' part of the magnetic field in the sun's radiative core (RC) and convection zone (CE) can be modeled as an analytical solution of the equation for magnetic diffusion in an incompressible medium of constant diffusivity whose field lines isorotate with the solar plasma. This solution is subjected to :

- (i) continuity of the normal component across the RC-CE boundary
- and (ii) merging with asymptotically uniform field of finite strength at large distances. The condition of isorotation enables determination of the values of the parameters in the first two

eigen modes of the diffusion equation.

The resulting model does not have any singularity , separatrix, or closed loop. It also yields a much better fit with the helioseismologically determined rotation in the radiative core than the fit given by the preliminary model.

The model enables us to estimate the 'initial ' (at Zero-Age-Main- Sequence) relative strengths of the two diffusion eigen modes as 4 : 1 . The characteristic diffusion time scales of these eigen modes are estimated to be ~ 10.6 and ~ 2.7 billion yr respectively.

These models also show that at the base of the convection zone , there is a discontinuity in the coefficients of isorotation. This implies a steady non-isorotation which can wind the poloidal field into a toroidal field ($\sim 10^6$ G) in $10^5 - 10^9$ years, if the discontinuities last that long.

From LF analysis of sun's inferred magnetic field , we know that the axisymmetric terms with odd values for the degree ' l ' have nearly same periodicity (~ 22 year). This indicates that the Alfven travel times may be approximately same along different field lines in the steady field. In order to check the admissibility of such global oscillations , we have computed the Alfven wave travel times along the field lines in the following

five models for the internal magnetic field. In the first model, the field is taken to be uniform and in the second it is assumed to be a dipole field. In the third model, the field is taken to be a combination of uniform and dipole field. The fourth and the fifth models are the models of the 'steady' part of the internal field as computed in chapters III and IV respectively. Results of the Alfvén wave travel time calculations are presented in chapter V. It is interesting to note that the last two models give the smallest relative bandwidth for the frequencies of global (Alfvén) oscillations. However, the last model (ie. the 'improved' model) is the admissible model that can sustain Alfvénic global oscillations.

The model of the steady part of the poloidal field specifies the steady part of the rotation also. The 'residual' part then represents the time-dependent part of the rotation, i.e. the torsional MHD perturbations in the interior of the Sun. The radial widths of this are found to be in the range of $\sim 0.1R_0 - 0.5R_0$, and their latitudinal widths are in the range of $\sim 10^\circ - 75^\circ$. Thus the time-dependent torsional perturbation seems to have global structure. It is shown that the time scales of these perturbations can be in the range 2-20 year, if the ratio of perturbations in the poloidal to the toroidal components of the magnetic field is in the range of $\sim 10-100$.

In the end of chapter V, I present the results obtained from the least square fitting of the residual rotation over the radial range $(0.4R_{\odot}-1.0R_{\odot})$ to a linear combination of the first three Legendre polynomials of even degree in $\cos\theta$. This fitting shows that the terms " $\ell = 2$ " and " $\ell = 4$ " are the dominant terms in the rotational perturbations as expected from the dominant terms $\ell = 3$ and $\ell = 5$ in the primarily excited oscillation (Gokhale and Javaraiah, 1994).

Thus, this study strengthens the idea that *the solar magnetic and the solar activity phenomena may be due to MHD oscillations superposed on the slowly diffusing steady part of the poloidal field in the interior.*

In chapter VI , I summarize the important conclusions of chapters II to V and discuss the directions for future work.

CONTENTS

Acknowledgements

List of Publications

Abstract (1)-(viii)

CHAPTER	PAGE
I INTRODUCTION	(1)
1.1 Historical Introduction	(1)
1.2 Periodic Phenomena On the Sun	(6)
1.2.1 <i>Short Periods</i>	(7)
1.2.2 <i>Intermediate Periods</i>	(8)
1.2.3 <i>Long Periods</i>	(8)
1.3 Sun's Magnetic Field	(11)
1.3.1 <i>Surface Magnetic Fields</i>	(12)
1.3.1.1 <i>Small Scale Fields</i>	(12)
1.3.1.2 <i>Large Scale Fields</i>	(13)
1.3.1.3 <i>Magnetic Activity Phenomena</i>	(14)
1.3.2 <i>The Internal Magnetic Fields Of the Sun</i>	(20)
1.4 Sun's Rotation	(22)
1.4.1 <i>Sun's Surface Rotation</i>	(23)

1.4.2 <i>Sun's Internal Rotation</i>	(24)
1.4.2.1 As Determined from Helioseismology.....	(24)
1.4.2.2 Theoretical Studies.....	(27)
1.5 Contents Of the Thesis.....	(28)

II THE SPECTRUM OF THE SUN'S HYDROMAGNETIC OSCILLATIONS FROM THE SUNSPOT DATA.....	(30)
2.1 Introduction.....	(30)
2.2 Use of Sunspot Data for Studying Global Distribution of the Solar Magnetic Field and its Variation.....	(32)
2.3 Nominal Toroidal Field.....	(34)
2.4 Legendre Fourier Analysis of the 'Nominal Toroidal Field'.....	(35)
2.4.1 Preliminary Results.....	(35)
2.4.1.1 The Amplitude Spectrum.....	(36)
2.4.1.2 The Approximate Constancy of Amplitudes.....	(37)
2.4.1.3 The Approximate Constancy of Phases.....	(37)
2.4.2 Indication of Existence of Global Oscillations of the Surface Magnetic Fields.....	(41)
2.5 Recent Results.....	(41)
2.5.1 'Forced' Nature of the Oscillations.....	(41)

2.5.2 Confirmation of the Global	
<i>Nature of the Oscillations</i>	(42)
2.5.2.1 Separation of LF terms in	
Coherent Global Oscillations.....	(42)
2.5.2.2 Verification of Superposition of	
‘Geometrical Eigen Modes’.....	(43)
2.6 ‘Reality’ Of the ‘Nominal’ Toroidal Field.....	(44)
2.7 The Mathematical Form of the Energy Spectrum.....	(44)
2.8 Physical Implications of	
the Independence of ν and l	(45)
Appendix 2.A.....	(47)
Appendix 2.B.....	(48)
III A PRELIMINARY MODEL OF THE ‘STEADY’ PART	
OF THE SUN’S INTERNAL MAGNETIC FIELD.....	(53)
3.1 Introduction.....	(53)
3.2 Determination of the ‘steady’ Field.....	(58)
3.2.1 <i>The Shapes of Isorotation Contours and the Sources</i>	
<i>for the ‘steady’ Poloidal Magnetic Field</i>	(58)
3.2.2 <i>The Feasibility of Existence of</i>	
<i>Iso-rotating Current free Poloidal Field</i>	
<i>with Central as well as External Sources</i>	(59)

3.2.3	<i>The Chosen Form of the relation</i> <i>between $\phi(r)$ and $\Omega(r)$.....</i>	(62)
3.2.4	<i>The 'data' used.....</i>	(62)
3.2.5	<i>The method of analysis.....</i>	(63)
3.2.6	<i>Estimation of the goodness of fit.....</i>	(66)
3.3	The Results.....	(67)
3.3.1	<i>Least-square fit for</i> <i>the Convection Zone.....</i>	(67)
3.3.2	<i>The Geometrical Structure of the Field</i>	(71)
3.4	A Slow Creation of Toroidal Magnetic Field Near S_*.....	(74)
3.4.1	<i>The Difference Between the Values</i> <i>of A_C and A_E.....</i>	(74)
3.4.2	<i>Slow Build up of Toroidal Field near S_*,</i> <i>its Form and Time Scale.....</i>	(76)
3.5	Conclusions and Discussion.....	(78)
	Appendix 3.A.....	(81)

IV	STEADY PART OF THE SUN'S INTERNAL MAGNETIC FIELD : IMPROVED MODEL.....	(83)
4.1	Introduction.....	(83)
4.2	Assumptions and the Resulting Form of the Basic Equations.....	(86)

4.3 Solution of Equation (3)	(89)
4.3.1 <i>Chandrasekhar's Solution of the Diffusion Equation</i>	(89)
4.3.2 <i>Modification for Large Diffusivity in CE and Asymptotically Uniform Field at Large Distances</i>	(91)
4.3.3 <i>The Boundary Conditions</i>	(93)
4.4 Evaluation of the Coefficients Using Equation (9)	(94)
4.4.1 <i>The Data and the Method</i>	(94)
4.4.2 <i>Procedure for Determining the 'Steady' Parts of the Rotation and the Poloidal Field</i>	(96)
4.5 The Model for the 'Steady' Parts of Rotation and Poloidal Magnetic Field	(97)
4.5.1 <i>The 'Steady' Parts of Rotation and Poloidal Field in CE</i>	(97)
4.5.2 <i>The 'Steady' Parts of Rotation and Poloidal Field in ORC</i>	(100)
4.5.3 <i>The Geometrical Structure of the Field</i>	(101)
4.5.4 <i>The Slow Field Winding at the ORC-CE Boundary and its Time Scales</i>	(101)
4.5.5 <i>The Form of the 'Steady' Part of the Toroidal Field</i>	(103)

4.6 Estimation of Diffusion Time Scales and the	
'Initial' Amplitudes of Diffusion Eigenmodes.....	(104)
4.7 Conclusions and Discussion.....	(105)
V TORSIONAL MHD OSCILLATIONS.....	(110)
5.1 Introduction.....	(110)
5.2 Theoretical Models of Solar Magnetic Cycle.....	(112)
5.2.1 <i>Theory of Dynamo Mechanisms.....</i>	<i>(112)</i>
5.2.2 <i>Difficulties in the Turbulent Dynamo Models</i>	
<i>of the Solar Cycle.....</i>	<i>(116)</i>
5.2.3 <i>MHD Oscillatory Dynamo Theories.....</i>	<i>(120)</i>
5.2.4 <i>Difficulties in the MHD Oscillatory</i>	
<i>Dynamo Theories.....</i>	<i>(121)</i>
5.3 Theoretical Formulation of	
Torsional Oscillations.....	(122)
5.4 Alfven Wave Travel Times.....	(124)
5.4.1 <i>Model 1 : Uniform Field.....</i>	<i>(125)</i>
5.4.2 <i>Model 2 : Dipole Field.....</i>	<i>(127)</i>
5.4.3 <i>Model 3 : Uniform and Dipole Field.....</i>	<i>(129)</i>
5.4.4 <i>Model 4 : Combination of Uniform, Dipole,</i>	
<i>and Hexapole Fields.....</i>	<i>(134)</i>

5.4.5 Model 5 : Travel Times in the Improved Model of the 'Steady' Field (Model in chapter IV).....	(136)
5.4.6 The Results.....	(139)
5.5 Study of the 'Time-Dependent' Torsional MHD Perturbation (Its Radial and Latitudinal Structure and Time scale).....	(142)
5.5.1 'Residual Rotation' as the Likely Time-Dependent Part of Rotation.....	(142)
5.5.2 Time-Dependent Parts in CE.....	(143)
5.5.3 Time-Dependent Parts in ORC.....	(144)
5.5.4 Scales of Radial Variations of the 'Torsional MHD Perturbations'.....	(148)
5.5.5 Time Scales of Variations of MHD Modes in the Perturbations.....	(149)
5.5.6 Latitudinal Structure of the Perturbations.....	(150)
5.6 Conclusions and Discussion.....	(153)
VI CONCLUSIONS AND FUTURE PROSPECTS.....	(156)
REFERENCES.....	(168)-(180)

CHAPTER I

INTRODUCTION

1.1 Historical Introduction

The first observations of sunspots through the telescope were made independently by four Europeans, viz., Thomas Harriot; Johannes Fabricius; Galileo Galilei and Christoph Scheiner (Hafbauer 1991). These blemishes on the Sun have always intrigued astronomers and astrophysicists. In 1843 Henrich Schwabe announced the discovery of the 11 year cycle of sunspots, which is now well known even among the non- scientists. In the mean time , Richard Carrington's (1863) observations of sunspots indicated that the latitude of occurrence of sunspots is around 40° north and south in the beginning of the cycle and drifts towards the equator as the cycle progresses. This is represented by the well known butterfly diagram of the sunspots (Maunder 1922a).

Meanwhile, the extensive study of the record of sunspot number by Wolf (1856,1868) from 1700 A.D onwards strengthened the belief that the cyclic behavior of sunspot activity is long lasting and fundamental in nature.

Since polar aurorae are believed to be the manifestations of sunspot activity, the 11 year periodicity is also evident in the records of polar arorae. These records have been found in the

historical documents in Europe, China, Korea and Japan

The most startling discovery by Maunder (1890,1922b) was that there was a lull in the solar activity in the period 1645-1715. This period of weakened solar activity is known as Maunder Minimum'. Recently, Eddy (1976) has presented a convincing evidence that the dearth of sunspot activity during this period was a real phenomenon and not an artifact of the data analyzed. Incidentally, during this period, most of the European countries witnessed a severe and unusual cold weather, known as the " Little Ice Age " .

From measurements of Zeeman effect, Hale (1908) showed that sunspots were associated with strong magnetic fields. He discovered (1913) that most sunspots occur in pairs, or in groups, which are oriented roughly parallel to the equator of the Sun. The leading and the following parts in a spot group have opposite polarities. Further, Hale et.al (1918) discovered that during each sunspot cycle, the leading parts of the spot groups in a given hemisphere have the same magnetic polarity as that of the polar region in the beginning of the cycle. During the next cycle, the polarities of the leading and the following spots in each hemisphere are reversed. Thus, when magnetic polarities are taken into account, a complete sunspot cycle has a period of about 22 years. This is known as ' 22 year magnetic cycle

The 11 year periodicity has also been revealed recently in the cyclic variability of the total solar irradiance (Frohlich

et.al 1991). It indicates that the Sun is more luminous (or brighter) during the maximum activity period than in the minimum activity period. As pointed out by Eddy, this may be a reason for the 'little ice age ' during the long sunspot minimum (Maunder minimum).

Similar ' long term ' variations in the solar activity also have been reported from the analysis of ^{10}Be and ^{14}C concentrations in ice core and tree rings respectively.

Thus , the study of the ' long term ' variations of solar activity may be crucial for understanding not only the solar structure and evolution, but also the solar terrestrial effects, including perhaps even the climatic effects.

Since sunspots are associated with strong magnetic fields with specific polarities on global scales, the 'long term ' variations in solar activity represent corresponding variations in the strength and structure of the solar magnetic field .

Hence theoretically, these phenomena have been modeled in terms of two types of dynamos : (i) a ' turbulent ' dynamo (Parker 1955 ; Steenbeck and Krause 1969 ; Krause 1976 ; Radler 1976) and (ii) an ' oscillatory ' dynamo (Walen 1949 ; Plumpton and Ferraro 1955 ; Vandakurov 1989).

In the turbulent dynamo mechanism, the magnetic field is generated , maintained, and periodically reversed by the rotation and the cyclonic turbulence of the solar plasma. The models based on this theory agree qualitatively with some of the observed

properties of the solar activity cycle (Yoshimura 1972 ; Gilman 1974). However, the radial gradient of the internal rotation needed in these models contradicts the gradient obtained from the helioseismological data (Dziembowski, Goode and Libbrecht 1989).

Because of the high conductivity of the solar gas, the electromagnetic induction in the Sun is very strong . Hence any disturbance of the plasma leads to strong electromagnetic restoring forces causing oscillations. These oscillations are called MHD oscillations. Perturbations in the form of displacements perpendicular to the field lines and propagating along the field lines constitute waves (called Alfvén waves) whose phase speed depends upon the field strength and the density of the plasma. The Alfvén mode oscillations have ' long periods ', viz, in the range of years to decades (Walen 1949 ; Plumpton and Ferraro 1955). For example, if we take the radial scale (110,000 kms) of density variation of the solar plasma in the radiative core and a uniform field strength of ~ 100 gauss, the Alfvén travel time from the center to the surface is of the same order as that of the period of the sunspot cycle, viz. ~ 11 year (i.e half the period of the Sun's magnetic cycle). The concept of an oscillatory dynamo is based on this fact .

Layzer et.al (1955), have pointed out that it may be possible to model the solar cycle as MHD oscillations of the Sun assuming the Sun to be threaded by an ambient poloidal magnetic

field. However, the computed periods turned out to be ~ 100 times longer than the solar activity cycle. So, one has to think of alternative models for understanding the 'periodic' behavior of the Sun's global magnetic field .

The detection of torsional oscillations in the photospheric rotation of the plasma (Howard and LaBonte 1980) as well as variations in Sun's internal rotation (Goode and Dziembowski, 1991; Gough and stark, 1993) strengthen the belief that sunspot cycle may be originating in global torsional MHD oscillations .

Supposing that the sunspot and the magnetic activity cycles are manifestations of torsional MHD oscillations , one has to answer the following questions, viz.,

- (i) what is the structure of the steady magnetic field, on which these MHD oscillations/waves are taking place ?
- (ii) can such a structure sustain global torsional (MHD) oscillations ?
- (iii) would the periods of such oscillations be in the range of the observed periods ?
- (iv) what is the form of their internal perturbations ?
- (v) what is the form of their amplitude spectrum ?

In the present study, the problems (i)-(v) have been addressed and answered to the following extent.

First, I review the results of the Legendre Fourier (LF) analysis of the latitude-time distribution of magnetic field

inferred from sunspot groups . This indicates that the solar magnetic cycle may be really originating in superposition of global stationary MHD oscillations. I use the helioseismological results on the Sun's internal rotation to develop a model for the ' steady ' part of the poloidal field . I then show that such a steady poloidal field can sustain global oscillations in the form of torsional Alfvén modes with periods in the range of periodicities observed in solar activity. The form of internal perturbations are detected from the large-scale systematic patterns in the residual rotation of the Sun.

Before presenting the above mentioned results in the subsequent chapters; I present a brief review of observational and theoretical knowledge of Sun's global magnetic field and rotation. At the end of this chapter, I describe the contents of the chapters II to VI .

1.2 Periodic Phenomena On the Sun

On the Sun, periodic phenomena have been observed with a wide variety of periods ranging from minutes to decades and perhaps even centuries . These periods can be classified (arbitrarily) into three groups, viz. ; (i) short periods (~ minutes), (ii) intermediate periods (~ solar rotation period) and , (iii) long periods (more than solar rotation period).

1.2.1 Short Periods

From the analysis of velocity dopplergrams, Leighton (1960) showed that there are coherent oscillations on the Sun, whose periods are in the range of 2-5 minutes. It is well established that these ' 5 minute ' oscillations are due to superposition of global acoustic 'p' modes, which are due to the restoring forces of the pressure gradient (Ulrich, 1970 ; Leibacher and Stein 1971; Deubner 1975; Ando and Osaki 1975). Similarly, 160 minute oscillations observed by Severney et.al. (1976), Brookes et.al (1976), etc., are believed to be global gravity (' g ') mode oscillations, which are due to restoring forces of gravity (/buoyancy) .

Oscillations with periods in the range of 120-200 sec were observed in the photosphere of sunspot umbrae (Beckers and Schultz, 1972; Thomas, et.al.1982; Lites 1986).

In the chromospheric region, different active phenomena, such as CaII structures, H α filaments, quiescent filaments and the prominences show the oscillatory behavior. For example, the CaII structures show the periodicities of \sim 150-300 seconds (Orall 1966; Punetha 1974; Liu 1974; Cram and Dame 1983; Rutten and Ultrenbrock 1991; Kariyappa 1992). The velocity oscillations in H α filaments show the periods in the range of \sim 150-250 seconds (Thompson and Schmieder, 1991). Quiescent filaments show the oscillatory variations in Doppler shift and central intensity of

the HeI (10830 Å) line. The periods vary from 5 to 15 min (Zang 1991). Prominence oscillations have periods of ~ few seconds to 6 minutes (Balthasar et.al. 1993 ; Wier et.al. 1984; Tsubaki 1988).

1.2.2 Intermediate Periods

27 day periodicity

Periodicity of ~ 27 day has been found in several activity related phenomena . This periodicity is detected (Lean 1991, and references there in) in the sunspot number, the HeI-1084 nm equivalent width, the plage index, and the 10.7 cm radio flux.

Note that , this periodicity is mainly due to the sun's rotation with a mean period of ~ 27 day.

1.2.3 Long Periods

155 day periodicity

A 155 day periodicity has been detected in the solar flare occurrence rate (Rieger et.al. 1984; Ichimota et. al.1985 ; Bai, 1987; Droge et.al. 1990); in the sunspot areas (Lean 1990); and in Zurich sunspot number (Lean and Brueckner, 1989).

240-330 day periods

By studying the monthly mean Zurich sunspot number from 1749

to 1979, Wolf (1983) reported a peak at 323 days. Delache et.al (1985) found this peak in the power spectrum of the solar diameter measurements from 1975 to 1984. Pap, et.al.(1990) claim the existence of periodicities between 240-330 days in the 10.7 cm radio flux, the CaK plage index, the UV flux at $L\alpha$ and MgII core to the wing ratio.

500-550 day periodicity

Several authors have claimed this range of periodicity in different manifestations of solar activity (eg : Oliver et.al. 1992 and references there in).

Quasi-biennial Oscillations (QBO)

Several analyses indicate the presence of QBO in different solar activity parameters : sunspot numbers (Shapiro and Ward 1962); solar neutrino flux (Sakurai 1979); solar radio flux at 10.7 cm (Hughes and Kesteven, 1981); coronal emission at 5303\AA line (Sykora 1980; Apostolov and Letfus 1985; Rusin et.al. 1987); CaK plages (Singh and Prabhu 1985) and in photospheric magnetic field (Csada 1974).

Periods of 2-22 years

In this range the 11 year period found in sunspot numbers, and in many other activity phenomena is the dominant period. Next dominant period is that of the 22 year magnetic cycle. There is

some evidence for presence of 80-90 year periodicity in many of these phenomena.

Sunspot cycle of '11' years discovered by Schwabe (1843) is the most well known phenomenon. In fact the power spectrum analysis of the annual mean relative sunspot numbers (Cole 1973) shows the periodicities of 10.45, 11.8 years along with 88, 59 and 190 years respectively. Cohen and Lintz (1974) computed the maximum entropy power spectrum of the annual mean sunspot numbers for the period 1793-1971. They discovered the peaks in the power spectrum of 8, 10 and 90 years in addition to the 11-year peak.

Power spectrum analysis of sunspot number (Wallenharst 1982) from 1711-1966 shows that 11 year periodicity is the only statistically significant one present in the sunspot data , whereas peaks of 8, 10 and 90 year appear to be statistically insignificant.

Eleven year periodicity has been detected in different activity phenomena : H α filaments (Makarov and Sivaraman 1988); ephemeral active regions (Martin and Harvey 1979) and X-ray bright points (Goulab et.al. 1989); magnetic field in the polar faculae (Makarov et al 1988) ; torsional oscillations (Howard and La Bonte 1980) ; the Sun's luminosity (Wilson 1991) and the magnetic flux (Harvey 1992).

This period has also been detected in the integral brightness of white light corona (K+F corona)(Rusin and Rybanski 1992); in the coronal green line intensity (Rusin et.al.1987) and in MgII

core to wing ratio index (Deland and Cebula 1992).

There is a good positive correlation of H α flare activity and x-ray luminosity , which vary together with the solar cycle (Pearce *et.al.* 1992).

In the range of long period variations , 22 year magnetic cycle detected by Hale *et.al.*(1918) is the dominant period , next to the 11 year cycle. From the Legendre Fourier analysis of magnetogram data , Stenflo and Vogel (1986) showed that the axisymmetric global oscillations with periods of \sim 22 year contribute predominantly to the evolution of large-scale photospheric field.

Recently, Javaraiah and Gokhale (1994) have found periodicities in the coefficient ' B ' of the differential rotation obtained from the sunspot groups during 1874-1976 . Their analysis show the periodicities of 18.9, 8.3, 3.9 , 3.1, 2.6, and 2.1 year respectively.

1.3 Sun's Magnetic Field

The discovery of polar plumes (or rays) in the corona at times of minimum solar activity led to a suggestion that the Sun possesses a large scale dipole magnetic field (Bigelow 1889; Stormer 1911). Hale (1908) initiated the measurement of zeeman splitting of photospheric lines and detected the strong magnetic fields in sunspots. Outside the sunspot regions, however, the

photospheric fields are weak and the zeeman components are not well separated. Hale *et al.* (1918) reported the existence of a general (background) magnetic field. The field was found to be of a dipole in character.

There is a wealth of observational information about the surface magnetic field, whereas the properties of the internal magnetic field have to be studied by theoretical methods only.

1.3.1 Surface Magnetic Fields

Howard (1967) has classified the surface magnetic fields as 'small scale' and 'large scale' fields. According to him, the small scale fields are associated with the small scale structures in the solar atmosphere, the development and the decay of active regions, etc. The large scale field consists of background field, the large-scale distribution of solar activity, and polar fields.

1.3.1.1 Small Scale Fields

Observations of solar magnetic field (Howard and Stenflo, 1972; Wang 1988) in a quiet region shows that the magnetic flux is concentrated in discrete clumps which are separated by apparently field-free areas. Most of these clumps are bipolar and the typical sizes of the elements in the clumps are ~ 100 Kms, with field strengths $\sim 1-2$ KG. These clumps are found every where on the surface of the disk. Stenflo (1989) has observed that, nearly 90% of the total magnetic flux penetrating the photosphere outside

the sunspots occurs in such clumps. Since , the sizes of these clumps are near the angular resolution limit, the mechanism of formation and evolution is poorly understood.

However, it is believed that the magnetic flux which appears to emerge from the solar interior as large coherent structures (for example the sunspots) decay by fragmentation at a rate of $\sim 10^{15} \text{ Mx sec}^{-1}$ (Gokhale and Zwaan 1972). The fragmentation implies transferring of flux from smaller to larger spatial wave numbers (Harvey and Harvey 1973; Stenflo 1976) leading to sizes of 100 Km flux tubes.

Theoretically, formation of ' KG ' flux tubes can be understood as an effect of instability caused by convective collapse (Parker 1978; Spruit and Zweibel 1979; Unno and Ando 1979). Hasan (1985, 1986) and Venkatakrisnan (1985,1986) have studied the process of collapse through numerical simulations using thin flux tube approximation. While they confirm the linear theory (Spruit and Zweibel 1979) of convective instability of weak magnetic fields , the results for strong fields and for the nonlinear evolution of the instability are uncertain (Schussler 1992).

1.3.1.2 Large Scale Fields

Howard (1967) showed the existence of large-scale monopolar and bipolar regions of photospheric fields with sizes $\sim 10^3$ times larger, field strengths $\sim 10^3$ times weaker (~ 5 Gauss) and fluxes

of the same order as that of the active regions. The unipolar regions seem to be created by breaking up the 'following' polarity parts of the active regions. These unipolar regions seem to migrate poleward and to build up a general polar magnetic field.

These photospheric large-scale fields lead to the large-scale structures in the corona which are seen in the white light photographs and in the x-ray pictures. The examples of these are : (i) prominences, (ii) loops, extending up to one solar radius, (iii) streamers, extending often beyond $\sim 10 R_0$ and (iii) coronal holes extending up to $0.1 R_0$.

1.3.1.3 Magnetic Activity Phenomena

Magnetic activity essentially consists of phenomena , which are manifestations of abnormal heating (or cooling) due to strong magnetic fields. For example, sunspots, pores and ephemeral active regions in the photosphere; faculae, filigree elements in the chromosphere; prominences , flares, and x-ray bright points in the corona.

Sunspots :

Sunspots are dark areas on the photosphere with the typical sizes of ~ 10 to 10^3 millionths of hemisphere (one millionth of hemisphere $\approx 3 \times 10^6 \text{ Km}^2$) and life times varying from several hours to several weeks depending upon the size. These are compact magnetic elements, with the magnetic fluxes in the range of

10^{20} - 10^{22} Mx which appear with the dark umbrae , usually surrounded by the penumbrae. In the umbrae the typical field strengths are $\sim 2900 \pm 400$ G and effective temperature of $\sim 4000 \pm 100$ K.

In sunspot groups, except for very large and complex active regions, the magnetic field has a bipolar pattern, with opposite polarities in the leading and the following parts. In most of these, the leading spot has the same polarity as that of the field near the pole in the same hemisphere, in the beginning of the sunspot cycle.

Pores :

Pores have field strengths of ~ 2000 - 2500 G, with fluxes in the range of 10^{19} - 10^{20} Mx. These have life times of few days only.

Sunspot Cycle :

Variation of the number of sunspots over the surface of the Sun with an average periodicity ~ 11 year is termed as ' sunspot cycle '. The length of sunspot cycle also varies between 9 and 12.5 years (Zwaan 1981). In the context of this study, it is interesting to note that 11-year cycle seems to be fairly regular (the underlying mechanism is exactly periodic) (Dicke 1978,1979b,1988 ; Nicolini 1977; Attolini et.al 1990; Morfil et.al. 1991). Correlation analyses of smoothed sunspot numbers

BUTTERFLY DIAGRAM OF SUNSPOT ACTIVITY 1874-1976

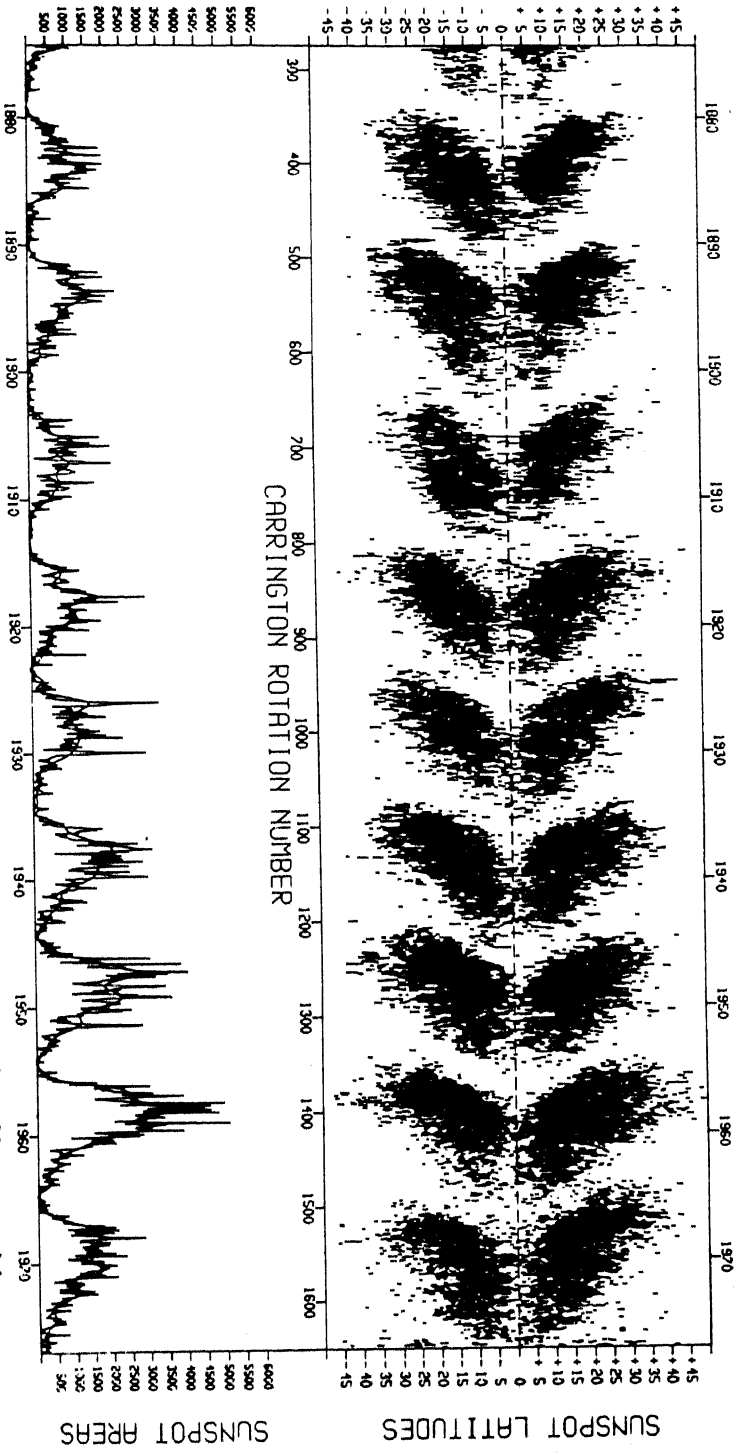


Fig 1.1.-In the upper half of the diagram 'butterfly diagram' is presented. In the lower half of the diagram the plot of mean total area for each synodic rotation is presented (adopted from Yallop and Hohenkerk, 1980).

(Ruzmaikin 1989; Kurtus and Ruzmaikin 1990; Hogenson 1992) have claimed that the sunspot cycle may be chaotic . Recent correlation analysis (Price et.al. 1993) of raw sunspot numbers rejects these results and confirms the regularity of the sunspot cycle .

Mostly, sunspot activity is confined within 40° latitude , on either side of the solar equator. Usually, the first sunspot of a cycle appears at such high latitudes. As time progresses, the sunspot activity on either side shifts closer to the equator. This tendency of drifting of sunspot activity from higher to lower latitudes, as the cycle progresses, is known as 'Spörer's law ' and is represented in a latitude time plot called Maunder's butterfly diagram. In Figure 1.1, we have given plots of butterfly diagram of sunspots and temporal variation of their mean area for each synodic rotation.

Solar Magnetic Cycle :

After the discovery of strong magnetic fields in sunspots, in 1908, Hale discovered the polarity laws . During a given cycle, the majority of the leading sunspots in the northern hemisphere are of the same polarity, whereas the leading sunspots on the southern hemisphere are of the opposite polarity. During the next cycle all polarities are reversed. Thus, the period of the magnetic activity cycle is twice as that of the sunspot cycle. This phenomenon is called " 22 year solar magnetic cycle ".

Ephemeral Active Regions :

These are tiny (30000 Kms), bipolar, short lived (~ 1 day) active regions found in the magnetograms. Many of them appear as bright dots on x-ray pictures of the Sun. They have a wide latitude distribution than that of the ordinary active regions. The magnetic flux of these elements is $\sim 10^{19} - 10^{20}$ Mx. Though, these features roughly follow the Hale polarity law as seen in active regions, they have broader distribution of orientations. Ephemeral active regions are randomly distributed over the surface, with high concentrations in active sunspot zones.

Faculae, Network, and Filigree Elements :

' Faculae ' are the bright chromospheric features, often associated with plages, and more widely arranged in the enhanced network. Outside the active regions, the bright elements form the ' quiet network ' outlining the supergranules. In filtergrams taken in extreme line wings, an intricate fine structure appears, which is called ' filigree ' (Dunn and Zirker 1973). Filigree elements always tend to lie between the granules and evolve along with them. Filigree have average flux $\sim 10^{17}$ Mx (Mehlretter 1974) with typical width ~ 100 Kms. Thus these are the magnetic structures at the limit of angular resolution in filtergrams.

Prominences :

Prominences are dense and relatively cool coronal clouds, 10,000-40,000 Kms high, ~ 5000 Kms thick, and with lengths

typically between 50,000 Kms to 300,000 Kms. Prominences are often associated either with active regions or with neutral lines separating large magnetic regions. These are called as 'filaments' when seen on the disk as dark ribbons especially in H α line .

The 'filaments' are located along the dividing line of opposite polarities in the large scale magnetic field. From the study of morphology of filaments and filament channels, it is shown (Makarov et.al. 1982) that they can be used as effective tracers for studying the evolution of large-scale magnetic fields. From the H α synoptic charts, Makarov and Sivaraman (1986) have found that in each hemisphere the magnetic neutral lines slowly migrate towards the pole and the signs of the magnetic field in the latitude zones 50° to 90° get reversed.

The Extended Solar Activity Cycle :

The coronal observations (Bretz and Billings 1959) in the emission line at 5303 Å° showed that a zone of enhanced emission appeared at high latitudes in each hemisphere, several years before the beginning of each sunspot cycle. This zone migrates towards the equator, reaching latitude ~ 40° in coincidence with the appearance of new-cycle sunspots at this latitude, apparently extending the butterfly diagram back in time to higher latitudes (Leroy and Neons 1983). This has been confirmed by the study of the variance of the 5303 Å° coronal emissivity from 1944 to 1974.

From the analyses of coronal green line emission , ephemeral active regions and torsional oscillation signal, Wilson et.al. (1988) concluded that the sunspot activity is simply the main phase of what they call 'an *extended-cycle*' . This '*extended-cycle*' begins at high latitudes before the maximum of a sunspot cycle and progresses towards the equator during the next 18-22 year.

1.3.2 *The Internal Magnetic Fields of the Sun*

It is impossible to measure the internal fields directly. Hence it is necessary to study the internal field only by theoretical modeling and comparing the consequence at the surface with the observed photospheric field. Many models have been developed for explaining the surface field during the solar cycle. According to the turbulent dynamo theory , this field is maintained and periodically reversed by cyclonic turbulence and rotation inside the sun (Parker 1955; Krause 1976; Radler 1976; Yoshimura 1972; Gilman 1974). A critical review of this theory is given in chapter V (section 5.2). For this mechanism, a weak seed field is required in order to produce the dynamo field.

Owing to the high conductivity of the solar plasma, the Sun might have retained some of the fossil field from the collapse in its protostar phase (Cowling 1953). In fact, the presence of such a field of primordial origin is possible on theoretical grounds only (Cowling 1953, Bachal and Ulrich 1971). Chitre et.al.(1973)

and Dicke (1977,1979a) had postulated the fields of $\sim 10^8$ G in the central regions of the Sun to explain the dearth of solar neutrinos. The large-scale internal magnetic field (Mestel and Thakar 1972) may induce meridional circulation which can lead to the mixing of material of the solar interior. It was suggested that this could also possibly explain the deficit of observed solar neutrinos and the splitting of acoustic modes of oscillations. Dziembowski and Goode (1991) by analyzing the Libbrecht's (1989) data on rotational splittings of acoustic frequencies, derived the presence of a 'steady' quadrupole toroidal field of $\sim 2 \pm 1$ MG at the bottom of the convection zone. However, such strong fields are expected to be unstable and hence unlikely in reality.

Mestel (1965) suggested that a field of ~ 1 G is required for uniform rotation. Parker (1984) and Moss (1987) explained the deficit of lithium with a normal beryllium abundance in the solar atmosphere, by proposing that a strong magnetic field ($\sim 10^6$ G) may be existing below the base of convection zone. Dudorov et.al. (1989) concluded that the presence of even a weak large-scale magnetic field (eg. ~ 1 G) in the radiative zone should lead to the establishment of rigid-body rotation in a short time scale compared with the age of the Sun.

The oscillatory theories of the solar magnetic cycle also require large-scale weak magnetic fields (eg. ~ 100 G) in the radiative interior of the Sun. Based on the analysis of global

magnetic resonances (Stenflo and Vogel, 1986), Gough (1986) has proposed that there may be large-scale weak field in the radiative core. From the analysis of rotational frequency splittings, Rosner and Weiss (1985) suggested that there may be large-scale poloidal field ($\sim 10^{-5} - 1\text{G}$) in the radiative core. On the grounds of evolution of Sun's angular momentum, Spruit (1990) suggested existence of a large-scale field of $\sim 1\text{G}$, with poloidal and toroidal components of similar strengths. Charbonneau and Macgregor (1993) demonstrated that the spin-down of a solar type star is possibly due to the existence of large-scale poloidal magnetic field, which may produce weak internal differential rotation in the star.

1.4 Sun's Rotation

Nearly 400 years ago (soon after the discovery of the sunspots), Sun's rotation was discovered from the movements of sunspots over the Sun's disk. Pioneers of this discovery were Goldshmit (1587-1615); Galileo Galilee (1564-1642); Thomas Harriot (1560-1621) and Scheiner (1575-1650) in Germany.

Systematic study of Sun's rotation was started from 1850 AD onwards. It was Richard Carrington (1826-1875), and Gustav Sporer (1822-1895), who undertook the long series of observations of the apparent motion of sunspots. They confirmed independently that the surface of the Sun does not rotate like a solid body,

i.e., it's period of rotation varies as a function of heliographic latitude. They showed that the rotation period is minimum at the equator and increases gradually toward the poles. After correcting for the annual motion of the Earth around the Sun, Carrington derived a mean rotation period of ~ 25 days at the solar equator.

1.4.1 Sun's Surface Rotation

Presently, Sun's surface rotation is determined from measurements of positions of the sunspots and the other magnetic features as tracers. It is also measured from Doppler effect on spectral lines.

By measuring the apparent motions of sunspots over the Sun's disk, one can derive Sun's surface rotation profile (Newton and Nunn 1951; Ward 1966 ; Balthasar and Wohl 1980 ; Godoli and Mazzucconi 1979). For example, a typical profile of Sun's rotation from sunspots as tracers given by Gilman and Howard (1984) in the following way :

$$\Omega(R_0, \phi) = 467.0(+0.2) - 91.4(\pm 1.4) \sin^2 \phi \quad \text{nHz}$$

where, ϕ is the solar latitude , and R_0 is the solar radius.

By measuring the doppler shift in the spectral lines at east and west limbs , one can derive the law of Sun's surface rotation (Snodgrass 1992), which is as follows :

$$\Omega(R_0, \phi) = 453.8(\pm 1.0) - 54.6(\pm 0.8) \sin^2 \phi - 75.5(\pm 1.1) \sin^4 \phi \text{ nHz.}$$

This is $\sim 4\%$ slower than the rate of rotation of sunspot groups. This significant difference, amounts to $\sim 80 \text{ m sec}^{-1}$ in relative velocity at the equator. Later measurements (Livingston and Duvall 1979 ; Duvall 1982) also confirm this result.

The rotation of photospheric magnetic fields outside sunspots was first examined by Wilcox and Howard (1970). This rotation is similar to the rotation of sunspots. Later studies (Stenflo 1974, 1977) confirmed this result. Snodgrass (1983) from the Mount Wilson magnetograph data determined the surface rotation of the photospheric magnetic fields as :

$$\Omega(R_0, \phi) = 461.9(\pm 0.3) - 73.8(\pm 2.9) \sin^2 \phi - 52(\pm 5) \sin^4 \phi \text{ nHz.}$$

1.4.2 Sun's Internal Rotation

1.4.2.1 As Determined from Helioseismology

Recently, the information on internal rotation is obtained from helioseismological observations (Christensen-Dalsgaard and Schou 1988 ; Dziembowski, Goode and Libbrecht 1989). In this, the observed frequencies of acoustic (p) modes are used for determining the internal rotation. In the absence of rotation the frequencies of these oscillations are independent of azimuthal order ' m ' , owing to absence of any preferred axis. However, rotation breaks this symmetry and remove the degeneracy of the

frequencies ν_{nlm} . Here n is radial order, l is spherical harmonic degree and m is the azimuthal order of the oscillations. Thus the splitting due to the rotation as given by observations is

$$\delta\nu_{nlm} = \nu_{nlm} - \nu_0$$

where ν_0 is the frequency of the mode which is free from effects of splitting. The observational splitting is related to the internal rotation in the following way (Christensen-Dalsgaard, 1992)

$$\delta\nu_{nlm} = m \sum_{\Delta} \int_0^R \mathcal{K}_{nlm}(r) \Omega_{\Delta}(r) dr$$

where $\mathcal{K}_{nlm}(r)$ are the kernels defined by the eigen functions of acoustic oscillations weighted by the latitudinal dependence of the internal rotation. Thus by knowing observationally determined rotational frequency splittings and theoretical eigen functions, the internal rotation can be determined. A typical internal rotation profile inferred from helioseismological data is given in Fig 1.2. Note that, the differential rotation exists down to base of the convection zone, whereas in the radiative core it is more like a rigid body rotation.

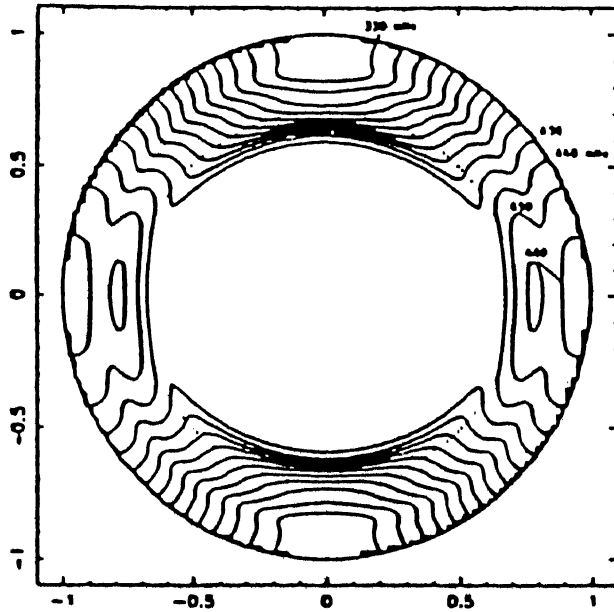


Fig 1.2.-Contours of constant angular velocity in the sun
(Adopted from Libbrecht, 1988)

1.4.2.2 Theoretical Studies

On the basis of the earlier works of Biermann (1951,1958), Kippenhan (1963) showed that steady axisymmetric fluid motions which allow the differential rotation are possible in an incompressible viscous fluid shell, if the viscosity is anisotropic.

Nakagawa and Trehan (1968) obtained the form of the steady-state differential rotation in a spherical shell of an incompressible inviscid fluid of infinite electrical conductivity in the presence of poloidal magnetic field and toroidal fluid motions. By imposing the boundary condition at the outer surface as given by the observed differential rotation and assuming a solid body rotation at the inner surface, they found that steady rotation exists only when the inner surface rotates slower than the outer surface at all latitudes.

Nakagawa (1969) examined the case in which the magnetic field and the fluid motions are both purely toroidal. He showed that a steady-state solution is possible if the Alfvén velocity associated with the toroidal magnetic field is comparable with the velocity of rotation. It is interesting to note that the theoretical isocontours of the internal rotation obtained by Nakagawa are similar to those given by helioseismological results (Libbrecht 1988).

Numerical simulations of convection (Gilman 1983; Glatzmaier 1985) predict that the internal rotation should be

constant on cylindrical surfaces throughout much of the convection zone. By applying different boundary conditions , Rosner and Weiss (1985) simulated the isorotation curves approximately as inferred by helioseismology.

1.5 Contents of the Thesis

The thesis is presented in six chapters.

In chapter II, I review the results obtained from the Legendre Fourier (LF) analysis of Sun's magnetic field inferred from sunspot data during 1874-1976.

The MHD oscillations need a framework of a ' steady ' poloidal field. In chapter III , I discuss the feasibility of such a field existing as a remnant of the primordial field and present a preliminary model of its structure. In this preliminary model, the 'steady ' part of the field is assumed to be current free and it's field lines to be isorotating according to the Sun's internal rotation derived from helioseismology .

Though the aforementioned model gives a satisfactory fit in the convective envelope (CE) , the fit is unsatisfactory in the outer radiative core (ORC) taken alone. Moreover, owing to the singularity at the center, it will not be possible to extend this

model when the rotation data in the inner radiative core is available in future. For these reasons, we have modified and improved the model (chapter IV). The model enables us to estimate the 'initial' relative strengths of the two diffusion eigen modes in the field. The characteristic diffusion time scales of these modes are also be estimated.

From LF analysis, we know that the axisymmetric terms with odd values for the degree ' l ' have nearly same periodicity (~ 22 year). In order to check the admissibility of such global MHD oscillations , we have computed (Chapter V) the Alfvén travel times along the field lines in the five different models. It is shown that the models in chapter III and IV give the smallest relative bandwidth for the frequencies of global (Alfvén) oscillations.

In the same chapter, I study the radial and the latitudinal structure in the possibly existing MHD oscillations from the 'residual rotation' (the part of the observed rotation which could not be fitted in the model of steady part of the rotation).

In chapter VI , I summarize the important conclusions of this study and discuss the directions for future work.

CHAPTER II

THE SPECTRUM OF THE SUN'S HYDROMAGNETIC OSCILLATIONS FROM THE SUNSPOT DATA

2.1 Introduction

As presented in chapter I, the possible connection of solar magnetic cycle to global oscillation of the sun was suggested by Alfvén (1943), Layzer *et.al.* (1979) and , Howard and LaBonte (1980). In principle the 22 and 11 year periodicity of the magnetic and the activity cycles could be related either to the periods of sufficiently slow global oscillations (Plumpton and Ferraro 1955) or the time scales of modulation (eg , beats) of fast global oscillations (Gokhale 1977, 1984) like 'g' modes. Theoretically slow MHD modes of global oscillations could have periods in years and decades depending upon the effective depth and intensity of the magnetic field in the solar interior.

Maunder's well-known ' butterfly diagrams ' show that the sunspot activity appears to be originating in ' waves ' with periods \sim 11 year (or multiples thereof), which propagate from middle latitudes in each solar hemisphere towards the solar equator (Becker 1955). Waves of one-way migrations of fast rotation zones (Snodgrass 1987 and references therein) and poleward migration of weak magnetic fields (Howard 1974), prominence belts (Ananthakrishnan and Nayar, 1953) and, polar faculae (Makarov and Sivaraman 1986) have been observed. All

these waves are in fact global . It could be that their confinement to certain latitude zones is only their manifestations in the respective observations. Supposing this to be true, each wave contributing to the overall pattern would be equivalent to a set of at least approximately stationary global oscillations of the Sun with appropriate phase differences. SHF analysis of Mount-Wilson and Kitt-Peak magnetogram data (1959-1984), shows (Stenflo and Vogel 1986; Stenflo 1988) that the axisymmetric ($m = 0$) global oscillations with specific periods (~ 22 yr and smaller) do contribute predominantly to the evolution of the large-scale photospheric field. The power spectra of this data showed that the modes of odd and even parity behave differently. All the odd parity modes have the same periodicity of ~ 22 years. For even parity modes , there appeared to be frequency increasing with the degree ' l ' which is similar to the observed p mode spectrum. If this is true it would indicate constructive and destructive interference of global waves (probably MHD waves).

In this chapter, I review the studies of the global distribution of the solar magnetic field and its temporal variation which are based on the sunspot data . Such studies have been carried out by Gokhale, Javaraiah and Hiremath (1990) ; Gokhale et.al. (1992) ; Gokhale and Javaraiah (1992) .

In section 2.2 , I describe the available data, and the data used in these studies . The results of the first study are presented in section 2.4. In sections 2.5-2.8, I have reviewed and discussed the conclusions of these studies.

2.2 Use Of Sunspot Data for Studying Global Distribution Of the Solar Magnetic Field and Its Variation

For studying the global distribution of the solar magnetic field and its variation, the sunspot data is more advantageous than the magnetogram data in the following two respects :

Magnetogram data is available from late 1950's. Thus the data length is ~ 33 years. This will give a resolution of $\sim 1/33 \text{ yr}^{-1}$ in the frequency of the magnetic cycle. On the other hand, the sunspot data extends for over 100 years. Hence it will give a substantially higher resolution for determining the frequencies and their bandwidths .

Secondly, if one wants to understand the physical nature of sun's global magnetic oscillations , one needs to study the variations in the amplitudes and the phases on time scales longer than the period . This can be studied with higher accuracy using the sunspot data .

Use of sunspot data has the following two disadvantages. Sunspots are distributed in the low heliographic latitudes ($\sim 40^\circ \text{N}$ to 40°S) only. This could in principle lead to substantial errors in the estimation of the amplitudes and phases of the LF terms . On the other hand , the magnetic data is distributed all over the sun's disc and thus will allow higher accuracy in the amplitudes and phases of up to the limit allowed by latitudinal resolution.

The other disadvantage of the sunspot data is that it is

discontinuously distributed in the heliographic latitudes and longitudes and the sizes of the sunspots are much smaller than the " latitudinal (longitudinal) wavelengths " of the oscillations . In fact, the data simulates a series of delta functions . On the contrary, magnetogram data is continuous . However, the sunspot data can be statistically used to describe the large-scale distribution of magnetic field on the surface and in time .

Presently the major astronomical centers which collect the data of white light pictures of sunspots are given in Appendix A.

Among the observatories listed therein, Greenwich Observatory has published the sunspot data from daily white light photographs of the sun , right from 1874 to 1976 in the series " Greenwich Photoheliographic Results "

The Greenwich photoheliographic results consist mainly of three sets of data, viz.; (i) positions and areas of sunspots and faculae for each day; (ii) positions and areas of the recurrent sunspot groups on each day of their observation (Ledger I) and (iii) similar data for the non-recurrent sunspot groups , which last for 2 or more days (Ledger II).

For the studies presented in this chapter the data from these Ledgers of the Greenwich photoheliographic results has been used . A magnetic tape of this data for the years 1874-1976 was kindly provided to the authors by H. Balthasar of Gottingen University. The heliographic colatitudes, and epochs (in days and fractions from 0.0 UT of January 1, 1874), for each sunspot group, on each day of its observation were taken for analysis .

2.3 Nominal Toroidal Field

From the bipolar nature of most of the sunspot groups, it is believed that the magnetic field associated with the sunspot groups is predominantly toroidal. This toroidal field is not directly measurable. However, by using Hale's laws of magnetic polarities and a mathematical function representing the distribution of sunspot activity on the sun's surface and in time, one can define quantitatively the sign and the strength of the field associated with a sunspot group. For example, the area or life time of a sunspot group can be taken as a measure of the associated toroidal magnetic flux. For normalizing the distribution of this toroidal magnetic flux on the surface of the sun and in time, we first define, the distribution of sunspot activity in terms of a probability function. Since the sunspot data is discontinuously distributed in heliographic latitude, longitude and in time, the distribution is represented by Dirac δ functions at the locations and the epochs of observed groups with suitable weightages attached to them. Thus the sunspot occurrence probability during a given time intervals (T_1, T_2) is defined as

$$p(\mu, \phi, t) = \begin{cases} W_i \delta(\mu - \mu_i, \phi - \phi_i, t - t_i) & \text{at } (\mu_i, \phi_i, t_i), i=1, 2, \dots, N, \\ 0 & \text{elsewhere in } (\mu, \phi, t) \text{ space} \end{cases} \quad (1)$$

where $\mu = \cos\theta$, θ is the heliographic co-latitude, ϕ is the heliographic longitude, δ represents a delta function in (μ, ϕ, t) , W_i is the weightage attached to the sunspot group 'i'. Here 'N' is the total number of sunspot groups.

is the number of data points during the interval (T_1, T_2) ; μ_i , ϕ_i are the values of μ and ϕ corresponding to the spot group ' i ' ; ' t_i ' is the time elapsed up to the epoch of observations in days, including the fraction of the day of the observation , from the zero hour of the first day of the interval (T_1, T_2) . In the works reported here , we adopted the weightage as $W_i = n_i/N$, where n_i is the life time of respective sunspot groups .

In reality the spot groups have finite extents . Hence , the delta functions used here are in fact mathematical idealizations of properly normalized ' physical ' delta functions which have large but finite values over small finite domains.

This leads to the following measure of the toroidal magnetic field $B_\phi(\mu, \phi, t)$

$$B_\phi(\mu, \phi, t) = \begin{cases} + p(\mu, \phi, t) & \text{in the northern hemisphere} \\ - p(\mu, \phi, t) & \text{in the southern hemisphere,} \end{cases} \quad (2)$$

the upper signs being taken during the ' even ' sunspot cycles and the lower ones during the ' odd ' cycles . This measure is named 'nominal toroidal field ' .

2.4 Legendre Fourier Analysis of the 'Nominal Toroidal Field'

2.4.1 Preliminary Results

This nominal toroidal field was subjected to Spherical Harmonic Fourier (SHF) analysis . The mathematical formulations

developed for this analysis is given in Appendix B . The SHF analysis consists of $m = 0$ (axisymmetric modes) and $m \neq 0$ (non-axisymmetric modes) terms. We present amplitude spectrum and phase variations of the axisymmetric (i.e., Legendre-Fourier) terms only for the following reasons : (i) with the exception of mode ($l = 1, m = 1$), amplitudes of axisymmetric terms are substantially higher than the non-axisymmetric terms (Gokhale and Javaraiah, 1990) (ii) the amplitudes and phases of non-axisymmetric terms are subject to errors due to those in determination of heliographic longitudes which are caused by variations in the law of differential rotation. The amplitude spectrum and the variation in the phases of the axisymmetric terms with a frequency $\nu = 1/22 \text{ yr}^{-1}$ obtained from analysis is given here.

2.4.1.1 The amplitude Spectrum

In Fig 2.1(a), the amplitudes $A_l = A(l, m, \nu)$ for $m = 0$ and $\nu = 1/22 \text{ yr}^{-1}$, derived from the data during the 82 intervals of 22 year length (i.e. 1874-1895, 1875-1896, etc) during 1874-1976, are shown for each value of l .

The values of A_l for even degree terms are much smaller than those of the odd degree terms. However, for $l > 21$, the amplitudes of the odd degree terms are also much smaller and are nearly comparable to those of the even degree terms . It is also interesting to note that the uncertainties in A_l values for odd degree terms are much smaller than the even degree terms.

2.4.1.2 The Approximate Constancy of Amplitudes

From Fig 2.1a, we note that for the odd degree terms , up to $l = 21$, the uncertainty of variation in each LF terms is smaller than the actual amplitudes of the LF terms . Thus the amplitudes of the odd degree terms remain approximately constant over the nine sunspot cycles by the data set. The amplitude spectrum for the odd degree terms has a 'main hump ' over $l = 1-11$ with a high peak at $l = 5,7$.

2.4.1.3 The approximate constancy of Phases

The temporal variation of the 'initial phases ' is represented by their values during the successive intervals . The pattern of the distribution of sunspot activity in latitude and time depends upon the relative phases of the LF terms . Here the phase of the term $l = 5$ is taken as the reference phase for computation of the relative phases.

In Fig 2.1(b), such relative phases of odd degree ' l ' terms are plotted for the 82 intervals of time. It is interesting to note that , the relative phases for the terms $l < 21$ remain approximately constant in time . The terms up to $l = 1,3,\dots,9$ describe a approximately stationary oscillation, since their relative phases are near 0° or 180° . Same is true for the terms $l = 13,15,\dots,21$. Thus the analysis shows possible presence of global oscillations represented by at least these two sets of LF terms .

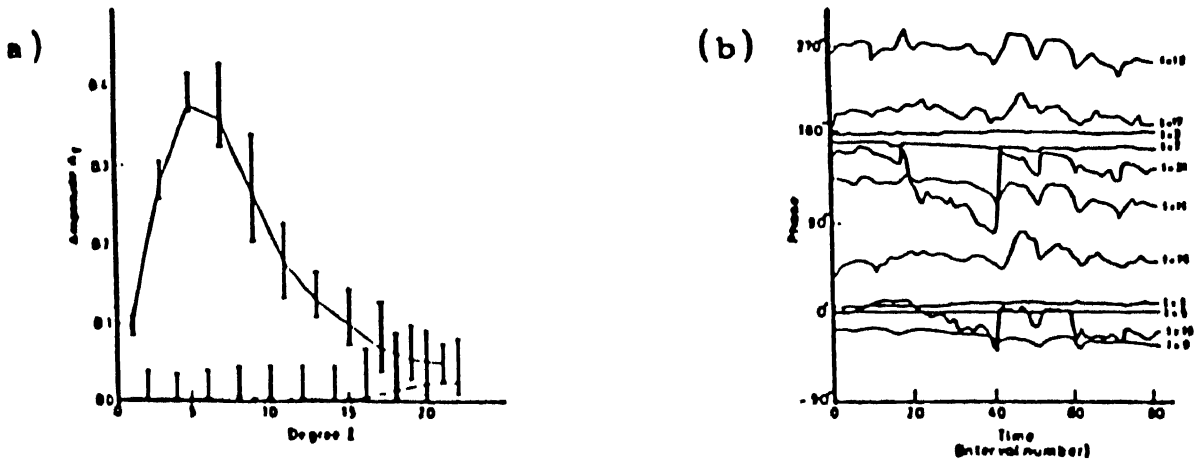


Fig 2.1(a).- Spectrum of relative amplitudes of the axisymmetric modes of 22 year periodicity in B_ϕ . The bars represent total scatter of the 82 values corresponding to the 82 intervals. The continuous curve represents the values obtained from the whole data set of the 103 years. (b) Relative phases $(\phi_l - \phi_5)$.

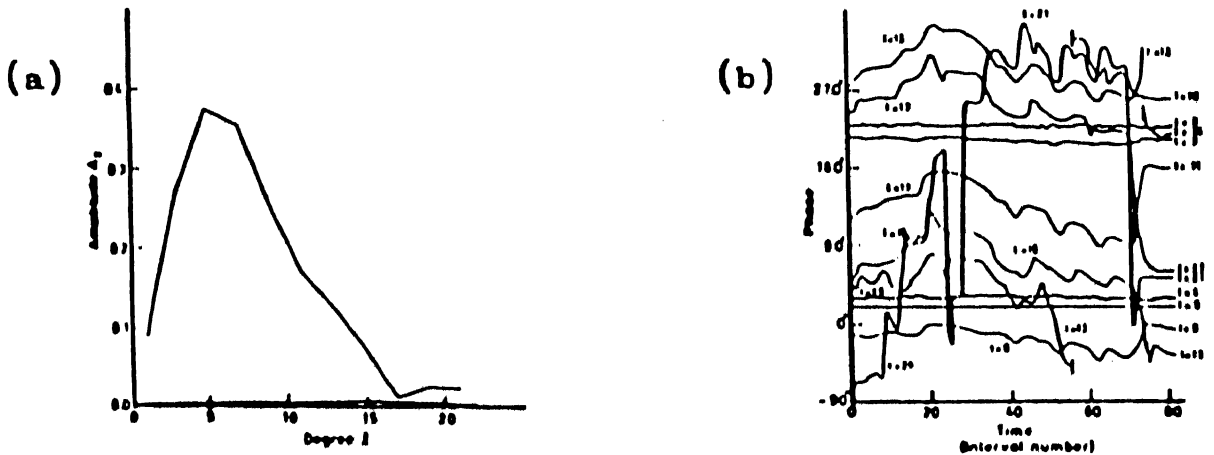


Fig 2.2.- (a) Relative amplitudes and (b) relative phases obtained from the 'simulated' data.

For examining whether the constancy of the amplitudes and the phases of the LF terms could be resulting by chance from a random distribution of sunspots, we generate a random data set, simulating the butterfly diagram in the following way. In this simulation the values of t_i are retained as in the real data but the values of latitudes $\lambda_i = (90^\circ - \phi_i)$ are assigned as follows : $\lambda_i = (\text{random sign}) \times (\lambda_0 + \Delta\lambda_i)$, in which, during the first seven years of each sunspot cycle, λ_0 varies linearly from 25° to 10° and $\Delta\lambda_i$ are random values between $(-9^\circ, +9^\circ)$. During the last four years of each cycle, λ_0 remains constant at 8° and $\Delta\lambda_i$ has random values between $(-6^\circ, +6^\circ)$. The relative amplitudes and the relative phases from this 'simulated' data set is given in Fig 2.2.

From comparison of Figures 2.1 and 2.2, it is clear that constancy of the relative amplitudes and the relative phases of the terms up to $\ell = 13$ can be reproduced by the simulated data. This is because the systematic variation of λ_0 truly reproduces the latitude-time correlation in the butterfly diagram on scales $\geq 14^\circ$. However, in Fig 2.2 the power in the terms $\ell > 13$ is much smaller than that in Fig 2.1. Also the phase variations of the term $\ell > 13$ are increasingly irregular with increasing ℓ . This shows that the constancy of the amplitudes and the phases up to $\ell \approx 21$ cannot be obtained by a simulated data set unless it reproduces $(\phi-t)$ correlations on all scales down to $\sim 9^\circ$. Such a simulation will need ad-hoc 'systematic' assumptions just for reproducing those correlations. Thus, this simulation shows that the

distribution of sunspot activity in the butterfly diagram is not produced by random process . Thus it was concluded that the correlations in real ϕ_i and t_i result from interference of the global oscillations of B_ϕ with amplitudes and phases as given by the LF analysis.

Here we list the results for the axisymmetric SHF terms.

(i) LF analysis of the Sun's inferred magnetic field shows that for $l \leq 21$, the odd parity terms have substantially larger amplitudes than the even parity terms .

(ii) For $l > 21$, the amplitudes of odd degree terms are much smaller than those for $l < 21$ and are comparable to those of the even parity terms .

(iii) The power spectrum has a ' main hump ' over $l = 1-11$, with a high peak at $l = 5, 7$ and a ' tail ' for $l \geq 21$.

(iv) The amplitudes and the phases of the dominant oscillations remain approximately constant for all 82 intervals of 22 years.

(v) Simulation of the butterfly diagram generated from the random data set shows that the distribution of sunspot activity is not produced by any random process.

2.4.2 Indication of Existence of Global Oscillations

of The Surface Magnetic Field

There is a possible presence of at least two global oscillations represented by the two sets of LF terms, viz., $\ell = 1, 3, 5, 7, 9$ and $\ell = 13, 15, 17, 19, 21$ with $\nu = 1/22 \text{ yr}^{-1}$. From constancy of amplitudes and phases which can not be reproduced by the simulated data (randomly distributed in butterfly diagram), we conclude that (i) the sunspot activity may originate in the interference of the global oscillations in sun's surface magnetic field ,with (ii) dominant contribution from axisymmetric terms of odd degrees up to $\ell \sim 13$ and periods ~ 22 year . This has been further confirmed (Gokhale *et.al.* 1992; Gokhale and Javaraiah, 1992) by two more types of simulated data sets with data randomly distributed with the real (observed) boundaries of the butterfly wings during each cycle.

2.5 Recent Results

2.5.1 ' Forced ' Nature of the Oscillations

Recently (Gokhale.*et.al* 1992), the LF analysis (up to $\ell = 35$) of the Sun's magnetic field inferred from the Greenwich sunspot data shows that in the LF power spectra there is no clear evidence for the existence of any relation between the harmonic degree and the temporal frequency of the power concentrations.

Apart from the power ' ridge ' in the narrow frequency band $\sim 1/21.4 \text{ yr}^{-1}$, and a few low ridges at odd multiples of this frequency, there are no other spectral features. In the spectrum for even degree modes features simulated to those obtained by Stenflo and Vogel (1986) are reproduced even by a randomly simulated data set. The authors conclude that the solar magnetic cycle could consist of global oscillations of the Sun ' forced ' at a frequency $\sim 1/21.4 \text{ yr}^{-1}$ and, perhaps, weak resonances at its odd harmonics. The band width of the forcing frequency seems to be much less than $1/107 \text{ yr}^{-1}$.

2.5.2 Confirmation of the Global Nature of the Oscillations

2.5.2.1 Separation of LF terms in Coherent Global Oscillations

As stated in section 2.4.1.3, the phases of the terms $\ell = 1, 3, 5, 7, 9$ are approximately but not exactly at 0° or 180° and those of $\ell = 11, 13, \dots$ are approximately but not exactly at 90° or 270° . By separating the $\cos\omega t$ and $\sin\omega t$ parts of these LF terms Gokhale and Javarajah (1992) showed that there must be four independent modes of global oscillations.

By computing the phases (δ_ℓ) and the standard deviations (Δ_ℓ) of δ_ℓ during the 82 intervals, the authors found that the terms fall into 3 categories, viz., (i) stationary modes which have constant phases ($\Delta_\ell \leq 15^\circ$) (ii) non-stationary modes which have approximately constant phases ($\Delta_\ell \leq 30^\circ$) and, (iii) non-stationary modes which have large phase variations ($\Delta_\ell \geq 30^\circ$).

When the authors separated the terms of the first two categories into two coherent groups of $\sin(\omega t)$ and $\cos(\omega t)$ components, they found that each coherent group separates into two power humps., viz., (i) B_1 ($l = 1$ to 11), (ii) B_2 ($l = 3$ to 17), (iii) B_3 ($l = 15$ to 29), and (iii) B_4 ($l = 21$ to 25). Since the full physics of these oscillations is not known, the authors named them as 'geometrical eigen modes'

2.5.2.2 Verification of Superposition of 'Geometrical Eigen Modes'

In the same paper, the authors showed that the large-scale latitude-time behavior (i.e. global properties) of the solar magnetic cycle can be reproduced even in high latitudes by superposing these four oscillations.

The mode B_1 acts for concentration of activity in latitude zones ($0^\circ - 30^\circ$) peaking at 15° . Superposition of B_1 and B_2 reproduces sunspot activity and starts giving agreement with observed behavior even in high latitudes. Finally, superposition of B_1 , B_2 , B_3 and B_4 reproduces the following observed characteristics: (i) butterfly diagrams, (ii) polar reversals near the sunspot maximum, (iii) migrations of neutral lines from middle latitudes all the way to the poles and (iv) 'high' ($\sim 10^3$), 'low' (~ 10) and, 'medium' ($\sim 10^2$) level flux concentrations in 'low' ($0-30^\circ$), 'middle' ($30^\circ - 75^\circ$) and 'high' ($\geq 75^\circ$) latitudes respectively.

Note that the behavior of these oscillations in the middle and the high latitudes is reproduced from the LF terms which are

computed from the data which comes only from the low latitudes. This cannot happen if basic mechanism of sunspot activity is operating only in low latitudes . And that these oscillations may provide basic mechanism of the solar magnetic cycle.

Thus, this analysis strongly supports that *the groups of LF terms used in the superposition must be representing real global oscillations of the Sun .*

2.6 ' Reality ' of the ' Nominal ' Toroidal Field

The 'nominal toroidal field ' defined in section 2.3 need not be same as the actual toroidal field. However, its spatial and temporal frequencies , as well as the amplitude spectrum, are similar to the radial field computed from the line of sight component of the field observed in the full disc magnetograms (Stenflo 1988) . Thus the nominal ' toroidal field ' simulates real field . Hence, the nominal toroidal field and the 'observed' radial field must be components of the same time-dependent vector magnetic field near the surface.

2.7 The Mathematical Form of the Energy Spectrum

From the approximate constancy of the phases of the odd LF degree terms in the nominal toroidal field , it was inferred that there are, in the sun, long period global MHD oscillations , i.e. standing MHD waves trapped in the sun (the small fluctuations in

the amplitudes and phases indicate a ' leakage ' of the trapped waves across the surface). The trapping of the waves generally leads to a spectrum with a power law for low frequencies and exponential fall at high frequencies (eg. Planckian spectrum of electromagnetic waves , Heisenberg spectrum of hydrodynamic turbulence, etc.). Hence, as a first step, it was attempted to fit the spectrum with a formula approximately $\sim al^2$ in a small l domain and $\sim al^3 \exp(-bl)$ in the large l domain (as in Plank spectrum). The power spectrum given by squares of the amplitudes in Fig 2.1a could be fitted excellently (χ^2 - confidence >99.98 %) to the form $al^3 \exp(-bl)$ with $a = 0.0142 \pm 0.011$ and $b = 0.552 \pm 0.015$. Note that , this mathematical form is good only for the main part of the hump of the spectrum. However, it does not fit the tail part of the spectrum. Later , this spectrum was fitted (Gokhale and Javaraiah, 1992) to the form given by Chandrasekhar's theory of MHD turbulence, which was good for the tail part of the spectrum also.

2.8 Physical Implications Of the Independence of ν and l

The approximate constancy of the frequency ν for all the odd values of ' l ' up to 29 may be due to the presence of some single ' forcing ' oscillation. Presence of such a forcing oscillations was suggested earlier by Alfven (1943) and Dicke (1977). In addition , the internal magnetic field (and the plasma density) must be so structured as to have the modes of free global MHD

oscillations with frequencies in the neighborhood of the forcing frequencies.

To decide whether such modes of ' free ' oscillations exist or not , it will be necessary to determine theoretically the oscillation modes allowed by the equations of MHD. This will require knowledge of steady part of the Sun's internal magnetic field . The latter can be inferred only by theoretical modeling . A model of such a field is presented in the next two chapters .

APPENDIX 2.A

- (i) Arectri Observatory, Islands Of Naples, Italy
- (ii) Beijing Solar Observatory, Beijing, China
- (iii) Catania Astrophysical Observatory, Italy
- (iv) Crimean Astrophysical Observatory, Simeiz, USSR
- (v) Greenwich Observatory, Greenwich, UK
- (vi) Hale Observatories, California, USA
- (vii) Heliophysical Observatory, Debrecen, Hungary
- (viii) Kiepenheuer Institute for Solar Physics, Frieberg,
Germany
- (ix) Kitt Peak National Observatory, Tucson, Arizona, USA
- (x) Kodiakanal Observatory, Kodiakanal, India
- (xi) Sayan Observatory, Lake Baikon, Siberia, USSR
- (xii) Sacramento Peak Observatory, Sunspot, New Mexico, USA
- (xiii) Tokyo Astronomical Observatory, Japan
- (xiv) Udaipur Solar Observatory, India
- (xv) Solar Observatory, Canaries Islands, Spain

APPENDIX 2.B

Formulae for SHF components

The harmonic components $H_{cc}(\ell, m, n | T_1, T_2)$, $H_{cs}(\ell, m, n | T_1, T_2)$, $H_{sc}(\ell, m, n | T_1, T_2)$, $H_{ss}(\ell, m, n | T_1, T_2)$ in the expansion

$$B_{\varphi}(\mu, \phi, \tau) = \sum_{\alpha, \ell, m, n} H_{\alpha}(\ell, m, n | T_1, T_2) P_{\ell}^m(\mu) \frac{\cos(m\phi)}{\sin} \frac{\cos(2\pi n\tau)}{\sin} \dots \dots \dots (B 1)$$

during the interval (T_1, T_2) are given by

$$H_{\alpha}(\ell, m, n | T_1, T_2) = C(\ell, m, n | T_1, T_2) \int_0^1 d\tau \int_0^{2\pi} d\phi \int_{-1}^{+1} B_{\varphi}(\mu, \phi, \tau) P_{\ell}^m(\mu) \frac{\cos(m\phi)}{\sin} \frac{\cos(2\pi n\tau)}{\sin} d\mu \dots \dots \dots (B 2)$$

$$= \frac{C(\ell, m, n)}{N} \sum P_{\ell}^m(\mu) \frac{\cos(m\phi)}{\sin} \frac{\cos(2\pi n\tau)}{\sin} \dots \dots \dots (B 3)$$

where α is a symbol representing the subscript 'cc', 'cs', 'sc' or 'ss', depending upon the combination of the cosines or sines of $(m\phi)$ and $(2\pi n\tau)$ in the respective term; $\tau = (t - T_1) / (T_1 - T_2)$, and

$$C(l, m, n) = \Lambda \frac{(l-m)!(2l+1)}{(l+m)!\pi}$$

with

$$\Lambda = \begin{cases} - & 1 \text{ for } m \neq 0, n \neq 0 \\ - & 1/2 \text{ if } m = 0 \text{ or } n = 0 \\ - & 1/4 \text{ if } m = 0 \text{ \& } n = 0 \end{cases}$$

Determination of amplitudes and phases

Referred to $t = T_1$ as zero epoch

The amplitudes $A_c(l, m, n)$ and $A_s(l, m, n)$ of the $P_\ell^m(\mu)\cos(m\phi)\exp(2\pi i n \tau)$ and $P_\ell^m(\mu)\sin(m\phi)\exp(2\pi i n \tau)$ during (T_1, T_2) are given by

$$A_c(l, m, n) = [H_{cc}^2(l, m, n) + H_{cs}^2(l, m, n)]^{1/2},$$

and

$$A_s(l, m, n) = [H_{sc}^2(l, m, n) + H_{ss}^2(l, m, n)]^{1/2}.$$

The rms amplitude of $P_\ell^m(\mu)$ term is defined as

$$A(l, m, n) = [A_c^2(l, m, n) + A_s^2(l, m, n)]^{1/2}$$

For $m = 0$, $A_c(l, m, n) = A(l, m, n)$.

The phases $\varphi_c(l, m, n)$ and $\varphi_s(l, m, n)$ of the above terms during (T_1, T_2) 'referred to $t = T_1$ as the zero epoch' are the values of φ in their dependence expressed as

$$\sin [2\pi\nu(t-T_1) + \varphi] ,$$

where

$$\nu = n / (T_1 - T_2) .$$

These phases are given by

$$\varphi_c(l, m, n) = \tan^{-1} [H_{cc}(l, m, n) / H_{cs}(l, m, n)] + 0 \text{ or } \pi \text{ and}$$

$$\varphi_s(l, m, n) = \tan^{-1} [H_{sc}(l, m, n) / H_{ss}(l, m, n)] + 0 \text{ or } \pi ,$$

where 0 or π is chosen to ensure the correct signs for the sines and cosines.

For axisymmetric ($m = 0$) terms φ_s is undefined and the symbol φ_c will be replaced by φ .

Amplitudes and phases referred to other zero epochs

It can be shown that the above formulae also give the amplitudes and phases referred to any epoch T_0 other than T_1 as the zero epoch if in equation (B 3) one takes

$$\tau = (t - T_0) / (T_2 - T_1) ,$$

instead of $(t - T_1)/(T_2 - T_1)$.

In such a shift of zero epoch, the amplitudes remain invariant and the phases shift by $2\pi\nu(T_1 - T_0)/(T_2 - T_1)$.

Estimates of uncertainties and errors

The uncertainties δA_c , δA_s , $\delta\varphi_c$ and $\delta\varphi_s$ in A_c , A_s , φ_c and φ_s arise from errors and uncertainties $\delta\theta$, $\delta\varphi$ and δt in θ , φ , t and from sunspot activity missed by observations.

The relative errors $\delta\theta/\theta$, $\delta\varphi/\varphi$ and $\delta t/t$ are $< 10^{-2}$. The correspond relative uncertainties $\delta A_c/A_c$, $\delta A_s/A_s$, etc. are $\sim (1/N^{1/2})(\delta\lambda/\lambda + \delta\varphi/\varphi + \delta t/t)$. These are $< 10^{-4}$ for A_c , A_s etc, computed from data lengths of a sunspot cycle or longer.

If each sunspot group is viewed as providing a single data point weighted by the number of days on which it is observed then the spread in t_i , together with those in θ_i and φ_i due to the proper motions of sunspots, will raise the above upper limit on $\delta A_c/A_c$, etc; but to a value still $< 10^{-3}\ell$. Further, the differential rotation will cause a spread in φ_i whose magnitude in degrees will be $\sim (2.7) \times (\sin^2\theta) \times (\text{life span in days})$. The upper limit on the average value of this spread will be $< 10^0$, i.e. less than 10 times the maximum error in the daily values of φ . Hence the upper limit on $\delta A_c/A_c$, etc. for non axisymmetric ($m \neq 0$) will be $< 10^{-2}m$. Thus, $\delta A_c/A_c$ etc., will be $< 10^{-3}\ell$ for the axisymmetric terms, and $< 10^{-2}m$ for the non axisymmetric terms.

Since, the definition of $p(\theta, \phi, t)$ is normalized with respect to $N(T_2 - T_1)$, the errors due to the 'missing' of activity on the unobservable side of the Sun will be small for $(T_2 - T_1) \gg 27$ day. Since the sunspot activity is confined to $\cos^2 \theta \leq 1/4$, the errors due to its 'under sampling' at different latitudes caused by the differential rotation $\Omega = (\Omega_0 - \Omega_1) \cos^2 \theta$, with $\Omega_1/\Omega_0 \approx 1/5$, will be < 5 per cent.

A PRELIMINARY MODEL OF THE 'STEADY' PART OF THE SUN'S
INTERNAL MAGNETIC FIELD

3.1 Introduction

As described in the previous chapter, the Legendre-Fourier analysis of the sun's inferred magnetic field strongly supports the idea that the sunspot activity could be resulting from superposition of global slow MHD oscillations. For such oscillations to be admissible there must exist inside the sun a 'steady' magnetic field that varies slowly (eg. on time scales much greater than 11 years). Since the activity related field is mainly toroidal, it is important to model 'steady' part of the poloidal field.

In this chapter and the next, we model this 'steady' part of the poloidal magnetic field which can remain in 'steady' state in the presence of internal differential rotation of the sun.

We consider the sun's internal rotation and the magnetic field at any epoch to be consisting of the 'steady' and the 'fluctuating' parts. The fluctuations themselves may be contributed, for example, by superposition of a large number of

sun's global MHD oscillations , on a hierarchy of 'dynamical' time scales. Here, the time scales of the ' steady ' parts of the rotation and the magnetic field must be larger than the periods of the slowest MHD oscillations . Thus they can be expected to be of the order of diffusion time scale . However, for determining the 'steady' part of the magnetic field, in the first step we approximate it as if it is absolutely steady.

On large scales of length and time, the distribution of activity is predominantly symmetric about the axis of solar rotation and has odd north south parity (cf. analysis given in chapter II). This implies that the 'steady' field assumed here must also be dominantly symmetric about the rotation axis and must have odd north-south parity . According to Cowling's theorem, this implies that in the induction equation , the resistive and the inductive terms for the steady part of the field must vanish separately. This in turn implies that the curl of the current density of the steady part of the internal field must vanish. As a first step, we take the simple special case where the field is current free (except near the 'boundaries'). Then it must also be in isorotation (Ferraro 1937) with the steady part of the rotation of the plasma. However, if the time dependent part of the rotation is small, then the isorotation of the field with the steady part of the plasma rotation implies approximate isorotation with the total rotation (i.e. steady and time

dependent parts) at any epoch , eg. the helioseismologically inferred rotation of the plasma. This is possible only if there exists a functional relation between the inferred rotation $\Omega(r)$ at a point r and the flux function $\phi(r)$ of the 'steady' poloidal field linking through the circle of revolution of the point. Here we have assumed that the meridional circulation part of the flow is negligible .

By assuming different arbitrary forms for the functional relation between $\phi(r)$ and the observed $\Omega(r)$, one may compute many models of the fields which isorotate with the observed rotation . However, since $\Omega(r)$ is known only in the form of numerical values, the models so computed will also be in numerical forms . Moreover, none of the models so computed will represent the steady field exactly, since the real steady field must be isorotating only with the unknown 'steady' part of helioseismologically inferred internal rotation. Therefore one has to model the 'steady' part of the real field by first choosing an analytical expression for the magnetic field and then determining the best combination of terms in the chosen form and the best set of values for their coefficients .

Thus, in such a model, the part of the 'observed' rotation which can be best fitted to the isorotation law represents the steady part of the rotation . The residual part of $\Omega(r)$ then

represents the fluctuating part of rotation.

In this chapter , we choose as a first step, the simplest expression for the magnetic field , viz., the multipole expansion of a potential field with odd north-south parity and consistent with asymptotically uniform field of intensity B_0 at large distances . In section 3.2, we give reasons why the steady part of the real field may be considered as current free . In the same section we also describe the data on internal rotation and the method of analysis .

In section 3.3, we find that the chosen form of the field yields a very good least square fit for a linear relation with the observed rotation in the outer part of the sun (especially the convective envelope). However , the best fit requires that the flux function $\phi(r)$ contains a term representing 'external' sources besides the term representing the 'central' sources . With the present accuracy of the rotational data, the best fit gives the internal source as a combination of a dipole field and a hexapole field , both located at the center, parallel to the rotation axis. The limits on the strength of B_0 can be estimated from the observed field on the surface , to be $\sim 10^{-4}$ and 1 G (section 3.4.2) . The strengths of the dipole and the hexapole is determined in terms of B_0 (as a free parameter) and the solar radius R_0 .

The field structure (Fig. 3.1) given by the best fit is presented in section 3.3.2 . This structure has a closed 'critical field line' $\phi = \phi_*$ running almost along the base of the convection zone in the 'sunspot' latitudes.

The observed rigid rotation in the outer radiative core (ORC) suggests that in the interior of the surface S_* generated by the rotation of the critical field line at the rate Ω_* ($=\Omega_0 + A\phi_*$), one may have $\Omega_0 \approx \Omega_*$ and ' A ' must be quite small .

However, we show in section 3.4 that the observed rotation just inside S_* could alternatively be expressed in the form of equation (10) , where $(A_C - A_E)$ may be ~ 7 nHz per unit flux . This difference between A_C and A_E corresponds to a small deviation from isorotation near S_* . Such a non-isorotation might result in winding of the poloidal field into strong toroidal field (eg the field inferred by Dziembowski and Goode 1991) . This may take in $\sim 10^6 - 10^9$ yr, depending upon the value of B_o .

In section 3.5 , some interesting properties of this model of the steady part of the field are presented . A possible role of the MHD oscillations is pointed out .

Finally we point out the main drawbacks of such a model.

3.2 Determination Of the ' Steady ' Field

3.2.1 *The shapes of iso-rotation contours and the sources for the 'steady' poloidal magnetic field*

Christensen-Dalsgaard & Schou (1988), Dziembowski et al (1989) and Sekii (1989) have analyzed the helioseismological data of Libbrecht (1989) in different ways. Except for the differences in the value and the gradient of rotation rate just below the base of the convection zone, the characteristics of internal rotation given by all the three investigations are qualitatively similar. In particular, all the three calculations yield considerable radial dependence of rotation rate along the polar axis so that the isorotation contours seem to intersect the rotation axis. If the contours really intersect the axis then the radial variation of $\Omega(r)$ along the rotation axis would make it impossible to have the Ferraro's isorotation law satisfied in the close neighborhood of the axis. However, there are considerable uncertainties in the estimation of rotation rates near the sun's center and near the rotation axis (Schou et al 1992). Consequently, it is not ruled out that in reality the iso-rotation contours actually turn near the axis and either (i) converge 'towards' the center (running close to the axis instead of intersecting it) or (ii) run crudely parallel to the rotation axis . This is equivalent to suggesting

the presence of either concentrated toroidal currents near the axis in the core or diffusing currents throughout the interior (eg see in chapter IV) . On the other hand the iso-rotation contours in convective envelope ('CE') are concave outwards, suggesting that the large scale steady field may have a contribution from 'external' sources.

Thus if there is a 'steady ' and axisymmetric poloidal field which (as argued earlier on the basis of the Cowling's theorem) as a special case is current free and iso-rotating with the contemporary internal rotation of the sun in outer radiative core ('ORC') and in 'CE' . Then it may have (i) internal sources (toroidal currents) concentrated near the axis and distributed inside the inner radiative core ('IRC') and (ii) 'external' sources at large distances .

3.2.2 The feasibility of existence of iso-rotating current free poloidal field with central as well as external sources

Toroidal currents of very high intensity might have been created in the sun during its formation by gravitational collapse. These currents must have dissipated during the fully convective (Hayashi) phase of the sun's subsequent evolution. However, as

shown by Spitzer (1956) such a diffusion would also create and maintain electric currents near the axis and the near surface. The 'steady' parts of the presently surviving internal field, and rotation, must constitute the slowest decaying solution of the MHD equations, with the end configuration of Hayashi phase as the initial configuration. In such a solution the magnetic field must be a solution of the induction equation (Chandrasekhar 1956a) :

$$\frac{\partial T}{\partial t} = \eta \Delta_5 T + \frac{1}{y} \left[\frac{\partial(\Omega, \phi)}{\partial(z, y)} - \frac{\partial(T, y^2 U)}{\partial(z, y)} \right]$$

where $T = y^{-1} B_T$, B_T is the steady part of the toroidal field, $y = r \sin \theta$, $z = r \cos \theta$, η is magnetic diffusivity,

$$\Delta_5 \equiv \left[\frac{\partial^2}{\partial y^2} + \frac{3}{y} \frac{\partial}{\partial y} + \frac{\partial^2}{\partial z^2} \right],$$

and U is a function defining meridional flow field in the same way as ϕ defines the poloidal field.

If in the post Hayashi evolution the effects of diffusion and that of the 'steady' part of the meridional circulation are small compared to the effect of rotation then in steady state, one must have :

$$\frac{\partial(\Omega, \phi)}{\partial(z, y)} = 0.$$

This is in fact Ferraro's law of isorotation in which all points on each field line rotate with the same angular velocity (which may differ from one field line to another). The slow evolution of the 'steady' part will be given by the diffusion and meridional circulation. Thus the 'steady' parts of the field and the rotation evolve slowly, maintaining the state of isorotation.

It follows from Spitzer's (1956) solution again that even in this evolution the currents will be maintained near the axis and near the surface. Whatever currents slowly diffuse into 'ORC' and 'CE' would decay fast owing to the MHD turbulence (ie. fluctuations on dynamical time scales) existing there. The currents diffusing into 'CE' will further decay by convective turbulence and will also be carried away by effects of magnetic buoyancy and finally by coronal expansion.

On these grounds we assume in this chapter, as a first step, that the large scale 'steady' field may be current-free in 'ORC' and 'CE', and has 'central' as well as 'external' sources.

There is also the following *a-posteriori* justification for this approximation. The photospheric field structure given by this approximation is almost same as that of a unique superposition of

the first two characteristic solutions of the magnetic diffusion equation, (Chandrasekhar 1956b), with appropriate parity (see Appendix A).

3.2.3 The chosen form of the relation between $\phi(r)$ and $\Omega(r)$

For the relation between $\phi(r)$ and $\Omega(r)$ we assume the linear relation

$$\Omega(r, \vartheta) = \Omega_0 + A \phi(r, \vartheta) \quad (1)$$

expecting it to serve as the first approximation to any non-linear relation that might exist.

Here $r = |r|$, ϑ is the co-latitude, Ω_0 and A are constants.

3.2.4 The 'data' used

Among the aforementioned (section 3.2.1) helio-seismological results of the internal rotation $\Omega(r)$, the one by Christensen-Dalsgaard & Schou yields the smallest uncertainties. We do not find in their paper general expressions which could be used for determining $\Omega(r, \vartheta)$ along directions other than $\vartheta = 0^\circ$, 45° and 90° . Hence we use the expressions given by Dziembowski et al (1989) to determine the rotation rates at selected sets of points (r, ϑ) and, (since the two rotation models are generally

similar) take the resulting values of $\Omega(r, \vartheta)$ as if obtained by the method of Christensen-Dalsgaard & Schou (1988) viz., with the correspondingly small uncertainties.

3.2.5 The method of analysis

Assuming the current free poloidal magnetic field to be symmetric about the axis of rotation, and of odd north-south parity, we write it as

$$\mathbf{B} = -\nabla V, \quad (2)$$

where

$$V = V_C(r, \vartheta) + V_E(r, \vartheta),$$

wherein

$$V_C(r, \vartheta) = \sum_{\ell=1} M_{\ell} r^{-(\ell+1)} P_{\ell}(\mu),$$

$$V_E(r, \vartheta) = -B_0 r P_1(\mu) + \sum_{\ell=3} M_{\ell} r^{\ell} P_{\ell}(\mu),$$

are the magnetic potentials due to the central and the external sources, $\mu = \cos\vartheta$, ϑ is the co-latitude, M_{ℓ} are the strengths of the magnetic moments, $P_{\ell}(\mu)$ are Legendre polynomials, and the summations are taken only over the odd integral values of ℓ .

Since we expect the *long-lived* external currents to be at

very large distances, we expect their field in the local neighborhood of the sun to be uniform. Hence we keep only the first term in $V_E(r, \theta)$ and remove the terms $\ell \geq 3$. This has been justified *a-posteriori* by the fact that inclusion of terms $\ell > 1$ or omission of the term $\ell = 1$ in V_E deteriorates the goodness of the least-square fit.

Thus we have

$$V(r, \theta) = (-B_0 r + M_1 r^{-2}) P_1(\mu) + M_3 r^{-4} P_3(\mu) + M_5 r^{-6} P_5(\mu) + \dots \quad (3)$$

From the above equation, we give the radial component of the magnetic field as

$$B_r = B_0 \cos \theta + 2M_1 \cos \theta r^{-3} + M_3 r^{-5} (10 \cos^2 \theta - 6) \cos \theta + \dots \quad (4)$$

This gives the following expression for the magnetic flux function

$$\begin{aligned} \phi(r, \theta) &= \int_0^\theta 2\pi r^2 B_r \sin \theta \, d\theta \\ &= \pi B_0 R_0^2 [(x^2 + 2\mu_1 x^{-1} + 4\mu_3 x^{-3} + \dots) \sin^2 \theta \\ &\quad + (-5\mu_3 x^{-3} + \dots) \sin^4 \theta + \dots], \quad (5) \end{aligned}$$

where $x = r/R_0$ and $\mu_\ell = M_\ell / (B_0 R_0^{\ell+2})$, $\ell = 1, 3, 5, \dots$

We write eq. (1) in terms of the 'normalized dimensionless rotation rate' :

$$\omega(r_1, \vartheta_1) = (\Omega(r_1, \vartheta_1) - \hat{\Omega}_{\text{obs}}) / \sigma_{\Omega\text{obs}} = a_0 + a_1 \phi(r_1, \vartheta_1) \quad , \quad (6)$$

where $a_0 = (\Omega_0 - \hat{\Omega}_{\text{obs}}) / \sigma_{\Omega\text{obs}}$ and $a_1 = A / \sigma_{\Omega\text{obs}}$, $\hat{\Omega}_{\text{obs}}$ and $\sigma_{\Omega\text{obs}}$ are the mean and the standard deviation of the whole set of the observationally determined values $\Omega(r_1, \vartheta_1)$ at the chosen set of points (r_1, ϑ_1) . Equation (6) can also be written as :

$$\Omega = \Omega_0 + \Omega_1 [(x^2 + 2\mu_1 x^{-1} + 4\mu_3 x^{-3} + \dots) \sin^2 \vartheta + (-5\mu_3 x^{-3} + \dots) \sin^4 \vartheta + \dots], \quad \dots (7)$$

where $\Omega_1 = \pi a_1 B_0 R_0^2 \sigma_{\Omega\text{obs}}$.

We determine the coefficients $\Omega_0, \Omega_1, \mu_1, \mu_3$, etc., by obtaining weighted least square fits for successive combinations of terms in equation (7) using the following three sets of data points :

'CE': 99 points in the convective envelope ($0.7 \leq x \leq 1.0$), consisting of 11 equi-spaced points along each of the directions

$\phi = 10^\circ, 20^\circ, \dots, 90^\circ,$

'ORC': a set of 72 points in the outer radiative core ($0.4 \leq x \leq 0.7$) consisting of 8 equi-spaced points along each of the directions just mentioned, and

'ORC+CE': a set of 189 points over the whole range ($0.4 \leq x \leq 1.0$)

The 'weights' have been assigned proportional to the reciprocals of the uncertainties as read off from Christensen-Dalsgaard & Schou (1988).

Values of the coefficients in equation (7) obtained from the the least-square fits for a_0 and a_1 in equation (6), by taking various combinations of terms in equation (7), are given in the three Tables along with the χ^2 probabilities.

3.2.6 Estimation of the goodness of fit

For determining the contribution from each point (r_i, ϕ_i) to the value of χ^2 the "observed normalized values" $\omega(i) = \omega(r_i, \phi_i)$ must be considered as if obtained from independent experiments. In reality this condition is not satisfied. However here we use the χ^2 values merely for the purpose of comparing the relative goodness of various least-square fits.

Further, in order that each $\omega(i)$ is a 'normal variate' distributed about the corresponding theoretical value $\omega_T(i)$, it is necessary that for each i , $\omega(i)$ and $\omega_T(i)$ are both measured in units of the standard deviation $\sigma_\omega(i)$ of the "distribution" of $\omega(i)$ about $\omega_T(i)$. However, for each i , $|\omega(i) - \omega_T(i)|$ is itself a measure of $\sigma_\omega(i)$. Hence we have:

$$\chi^2 = \sum_i |\omega(i) - \omega_T(i)| / \omega_T(i) .$$

We have verified that at least in 'CE' the values of the least square difference $\left(\sum [\omega(i) - \omega_T(i)] \right)$ also give the same conclusions about the relative goodness of the fits as given by the χ^2 values.

3.3 The Results

3.3.1 Least-square fit for the convection zone

Results of least-square fits of successive combinations of terms in equation (7) to the three data sets are presented in three tables, viz., Table 3.1, Table 3.2 and Table 3.3.

Table 3.1

Results of least-square fits of successive combinations
of terms in equation (7) to the data set 'CE'

Terms Taken	Ω_0 (nHz)	Ω_1 (nHz)	μ_l	$\Delta\mu$ (%)	$\frac{\mu_3}{\mu_1}$	χ^2	Goodness of Fit (%)
(1)	(2)	(3)	(4)	(5)	(6)	(7)	(8)
P1	349 ± 9	62 ± 5	$\mu_1=0.484$	10	—	42.5	99.99
P_1, P_3	326 ± 12	68 ± 11	$\mu_1=0.624$ $\mu_3=0.156$	17 30	0.250	17.9	100*
P_1, P_3 and P_5	321 ± 13	57 ± 2	$\mu_1=0.905$ $\mu_3=0.227$ $\mu_5=0.001$	23 26 ...	0.251	19.0	100*

(* χ^2 - probability $< 10^{-7}$) In column 5 uncertainties exceeding 100% are not given.

Table 3.2

Results of least-square fits of successive combinations
of terms in equation (7) to the data set ' ORC+CE '

Terms Taken	Ω_0 (nHz)	Ω_1 (nHz)	μ_ℓ	$\Delta\mu$ (%)	$\frac{\mu_3}{\mu_1}$	χ^2	Goodness of Fit (%)
(1)	(2)	(3)	(4)	(5)	(6)	(7)	(8)
P1	364	32	$\mu_1=0.218$	33	—	134	99.74
	± 4	± 2					
P ₁ , P ₃	332	73	$\mu_1=0.490$	31	0.229	156	96.00
	± 8	± 15	$\mu_3=0.112$	22			
P ₁ , P ₃	322	64	$\mu_1=0.727$	15			
& P ₅	± 10	± 2	$\mu_3=0.187$	16	0.257	143	99.00
			$\mu_5=0.0003$..			

In column 5 uncertainties exceeding 100% are not given.

Table 3.3

Results of least-square fits of successive combinations
of terms in equation (7) to the data set ' ORC '

Terms Taken	Ω_0 (nHz)	Ω_1 (nHz)	μ_l	$\Delta\mu$ (%)	$\frac{\mu_3}{\mu_1}$	χ^2	Goodness of Fit (%)
(1)	(2)	(3)	(4)	(5)	(6)	(7)	(8)
P1	434 ± 16	32 ± 26	$\mu_1 = -0.102$..	—	163	0.0
P1, P3	429 ± 3	8 ± 34	$\mu_1 = -0.314$..			
			$\mu_3 = -0.001$..	0.004	1008	0.0
P ₁ , P ₃	426	-10	$\mu_1 = -0.349$..			
& P ₅	± 150	± 5	$\mu_3 = -0.013$..	0.037	57	89
			$\mu_5 = -0.0001$..			

In column 5 uncertainties exceeding 100% are not given.

From the values of χ^2 in the tables it is clear that in the convective envelope ('CE') (Table 3.1) the best fit for equation (7) is given by the combination $\ell = 1$ and 3 (the dipole and the linear hexapole terms) whose strengths in terms of B_0 are given by

$$M_1 = (0.624 \pm 0.106)B_0 R_0^3 \text{ and } M_3 = (0.156 \pm 0.046)B_0 R_0^5 . \quad (8)$$

This corresponds to a total 'flux' across the solar hemisphere:

$$\phi(R_0, \pi/2) \approx 2.09\pi B_0 R_0^2 ,$$

which gives the following upper limit on B_0 :

$$B_0 \leq 1 \text{ G} ,$$

since the total observed magnetic flux on the photosphere does not exceed 3×10^{22} Mx (Howard 1974).

3.3.2 *The geometrical structure of the field*

The field lines of the field given by equations (5) and (8) in the range $0.7 \leq r/R_0 \leq 1.0$ are plotted in Fig.3.1. These simulate quite satisfactorily (in CE) the pattern of the isorotation lines given by helioseismology (Libbrecht 1988), except very near the axis, where the uncertainties in the 'observed' rotation rates are large.

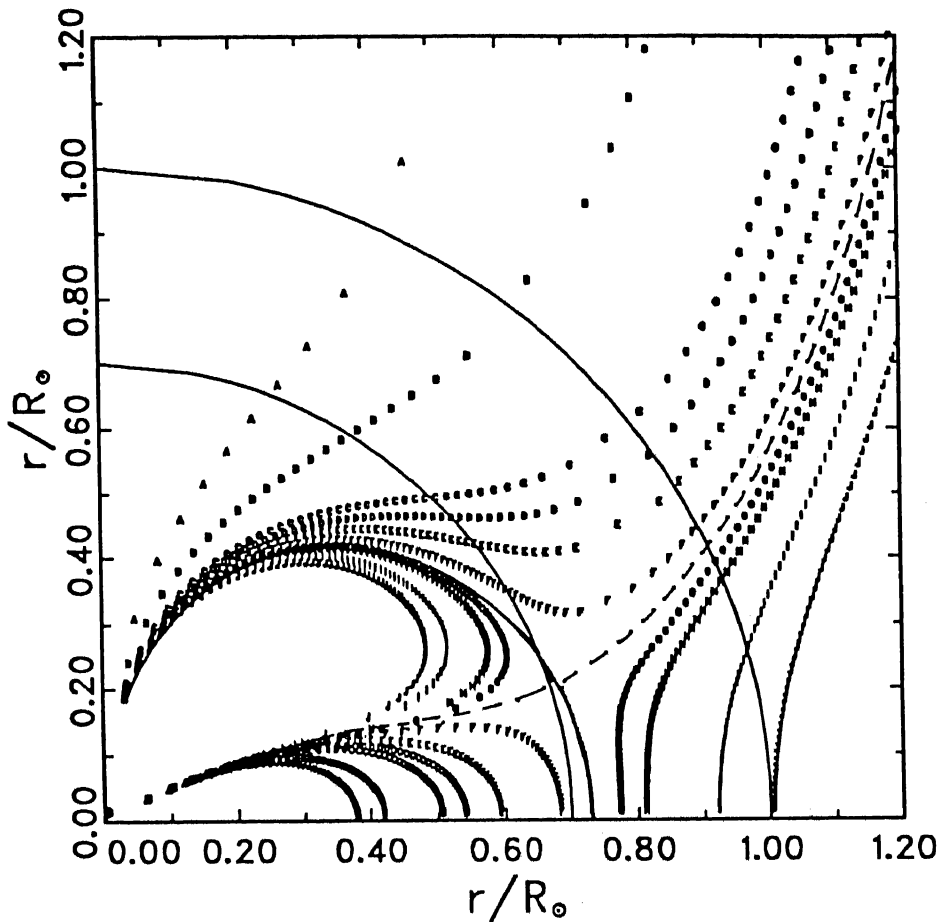


Fig. 3.1.- Structure of the 'steady' part of the poloidal field in one quadrant of a meridional plane as defined by the combination of terms $\ell=1$ and 3 in equation (5) with the 'best estimates' : $\mu_1 = 0.624$ and $\mu_3 = 0.156$ (cf. equation 8). The field lines correspond to flux values A:0.50, B:1.00, C:1.50, D:1.60, E:1.70, F: 1.80, G:1.87, H: 1.90, I: 2.00, J: 2.10, in units of $\pi B_0 R_0^2$. The continuous and the broken lines represent branches of the separatrix S_* defined by $\phi = \phi_* = 1.84$ units. The field directions can be marked relative to that of B_0 , which is presently indeterminate. The field at the surface and that outside is subject to deformation by several processes into observationally unrecognizable patterns.

The field structure also contains a 'separatrix' which has two branches (shown by the thick and dashed lines) intersecting at the neutral point (r_*, ϑ_*) where

$$r_* = 0.71 R_0 \quad \text{and} \quad \vartheta_* = 73^\circ.$$

The revolution of the branch shown by the thick line defines a closed 'critical surface', S_* , running close to the base of the convection zone in latitudes $\leq 45^\circ$.

At S_* , the flux function $\phi(r, \vartheta)$ and the rotation rate $\Omega(r, \vartheta)$ are given by equation (7), along with values of Ω_0 , Ω_1 in the best fit in 'CE', as

$$\phi_* = \phi(r_*, \vartheta_*) \approx 1.84 (\pi B_0 R_0^2) ,$$

and $\Omega_* = \Omega(r_*, \vartheta_*) \approx 450 \text{ nHz} .$

The helioseismological studies referred earlier (Christensen-Dalsgaard & Schou 1988 ; Dziembowski et al 1989 ; Sekii 1989) , suggest that sun's rotation undergoes a transition from an approximately rigid rotation within 'ORC' to a differential rotation within 'CE'. Within 'ORC' the small radial variations in the equatorial plane seem to be time

dependent (Goode & Dziembowski 1991) so that the steady part of equatorial rotation may be uniform.

3.4 A Slow Creation Of Toroidal Magnetic Field Near S_*

3.4.1 The difference between the values of A_C and A_E

All the three helioseismological results of inferred rotation referred in the previous section suggest that the transition from differential rotation to rigid rotation occurs at the base of the convection zone. However, this model suggests at S_* instead of occurring at the base of the convection zone.

Thus the isorotation in the steady state takes the form :

$$(\Omega - \Omega_*) = A(\phi - \phi_*) \quad (9)$$

where 'A' changes to some small value inside S_* from ~ 68 nHz per unit flux outside S_* . This implies a 'discontinuity' in $d\Omega/d\phi$ without a discontinuity in Ω .

From the results of the best fits in 'CE' (Table 3.1) and 'ORC+CE' (Table 3.2), it appears that neither Ω_0 nor A changes significantly across S_* . However, from 'CE' to 'ORC+CE' the estimates of both μ_1 and μ_3 increase significantly by the same

ratio (viz. 7/6). Such a change is not physically meaningful. Mathematically it must be the effect of a change only in the coefficient of the terms in $\mu_1, \mu_3 \dots$, i.e. the coefficient of the terms contributed by the 'internal' sources. Thus it seems necessary to re-write equation (7), separating the terms contributed by the 'internal' and 'external' sources of the field, as :

$$\Omega(r, \vartheta) = \Omega_0 + A_E \phi_E + A_C \phi_C, \quad (10)$$

where,

$$\phi_E = \pi B_o R_o^2 (x^2 \sin^2 \vartheta) \quad (11)$$

and

$$\phi_C = (\pi B_o R_o^2) (2\mu_1 x^{-1} \sin^2 \vartheta + \dots) \quad (12)$$

of $\phi(x, \vartheta)$ correspond to the parts $V_E(r, \vartheta)$ and $V_C(r, \vartheta)$ of the magnetic potential $V(r, \vartheta)$ defined in section 3.2.5. The apparent increase in μ_1, μ_3 can then be understood as a change in A_C alone, by factor $\sim 7/6$, from 'CE' to 'ORC+CE' [In fact, it is this jump in A_C which appears in Table 3.1 as a jump in μ_1, μ_3 owing to the combined effect of the following facts : (i) μ_1, μ_3 were determined only through the products $A_C \mu_1, A_C \mu_3$, (ii) A_C was not distinguished from A_E and (iii) A_E could change only from 68 to 64 nHz per unit flux from 'CE' to 'ORC+CE'].

In view of the high relative accuracy of the data in 'CE', we assume that the true values of μ_1 , μ_3 are as given by the ('best') fit in 'CE' (Table 3.1). Since the values of μ_1 , μ_3 must be continuous across S_* , the value of A_C in 'ORC+CE' must be $\sim 7/6$ times that given by the corresponding best fit in Table 3.1. Thus, in 'ORC+CE', $A_C \sim 75$ nHz per unit flux giving $(A_C - A_E) \sim 7$ nHz per unit flux.

3.4.2 Slow Build up of Toroidal Field near S_* , its Form and Time Scale

Equation (10) can be written as

$$(\Omega - \Omega_*) = A_C(\phi - \phi_*) + (A_E - A_C)(\phi_E - \phi_E^*)$$

The difference between A_C and A_E in the last term implies a slow winding of the 'steady' poloidal field into a toroidal field (B_T) in the neighborhood of S_* . This follows from the law of induction in MHD which takes the following form as a corollary of the form given by Chandrasekhar (1956a) for axisymmetric fields (when the relatively small effects of diffusion and meridional circulation are neglected):

$$\frac{\partial B_T}{\partial t} = \frac{\partial (\Omega, \phi)}{\partial (z, \rho)} = \frac{\partial \Omega}{\partial z} \frac{\partial \phi}{\partial \rho} - \frac{\partial \Omega}{\partial \rho} \frac{\partial \phi}{\partial z}$$

where $z = x R_0 \cos\theta$ and $\rho = x R_0 \sin\theta$.

In the neighborhood of S_* this reduces to :

$$\frac{\partial}{\partial t} \left(\frac{B_T}{B_0} \right) \sim (A_C - A_E) \frac{\partial(\phi_C, \phi_E)}{\partial(z, \rho)}$$

$$\sim -12\pi^2 B_0^2 R_0^2 (A_C - A_E) \mu_1 \sin^3\theta \cos\theta$$

Taking $(A_C - A_E) = 7$ nHz per unit flux, we have

$$\frac{\partial}{\partial t} \left(\frac{B_T}{B_0} \right) \sim (50\pi) \sin^3\theta \cos\theta \quad \text{nHz} \quad . \quad (13)$$

The maximum estimate of this is $\sim 50\pi$ nHz .

Consequently, the time scale of creation of the toroidal field is:

$$\tau_{\text{tor}} \simeq (10^9 / 50\pi) (B_T / B_0) \quad \text{sec} \quad .$$

If $B_T \sim 2 \times 10^6$ G as derived by Goode & Dziembowski(1991), then
 , since $B_0 < 1$ G ,

$$\tau_{\text{tor}} > 3 \times 10^5 \quad \text{yr} \quad .$$

For the meridional circulation effects to be negligible in the present stage of sun's MHD evolution, as assumed by us, τ_{tor} must be $\ll \tau_{\text{mc}}$ (time scale of meridional circulation). If $\tau_{\text{mc}} \sim 10^9$ yr (eg. Zappala 1972), this requires $B_o > 3 \times 10^{-4}$ G.

Finally for τ_{tor} to be less than the age of the sun, (4.5×10^9 yr) one must have :

$$B_o > 10^{-4} \text{ G .}$$

This gives the lower limit on the order of magnitude of B_o .

It is interesting to note that in the low latitudes (which are significant for observations) , the leading term in the ϑ - dependence of the toroidal field created near S_* is \sim 'sin ϑ cos ϑ ' ie. same as that deduced by Dziembowski & Goode (1991).

3.5 Conclusions and Discussion

We have shown in this model that a large-scale steady part of the magnetic field which can be expressed in the form of a potential field given by the terms $\ell = 1$ and $\ell = 3$ in equation (3) can be isorotating with the helioseismologically inferred internal rotation of the sun.

The linear form of equation (1) has served well for modeling the steady part of the poloidal magnetic field . We have repeated the modeling procedure by choosing the exponential form for the relation between Ω and ϕ . However, such a form cannot give a good fit . Thus , with the present accuracy in the rotation data, non-linear terms are not needed.

The best estimates of the strengths of the terms $l=1$ and $l=3$ obtained from 'CE' (Table 3.1), where the uncertainties in Ω are smallest, are given in equation (8).

The field structure presented in Fig.3.1 shows clearly the distinct different patterns in the high ($\geq 30^\circ$) and the low ($< 30^\circ$) latitude zones. This could provide a natural framework for the remarkably different behaviors of the surface fields observed in these zones.

The field structure also shows a clear separation of a part of the flux of the 'steady' field 'trapped' near the sun's center and the other part of the flux which seems to be in the process of diffusing out of the sun, across the convection zone.

We find a small steady deviation from isorotation near the base of the convection zone which winds the ' steady ' poloidal field into a toroidal field . The strength of this field can reach ~ 2 mega gauss in $10^6 - 10^9$ yr, depending upon the value of B_0 .

However, this model has the following drawbacks .

(i) We have assumed in this model that the field is current free in the interior of the sun. This approximation is good only in the convective envelope , where buoyancy and convection play the dominant role in fast disposal of the currents. However, it is not so good in the radiative core. In fact this is evident from Table 3.3 that it is not possible to get a good fit for a current free field in the radiative core, where uncertainties in the coefficients μ_1 , μ_3 , ..are exceeding 100 % .

(ii) The current free fields have the multipole singularities near the center (eg. dipole and hexapole).

Thus , it is necessary to improve the ' preliminary ' model for the realistic magnetic field structures in the sun's interior. We present such a realistic model in the next chapter.

APPENDIX 3.A

Consistency of the ϑ -dependence of the photospheric field in the present model with a unique superposition of the first two characteristic solutions of the diffusion equation for the magnetic fields.

Here we show that the values of μ_1 and μ_3 obtained by us in section 3.3 are such that $\phi(1, \vartheta)$ can be expressed as

$$\phi(1, \vartheta) \equiv \psi_0(1, \vartheta) + \Lambda \psi_2(1, \vartheta) \quad (\text{A1})$$

where ψ_0 and ψ_2 are the first two even-parity characteristic solutions of the diffusion equation given by Chandrasekhar (1956b), and Λ is a constant.

Our model (equations 5 and 8) gives

$$\phi(1, \vartheta) = \alpha_0 + \alpha_2 (\cos^2 \vartheta) + \alpha_4 (\cos^4 \vartheta) \quad (\text{A2})$$

where $\alpha_0 = (1 + 2\mu_1 - \mu_3) = 2.092$, $\alpha_2 = -(1 + 2\mu_1 - 6\mu_3) = -1.312$

and $\alpha_4 = -5\mu_3 = -0.78$.

Using definition of Gegenbauer polynomials, which occur in Chandrasekhar's solution, equation (A1) can be written as

$$\phi(1, \vartheta) \equiv (1 - 3\Lambda/2) + (-1 + 9\Lambda) \cos^2 \vartheta + (-15\Lambda/2) \cos^4 \vartheta. \quad (\text{A3})$$

Equations (A2) and (A3) together require that

$$\frac{-15\Lambda/2}{9\Lambda-1} = \frac{\alpha_4}{\alpha_2} = 0.5945 \quad (\text{A4})$$

and

$$\frac{9\Lambda-1}{1-3\Lambda/2} = \frac{\alpha_2}{\alpha_1} = -0.6272 \quad (\text{A5})$$

It is important to note that (A4) and (A5) yield almost identical values of Λ viz., $\Lambda = 0.0462628$ and 0.0462571 respectively .

Thus for the values of μ_1 and μ_3 obtained in section 3.3.1 , a unique value of Λ exists such that on the photosphere the ϕ dependence of the flux function $\phi(1, \phi)$ can be written in the form (A1) .

This shows that near the photosphere the steady field obtained by assuming a current free form is almost same as that obtainable by assuming it to be in the form of a solution of the diffusion equation with appropriate parity .

CHAPTER IV

' STEADY ' PART OF THE SUN'S INTERNAL MAGNETIC FIELD : IMPROVED MODEL

4.1 Introduction

In the previous chapter , we have developed a preliminary model of the steady part of the sun's magnetic field in the outer radiative core and the convective envelope . This model consists of a 'current-free' field whose field lines isorotate according to the sun's internal rotation as determined from helioseismology (Dziembowki ,Goode & Libbrecht 1989).

However, as pointed out in the previous chapter, current free approximation of the magnetic fields and singularity of these fields at the center are the main drawbacks. Thus, it is necessary to improve the preliminary model with some realistic solution of the basic equations. In this chapter , we present such an improved ' model.

In section 4.2, we show that if the steady part of the field is weak compared to the rotation, then the field must be a solution of the diffusion equation, whose field lines isorotate with the plasma.

We assume that magnetic diffusivity must be uniform and constant with a value represented by a suitable average . In the convective envelope the convection and the magnetic buoyancy lead to fast disposal of the electric currents . Hence, the effective average value of diffusivity in the convective envelope must be several orders of magnitudes higher than the average value of diffusivity in the radiative core . Thus , in the convective envelope, one has to take the limiting form of the solution for the diffusivity tending to infinity. Chandrasekar (1956 b) has given a solution of the diffusion equation in a sphere of uniform and constant diffusivity , which is embedded in a current-free field (section 4.3.1) . We modify Chandrasekar's solution of magnetic diffusion equation by incorporating the boundary condition imposed by the presence of a locally uniform interstellar field. From this solution we obtain the mathematical forms (section 4.3.2) of flux function in the radiative core (Φ_{RC}) and in the convective envelope (Φ_{CE}) respectively .

For improving the earlier model, we take this modified solution and determine the coefficients by least square fitting as in section 4.4.

As in the previous chapter, we assume (section 4.4) a linear relation between the internal rotation Ω and the flux function Φ and express Ω^{RC} (in the radiative core) and Ω^{CE} (in the convective envelope) for the sun's internal rotation $\Omega(r,\theta)$ in terms of the flux functions Φ^{RC} and Φ^{CE} . First we determine the

parameters Ω_0^{CE} and Ω_1^{CE} , and the coefficients in Φ^{CE} by least square fitting Ω^{CE} to the helioseismologically inferred rotation in the convective envelope . From the boundary conditions at the base of the convection zone , we then determine the coefficients in Φ_{RC} . Finally , the parameters Ω_0^{RC} and Ω_1^{RC} in the radiative core are determined by least square fitting the helioseismologically inferred rotation in the radiative core .

In section 4.5, we obtain excellent simultaneous least square fits both in outer radiative core (ORC) and in the convective envelope , for the fields in their respective assumed forms . The resulting field geometry is much simpler and it is free from any singularity, separatrix or closed loops as were present in the previous model .

Even in the improved model , we find that the conclusion of the preliminary model about the presence of a long term non-isorotation in the neighborhood of the convection zone is valid .

We determine (section 4.6) the present values of the relative magnitudes of the first two eigenmodes of diffusion in RC, and their characteristic time scales in terms of the magnetic diffusivity. From these we obtain a crude estimate of the 'initial' (Zero Age Main Sequence) relative strengths of the two diffusion eigenmodes.

In section 4.7 we summarize the important features of the model and discuss their implications.

4.2 Assumptions and the Resulting Form of the Basic Equations

We assume that the magnetic fields and the fluid motions are symmetric about the Sun's rotation axis, and note that on the relevant time scales, the fluid motions can be considered as incompressible. For simplicity the magnetic diffusivity η is assumed to be uniform and constant. Thus the density ρ and the diffusivity η are represented by their suitable averages. In CE, the convection and the magnetic buoyancy leads to fast disposal of the electric currents. Hence the effective average value η_{CE} of η in the convective envelope must be *several orders of magnitudes higher* than the average value η_{RC} in the radiative core.

Following Chandrasekar (1956a), the magnetic field \mathbf{B} and the velocity field \mathbf{v} can be expressed as

$$\mathbf{h} = -\zeta \frac{\partial P}{\partial z} \mathbf{1}_\zeta + (\zeta T) \mathbf{1}_\phi + \zeta^{-1} \frac{\partial(\zeta^2 P)}{\partial \zeta} \mathbf{1}_z \quad (1)$$

$$\mathbf{v} = -\zeta \frac{\partial U}{\partial z} \mathbf{1}_\zeta + (\zeta \Omega) \mathbf{1}_\phi + \zeta^{-1} \frac{\partial(\zeta^2 U)}{\partial \zeta} \mathbf{1}_z \quad (2)$$

where $h = B/(4\pi\rho)^{1/2}$; ρ is the density ; ζ , ϕ and z are the cylindrical polar coordinates with their axis along the axis of solar rotation ; $\mathbf{1}_\zeta$, $\mathbf{1}_\phi$ and $\mathbf{1}_z$ are the corresponding unit vectors ; T, P, Ω and U are scalar functions which are independent of ϕ .

For the reasons given in the preliminary model , we neglect the meridional motions and write Chandrasekar's MHD equations in the form :

$$\eta\Delta_5 P - \frac{\partial P}{\partial t} = 0 , \quad (3)$$

$$\eta\Delta_5 T - \frac{\partial T}{\partial t} = - \zeta^{-1} [\Omega , \zeta^2 P] \quad (4)$$

$$\frac{\partial \Omega}{\partial t} = \zeta^{-3} [\zeta^2 T , \zeta^2 P] \quad (5)$$

$$[\Delta_5 P , \zeta^2 P] = \zeta \frac{\partial}{\partial z} (T^2 - \Omega^2) \quad (6)$$

where for any two functions f and g ,

$$[f , g] = \frac{\partial f}{\partial z} \frac{\partial g}{\partial \zeta} - \frac{\partial f}{\partial \zeta} \frac{\partial g}{\partial z} \quad (7)$$

and

$$\Delta_5 = \frac{\partial^2}{\partial z^2} + \frac{3}{\zeta} \frac{\partial}{\partial \zeta} + \frac{\partial^2}{\partial \zeta^2} \quad (8)$$

Next we assume that the 'steady' part of the poloidal field is very weak compared to the 'steady' part of the rotation and

that the 'steady' part of the toroidal field is weaker than (or at the most of comparable strength to) that of the 'steady' part of rotation. These assumptions are quite reasonable on physical grounds (e.g. Mestel and Weiss, 1987; Spruit, 1990) .

Equation (4) itself can then be written, to the first approximation, a:

$$[\Omega, \zeta^2 P] = 0 \quad (9)$$

which is same as

$$\Omega = \text{function}(\Phi) \quad (9)$$

where

$$\Phi(\zeta, z) = \zeta^2 P(\zeta, z) \quad (10)$$

is the flux function representing the flux of the poloidal field through the circle of axi-symmetry passing through (ζ, z) .

Physically this means that in the lowest order the plasma rotation imposes isorotation on the poloidal field. In the next order the small deviation from isorotation will produce a time-dependent part of the toroidal field.

Thus the 'steady' (slowly varying) part of the Sun's internal poloidal field must satisfy diffusion equation (3), [with $\eta = \eta_{RC}$ in the radiative core and $\eta = \eta_{CE}$ ($\gg \eta_{RC}$) in the convective envelope], and must also satisfy isorotation, (viz. equation 9).

4.3 Solution of Equation (3)

4.3.1 Chandrasekhar's Solution of the Diffusion Equation

Chandrasekhar (1956b) has given a solution of the diffusion equation (3), in a sphere of radius R_c of uniform and constant diffusivity η , which is embedded in a current-free field in the form :

$$P(r, \vartheta, t) = \mathcal{P}(x, \mu) \exp(-t/\tau) \quad (11)$$

where $x = r/R_c$, $\mu = \cos\vartheta$, r and ϑ being the radial distance and co-latitude of a point, and $\mathcal{P}(x, \mu)$ is a solution of :

$$\Delta_S \mathcal{P} + (\eta\tau)^{-1} \mathcal{P} = 0, \quad \text{in } x \leq 1, \quad (12 \text{ A})$$

and

$$\Delta_S \mathcal{P} = 0 \quad \text{in } x > 1. \quad (12 \text{ B})$$

The solution of equation (12 A) which is finite at origin has the form :

$$\mathcal{P}_n(x, \mu) = x^{-3/2} J_{n+3/2}(\alpha_n x) C_n^{3/2}(\mu)$$

$$\text{for } x \leq 1 \quad (13 \text{ A})$$

and the solution of (12 B) which vanishes as $x \rightarrow \infty$ has the form :

$$\mathcal{P}_n(x, \mu) = x^{-(n+3)} C_n^{3/2}(\mu)$$

$$\text{for } x > 1 \quad (13 \text{ B})$$

where n is any non-negative integer, τ has value $\tau_n = R_c^2 / \eta \alpha_n^2$, $C_n^{3/2}(\mu)$ is Gegenbauer's polynomial of degree n , and $J_{n+3/2}$ represents Bessel function of order $n+3/2$.

Hence the solution of equation (11) is

$$P(r, \vartheta, t) = \sum_{n=0}^{\infty} A_n x^{-3/2} J_{n+3/2}(\alpha_n x) C_n^{3/2}(\mu) \exp(-t/\tau)$$

$$\text{for } x \leq 1 \quad (14 \text{ A})$$

and

$$P(r, \vartheta, t) = \sum_{n=0}^{\infty} M_n x^{-(n+3)} C_n^{3/2}(\mu) \exp(-t/\tau)$$

$$\text{for } x > 1 \quad (14 \text{ B})$$

where the values of α_n , and the coefficients A_n and M_n are to be determined using the boundary conditions.

4.3.2 Modification for Large Diffusivity in CE and Asymptotically Uniform Field at Large Distances

For modeling the 'steady' (slowly varying) part of the poloidal field in RC and CE we adopt the above solution with R_c as the RC-CE boundary (*i.e.* with $R_c = 0.7 R_0$). This is possible because $\eta_{CE} \gg \eta_{RC}$ (section 4.2) and equation (12 B) is the limiting form of equation (12 A) in the limit $\eta \rightarrow \infty$.

However, here we introduce the following important modification. In the solution (13 B) of equation (12B) the terms with positive powers of x were dropped for ensuring that the field vanishes as $x \rightarrow \infty$. However, the Sun's poloidal field must merge with the interstellar field at large distances which is non-zero and which can be considered as uniform on scales of the solar system. Hence on the right side of (13 B), we introduce a term B_0 corresponding to a uniform field. Moreover, we assume that the field has odd north-south parity (which allows \mathcal{P}_n only with even values of n). Thus, we modify equations (13 A,B) as

$$\mathcal{P}_n(x, \mu) = x^{-3/2} \sum_{\substack{n=0 \\ \text{(even)}}}^{\infty} A_n J_{n+3/2}(\alpha_n x) C_n^{3/2}(\mu) \quad \text{for } x \leq 1 \quad (15)$$

and

$$= B_0 C_0^{3/2}(\mu) + \sum_{\substack{n=0 \\ \text{(even)}}}^{\infty} M_n x^{-(n+3)} C_n^{3/2}(\mu) \quad \text{for } x > 1 \quad (16)$$

These solutions give the following forms for the magnetic flux functions in the radiative core and in the convective envelope :

$$\Phi_{RC}(x, \vartheta) = 2 \pi A_0 R_c^2 x^{1/2} \sin^2 \vartheta \sum_{\substack{n=0 \\ \text{(even)}}}^{\infty} \lambda_n J_{n+3/2}(\alpha_n x) C_n^{3/2}(\mu) \quad (17)$$

where A_0 is taken as a scale factor for the field, $\lambda_n = A_n/A_0$, and

$$\Phi_{CE}(x, \vartheta) = \pi B_0 R_c^2 \sin^2 \vartheta \left\{ x^2 C_0^{3/2}(\mu) + \sum_{\substack{n \geq 0 \\ \text{even}}} \hat{\mu}_{n+1} x^{-(n+1)} C_n^{3/2}(\mu) \right\}, \quad \dots \dots \dots (18)$$

where $\hat{\mu}_{n+1} = M_n / (\pi B_0 R_c^{n+3})$ are strengths of the central multipoles. Equation (18) can be re-written in a form similar to that of Φ_{CE} in the previous chapter , as follows :

$$\begin{aligned} \Phi_{CE}(x, \theta) = \pi B_0 R_c^2 \{ & (x^2 + 2\mu_1 x^{-1} + 4\mu_3 x^{-3} + \dots) \sin^2 \theta \\ & + (-5\mu_3 x^{-3} + \dots) \sin^4 \theta + \dots \} , \end{aligned} \quad (19)$$

$$\text{where } \mu_1 = \hat{\mu}_1 / 2 , \quad \mu_3 = 3/2 \hat{\mu}_3 \quad (19A)$$

It may be noted that here the magnetic field is not current free even in CE though the poloidal part of this field is same as that of the current free field of chapter III. (The field here has a non zero toroidal component)

4.3.3 The Boundary Conditions

At $x = 1$, i.e. $r = R_c$, the flux function $\Phi(x, \theta)$ and the radial component B_r of the magnetic field must be continuous. Following Chandrasekhar's (1956b) method, with the modification necessitated by the presence of the uniform field term in Φ_{CE} , the boundary conditions can be reduced to the following pairs of equations for each value of n .

For $n = 0$:

$$A_0 J_{3/2}(\alpha_0) = (1 + \hat{\mu}_1) B_0$$

and

$$A_0 [1/2 J_{3/2}(\alpha_0) + \alpha_0 J'_{3/2}(\alpha_0)] = (2 - \hat{\mu}_1) B_0$$

where $J_n'(x) = (d/dx) J_n(x)$. These two equations give :

$$3J_{3/2}(\alpha_0)/\alpha_0 J_{1/2}(\alpha_0) = (1 + \hat{\mu}_1) \quad (20)$$

and
$$A_0 = 3B_0/\alpha_0 J_{1/2}(\alpha_0) \quad (21)$$

For $n = 2$:

$$A_2 J_{7/2}(\alpha_2) = \hat{\mu}_3 B_0$$

$$A_2 [1/2 J_{7/2}(\alpha_2) + \alpha_2 J_{7/2}'(\alpha_2)] = -3\hat{\mu}_3 B_0$$

These give :

$$J_{5/2}(\alpha_2) = 0 \quad (22)$$

and
$$A_2 = \hat{\mu}_3 B_0 / J_{7/2}(\alpha_2) \quad (23)$$

4.4 Evaluation of the Coefficients Using Equation (9)

4.4.1 The Data and the Method

The 'data' used here is same as that used in the preliminary model , viz. the values of the angular velocity of the Sun's

internal rotation as determined by Dziembowski *et al* (1989), with uncertainties as quoted by Christensen-Dalsgaard & Schou (1988). The method of analysis is also somewhat similar. As in chapter III, the law of isorotation (equation 9) is assumed to be linear and written in the form :

$$\Omega_{\text{mod}}(x, \vartheta) = \Omega_0 + \Omega_1 \Phi(x, \vartheta) \quad , \quad (24)$$

and the parameter Ω_0 and the products of the coefficient ' Ω_1 ' with the coefficients in $\Phi(x, \vartheta)$ are determined by least square fitting $\Omega_{\text{mod}}(x, \vartheta)$ to the helioseismologically determined plasma rotation $\Omega_{\text{obs}}(x, \vartheta)$. The difference is in the assumptions about the fields in RC and in CE that yield different forms for $\Phi(x, \vartheta)$, and in the order in which the various parameters are determined.

Since the forms of $\Phi(x, \vartheta)$ as well as the levels of uncertainties in Ω_{obs} are different in CE and in ORC, we write equation (24) separately in CE and ORC as :

$$\Omega_{\text{mod}}^{\text{CE}}(x, \vartheta) = \Omega_0^{\text{CE}} + \Omega_1^{\text{CE}} \Phi_{\text{CE}}(x, \vartheta) \quad (25)$$

and

$$\Omega_{\text{mod}}^{\text{ORC}}(x, \vartheta) = \Omega_0^{\text{ORC}} + \Omega_1^{\text{ORC}} \Phi_{\text{RC}}(x, \vartheta) \quad ,$$

where Φ_{RC} and Φ_{CE} represent the flux functions in RC and CE given in equations (17) and (18) respectively.

As in the previous chapter , we define a dimensionless

rotation $\omega_{\text{obs}}(x, \vartheta)$ as

$$\omega_{\text{obs}}(x, \vartheta) = [\Omega_{\text{obs}}(x, \vartheta) - \hat{\Omega}] / \sigma_{\Omega_{\text{obs}}}$$

where $\hat{\Omega}$ is the mean and $\sigma_{\Omega_{\text{obs}}}$ is the standard deviation in the set of the values of $\Omega_{\text{obs}}(x, \vartheta)$ used. However, instead of determining $\hat{\Omega}$ and $\sigma_{\Omega_{\text{obs}}}$ separately in ORC and CE, here we have determined these for the combined data from ORC and CE.

We then fit $\omega_{\text{obs}}(x, \vartheta)$ in CE and ORC to the forms :

$$\omega_{\text{mod}}^{\text{CE}}(x, \vartheta) = \omega_0^{\text{CE}} + a^{\text{CE}} \Phi_{\text{CE}}(x, \vartheta) \quad (26 \text{ A})$$

and
$$\omega_{\text{mod}}^{\text{ORC}}(x, \vartheta) = \omega_0^{\text{ORC}} + a^{\text{ORC}} \Phi_{\text{RC}}(x, \vartheta) \quad (26 \text{ B})$$

4.4.2 Procedure for determining the 'Steady' Parts of the Rotation and the Poloidal Field

As before, the uniform field at the large distances, B_0 is essentially a scaling factor for the Sun's field. Hence we choose

$$B_0 = 1 \quad \text{'unit'}$$

The uncertainties in $\Omega_{\text{obs}}^{\text{CE}}$ are much smaller than those in $\Omega_{\text{obs}}^{\text{RC}}$. Hence, the parameters $\Omega_0^{\text{CE}} (= \hat{\Omega} + \omega_0^{\text{CE}} \sigma_{\text{obs}})$, $\Omega_1^{\text{CE}} (= \pi B_0 R_c^2 a^{\text{CE}} \sigma_{\text{obs}})$, $\hat{\mu}_1$ and $\hat{\mu}_3$ for 'steady' parts of rotation and

magnetic field in CE are computed first by *least-square fitting* of $\omega_{\text{mod}}^{\text{CE}}(x, \mu)$ to $\omega_{\text{obs}}^{\text{CE}}(x, \mu)$. As shown in the preliminary model, a two term fit is the best fit in CE (i.e., it is not enough to take only the first term in Φ_{CE} and there is no gain in including the third term). The goodness of the fit and the uncertainties in the parameters are also computed in the same way as in the previous chapter.

The parameters α_0 , A_0 , α_2 and A_2 must then be determined using the boundary conditions. Equation (20) gives a single positive value of α_0 . Equation (22) gives a series of positive values $\alpha_{2,i}$ ($i = 1, 2, 3, \dots$). Equations (21) and (23) are used to determine the values of the parameters A_0 and $A_{2,i}$ corresponding to $\alpha_{2,i}$, $i = 1, 2, 3, \dots$ etc.

Lastly the parameters $\Omega_0^{\text{ORC}} (= \hat{\Omega} + \omega_0^{\text{ORC}} \sigma_{\text{obs}})$ and $\Omega_1^{\text{ORC}} (= \pi B_{\text{c}}^2 R_{\text{c}}^2 a_{\text{obs}}^{\text{ORC}} \sigma_{\text{obs}})$ are determined by fitting $\omega_{\text{mod}}^{\text{ORC}}(x, \mu)$ to $\omega_{\text{obs}}^{\text{ORC}}(x, \mu)$.

4.5 The Model for the ' Steady ' Parts of

Rotation and Poloidal Magnetic Field

4.5.1 The ' Steady ' Parts of Rotation and Poloidal Field in CE

The above mentioned computations yield the following results for the 'steady' part of the field in CE :

$$\hat{\mu}_1 = 3.638 \pm 0.212 ,$$

(27)

$$\hat{\mu}_3 = 0.621 \pm 0.063 .$$

Here we note that this value of $\hat{\mu}_1$ is exactly equal to $\hat{\mu}_1$ and $\hat{\mu}_3$ is almost exactly equal to $\hat{\mu}_3$, where $\hat{\mu}_1$, $\hat{\mu}_3$ are the values obtained from the values of μ_1 and μ_3 determined in previous chapter of $\hat{\mu}_1$, $\hat{\mu}_3$ by inverting the relations (19A). This confirms once again that the field in CE is almost current-free up to the accuracy of $\Omega_{\text{obs}}^{\text{CE}}$.

For the 'steady' part of the rotation in CE we obtain :

$$\Omega_0^{\text{CE}} = 325.9 \pm 4.1 \text{ nHz} ,$$

(28)

$$\Omega_1^{\text{CE}} = 33.2 \pm 1.9 \text{ nHz/unit flux}$$

The corresponding χ^2 is = 42.95 and the *confidence for goodness of fit* is = 99.9943 %.

Table 4.1

RESULTS OF THE LEAST-SQUARES FITS FOR $\alpha_0 = 2.904, A_0 = 9.374$ WITH THE FIRST FEW VALUES OF α_2 AND THE CORRESPONDING VALUES OF A_2 HERE $\Delta\Omega$ AND $\Delta\Omega$ ARE THE UNCERTAINTIES IN Ω AND Ω RESPECTIVELY

VALUES OF α_2	A_2	Ω_0 (nHz)	$\Delta\Omega_0$ (nHz)	Ω_1 nHZ unit flux	$\frac{\Delta\Omega_1}{\Omega_1}$	χ^2
5.763	1.955	450	5.0	-3.89	0.17	11.58
9.095	-2.389	439	3.0	-0.31	0.16	13.51
12.32	2.754	437	2.4	0.11	0.18	13.69
15.51	-3.079	434	1.8	0.98	0.16	13.93

4.5.2 The 'Steady' Parts of Rotation and Poloidal Field in ORC

With the value of $\hat{\mu}_1$ given in (27), equations (20) and (21) yield unique values $\alpha_0 = 2.904$ and $A_0 = 9.374$. On the contrary, equation (22) has many roots, and the corresponding values of A_2 are given by (23). For different values of α_2 and the corresponding values of A_2 , the least square fits of $\Omega_{\text{mod}}^{\text{ORC}}$ to $\Omega_{\text{obs}}^{\text{ORC}}$ yield the results given in Table 4.1.

According to Table 4.1, the different values of α_2 yield very low value of χ^2 (all with probabilities $< 10^{-7}$), the smallest being given by the smallest positive root $\alpha_{2,1}$ of α_2 . The differences between the values of χ^2 are so small that the significance of these differences cannot be estimated. However, this is mainly because of the large uncertainties in Ω_{obs} near the rotation axis, where the polynomials $C_n^{3/2}(\mu)$ have the largest amplitudes. Hence the difficulty can be avoided by rewriting Φ_{RC} and Φ_{CE} in terms of $\sin^2\vartheta$ and $\sin^4\vartheta$ (since $\sin\vartheta$ has large values near the equator where helioseismic data is more reliable). When this is done and the condition of continuity of magnetic flux is re-checked, we find that the continuity condition is satisfied only by the *smallest* value of α_2 viz., 5.763.

Hence the corresponding parameters for the 'steady' part of the field and the rotation are :

$$\alpha_0 = 2.904, \Lambda_0 = 9.374, \alpha_2 = 5.763, \Lambda_2 = 1.955, \quad (29)$$

and

$$\Omega_0^{\text{ORC}} = 450.2 \pm 5.0 \text{ nHz},$$

(30)

$$\Omega_1^{\text{ORC}} = -3.9 \pm 0.6 \text{ nHz/unit flux.}$$

4.5.3 The Geometrical Structure of the Field

The field lines of the field given by equations (17) and (18) in the region $0.0 \leq r/R_0 \leq 1.0$ are plotted in Fig 4.1. In CE ($0.7 \leq r/R_0 \leq 1$) the field structure is similar to that of the field in the preliminary model. However in RC it is entirely different. It is interesting to note that, in this model the field in RC is much simpler than the preliminary model: it has *no closed loops*, and *no singularity* (see equation 17).

4.5.4 The Slow Field Winding at the ORC-CE Boundary and Its Time Scales

Equations (26) yield different values for the angular velocity Ω on the two sides of the ORC-CE boundary, suggesting a steep radial gradient across the boundary. In the present model, the values of $[\Omega]$ i.e. the apparent 'jump' in Ω defined by

$$[\Omega] = \left\{ \Omega_{\text{mod}}^{\text{ORC}}(1, \theta) - \Omega_{\text{mod}}^{\text{CE}}(1, \theta) \right\},$$

vary from ~ 125 nHz at $\theta = 10^\circ$ to ~ 50 nHz at $\theta = 90^\circ$.

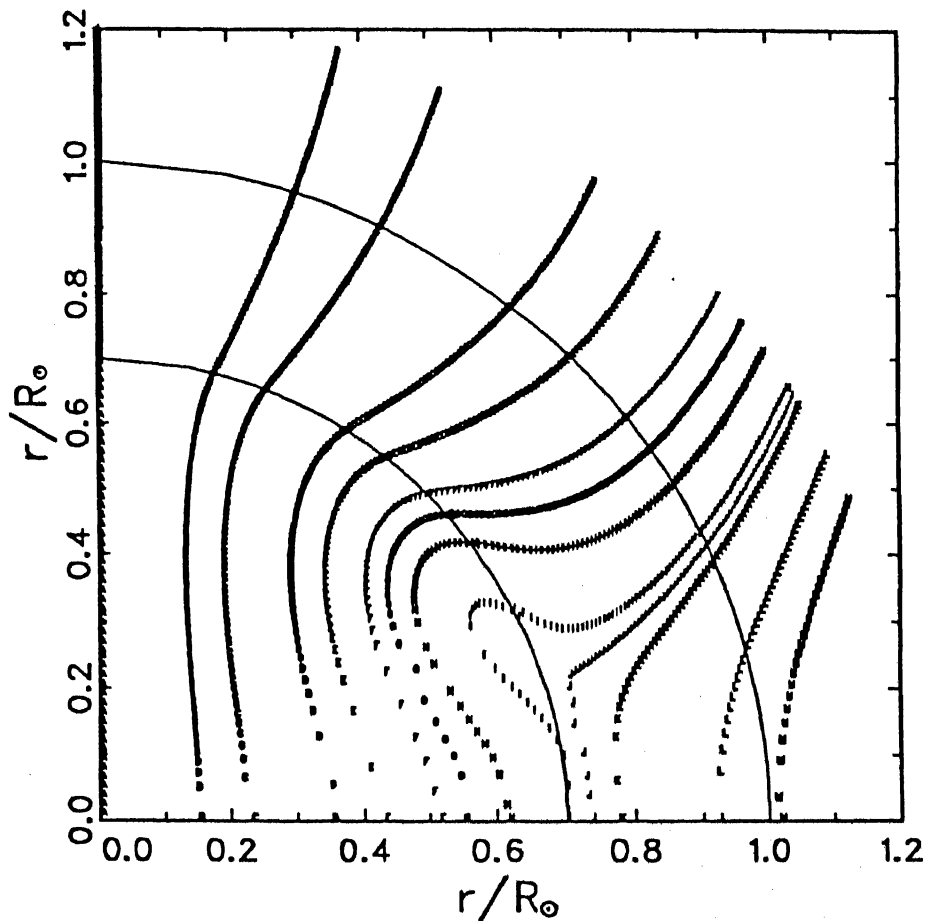


Fig 4.1.- Structure of the " steady " part of the magnetic field as given by flux functions (17) and (18) with values of parameters given in equations (27) and (29). The field line correspond to flux values A : 0.0, B : 0.51, C : 1.02, D : 2.04, E : 2.55, F : 3.06, G : 3.27, H : 3.47, I : 3.71, J : 3.76, K : 3.82, L : 4.08, M : 4.29, in units of $\pi B_0 R_c^2$.

How much of the 'jump' $[\Omega]$ is time dependent (varying on short time scales) and how much is 'steady' (varying on long time scales) is not known at present. If a substantial part of this $[\Omega]$ is sufficiently long lived then the time scale τ_ϕ of field winding will be given by :

$$\tau_\phi = |B_\phi| / \{ |B_p| [\Omega] \}$$

where, $|B_\phi|$ is the strength of the long lived part of the toroidal field and $|B_p|$ is the strength of the poloidal field at the point considered. The values of $|B_p|$ at $r = R_c$ (ie. at ORC-CE boundary) range from $\sim 36B_0$ at $\vartheta = 10^\circ$ to $\sim 6B_0$ at 90° (equator).

If $B_\phi \sim 10^6$ G, (e.g. as estimated by Dziembowski & Goode, 1991), and $B_0 \sim 10^{-2}$ G as suggested from Alfvén travel time calculations along the part of the steady field (cf, in chapter V), the time scales of winding range from $\sim 10^7$ yr in the polar regions to $\sim 10^8$ yr in the neighborhood of the equator.

4.5.5 The Form of the 'steady' Part of the Toroidal Field

To the order of the present approximation in which the dominant term viz. $[\Omega, \zeta^2 P]$ in equation (4) is equated to zero, equations (3) and (4) will both have the same form. Hence the function $T(r, \vartheta, t)$ describing the slowly varying toroidal field

will also have the form similar to that of P in equation (11),
e.g.

$$T(r, \theta, t) = \mathcal{T}(x, \mu) \exp(-t/\tau)$$

with \mathcal{T} given by equation similar to (13 A), *except* in the spherical shell near $r = R_c$ across which the 'jump' $[\Omega]$ occurs. Within this shell \mathcal{T} will be given by the equation

$$\Delta_s \mathcal{T} + (\eta\tau)^{-1} \mathcal{T} = -\zeta^{-1}[\Omega, \zeta^2 \mathcal{P}_n]$$

subject to the boundary conditions at the boundaries of the shell. However, details of such a solution remain to be worked out.

4.6 Estimation of Diffusion Time Scales and the ' Initial ' Amplitudes of Diffusion Eigenmodes

From the values of α_0 and α_2 obtained in section 4.5.2, we estimate the diffusion time scales for the two terms in (17) as :

$$\tau_0 = R_c^2 / (\eta_{RC} \alpha_0^2) \approx 10.6 \text{ billion yr}$$

$$\tau_2 = R_c^2 / (\eta_{RC} \alpha_2^2) \approx 2.7 \text{ billion yr}$$

taking $\eta_{RC} = 35 \text{ cm}^2 \text{ s}^{-1}$ in the radiative core.

This enables us to estimate the ratio of the 'initial' (ZAMS) relative amplitudes of these two terms A_2^* and A_0^* as :

$$\frac{A_2^*}{A_0^*} = \frac{A_2}{A_0} \exp \{ \eta_{RC} [\alpha_2^2 - \alpha_0^2] t / R_c^2 \}$$

$$\approx 0.276$$

where 't' is the present epoch.

4.7 Conclusions and Discussion

Compared to the preliminary model of the steady part of the poloidal magnetic field in the sun's interior, the present model incorporates important improvements in the following respects. (i) The field structure of this model is much simpler. Unlike the preliminary model, it is free from central singularity, separatrix or closed loops. (ii) In the outer radiative core the field lines in this model have a much better fit with the helio-seismologically inferred isorotation contours.

The opposite signs of Ω_1^{ORC} and Ω_1^{CE} suggest that the rotation and the field in the radiative core and the convective envelope evolve separately in separate frames of rotation,

rotating with angular velocities Ω_0^{ORC} and Ω_0^{CE} respectively.

With the present accuracy of sun's internal rotational data (the latitude dependence in which is known only up to $\sin^4 \theta$), as in the preliminary model, we have determined only the leading two terms in the magnetic flux function in the radiative core .

The determination of A_2^*/A_0^* will provide a good starting point for studying the complexity of the 'initial' (ZAMS) configuration of the magnetic field . The field diffusion may be modified by the possible presence of MHD oscillations throughout the evolution of the field and the rotation .

From the observed low degree rotational splittings , one can determine the rotation near the solar core . Presently, observed low degree rotational splittings have poor signal to noise ratio. It is extremely difficult to resolve the splittings of low degree modes (Palle et.al. 1990; Hill et.al. 1990; Toutain and Frollich 1992) and leads to uncertainty in the determination of angular velocity near the sun's interior. Thus, it is of considerable interest to know the rotation in the inner radiative core. In fact, since this improved model has no singularity at the center , it enables us to draw inferences about the core rotation. The present model suggests that the rotation near the center is uniform, with angular velocity $\Omega_0 = 450$ nHz. Note

that the estimated value of core rotation is similar to that of the value derived by $\ell = 1$ degree rotational splitting (Loudagh et.al. 1993; Toutain and Kosovichev, 1994).

In this improved model , we have obtained the relative magnitudes of the first two eigen modes of the diffusion in ORC to be ~ 10.6 billion yr and ~ 2.7 billion yr respectively . We also obtain a crude estimate of the ' initial' (zero Age Main Sequence) relative strengths of the two diffusion eigen modes to be in the ratio of 4 : 1 .

By satisfying the continuity of the radial component of the steady part of the magnetic field at the common boundary , the field lines in each region isorotate with the plasma rotation given by helioseismology. In an independent calculation, we have found that if the values of A_0 and A_2 are determined by least square fit without using the boundary conditions , then the fit is not so good . Thus the Sun seems to have " preferred to satisfy the boundary conditions " . This strongly suggests that the computed fields are realistic .

The steady part of the sun's internal magnetic field from the improved model gives a very good least square fit with the helioseismologically inferred rotation. The sun's inferred internal rotational data has large uncertainties in high

heliographic latitudes and near the rotation axis. Thus for further refinements of the model, more accurate data will be needed in those regions .

It is very difficult observationally to detect the 'steady' part of the solar magnetic field for the following reasons . The first order perturbations, if excited as MHD waves in the central regions , will grow as they approach the surface. Their interferences may create very strong field . Convective flows may introduce further complications in the convection zone. Moreover , non-axisymmetry of the perturbations, formation of flux tubes and eruption of toroidal flux by magnetic buoyancy will create strong noise in the magnetic field at the surface. Consequently , one expects considerable difficulties in detecting such a 'steady' field at and above the photosphere .

In chapter III (section 3.4.2), we have only given the limits on B_0 . It is difficult to determine its value observationally . However, long term space observations at high heliographic latitudes will be needed to detect the steady part of the field if it is there. It might also be detected and determined as 'd.c.' components in the spherical harmonic Fourier analysis of a long enough time series (i.e much longer than 22 yrs) of the magnetograms with high sensitivity. From the fourier analysis of 33 years of the full disk magnetogram data , Stenflo (1993) has set 0.1 G as an upper limit on the average strength of the dipole

component of the steady field .

On MHD time scales, the MHD perturbations convert rotational energy into magnetic energy . Together with the other 'activity generating ' processes such as flux tube formations, magnetic buoyancy etc, the MHD waves can provide a non-radiative mechanism of transport of energy , magnetic flux , and momentum . The leakage of waves across the surface may contribute similar transport outside the sun also.

The uncertainties in the computed coefficients will be smaller if one determines the internal rotation and the coefficients of steady magnetic field simultaneously and directly from the observed rotational splittings of acoustic frequencies .

Such determination in all phases of the solar magnetic cycle will lead to better understanding of properties of the steady as well as the time-dependent part of the sun's internal magnetic field .

TORSIONAL MHD OSCILLATIONS

5.1. Introduction

As mentioned in chapter I, there are two schools of studies for modeling the solar magnetic and the solar activity cycles which lead to two types of models : the turbulent ' dynamo ' models and the ' MHD oscillations ' models.

In section 5.2 of this chapter we describe the basic ideas in these two types of models. We also describe the difficulties and questions arising in each and explain why it is necessary and worth while to examine in further detail the possibility pointed out in chapter II that *solar activity and magnetic cycle may be due to MHD torsional oscillation(/s) of the Sun.* This is done in section 5.3 to 5.5 in the following way.

In section 5.3, the basic physics of torsional oscillations is briefly explained.

We recall here that the SHF analysis of sun's inferred magnetic field (chapter II) shows that all the axisymmetric LF terms with odd values for the spherical harmonic degree ' l ' have nearly same dominant periodicity (\sim 22 year). If these terms represent global MHD oscillations then the Alfvén wave travel times along different field lines of steady axisymmetric field should be independent of the latitudes of the photospheric

intersections. In order to get an idea as to what type of steady field structure can satisfy this condition, we have computed in section 5.4, the Alfvén wave travel times along the field lines in the following five models for the steady part of the field. The first three of these five models are ad-hoc. In the first model, the field is taken to be uniform and in the second it is assumed to be a dipole field. In the third model, the field is taken to be a combination of uniform field and a dipole field. The fourth and the fifth models are the models of the 'steady' part of the internal field determined in chapters III and IV respectively. The last two models give the smallest spread in the values of Alfvén wave travel times along their field lines.

In order to investigate if in the helioseismologically determined internal rotation of the sun, there is any indication of existence of torsional MHD oscillations, we study in section 5.5 the 'residual rotation' (viz., the difference between the observed and the modeled values of rotation). The 'residual rotation' may in fact represent the time-dependent part of rotation. We find that in this residual rotation there exist *systematic large-scale torsional patterns* representing fast and slow rotational velocity bands in the sun's interior. From these we have also estimated the possible order of the radial wavelength, the latitudinal wavelength, and the order of amplitude of angular velocity in these rotational perturbations. From the least square fits of the radial integral of the residual rotation over $(0.4R_{\odot} - 1.0R_{\odot})$, to linear combinations of even

degree Legendre polynomials, we find that ' $l = 4$ ' and ' $l = 2$ ' are the dominant modes in the rotational perturbation.

In section 5.6 , we summarize the conclusions of sections 5.3-5.5 and discuss their implications.

5.2 Theoretical Models of Solar Magnetic Cycle

5.2.1 Theory of Dynamo Mechanisms

In the Sun, the time scale of global magnetic diffusion is ~ of billion years, i.e., larger than the Sun,s age. Hence the Sun is expected to retain some of its primordial magnetic field, which would vary on time scales much larger than the dynamical time scales. Thus it would be easy to understand the existence of the Sun's magnetic field , if it were found to be steady with time.

However, the large-scale field observed at surface varies in a cyclic manner with time scales of ~ decades. Thus, one has to seek the explanation not only for the maintenance of Sun's magnetic field but also for it's periodic behavior. This would essentially require the presence of a dynamo mechanism in the Sun.

Basically, a dynamo mechanism maintains electromagnetic field against dissipation at the cost of energy provided by some source.

The dynamo theories are of two kinds : *kinematic dynamo theory*, in which velocity is specified and the evolution of magnetic field follows in accordance with the induction equation

alone ; and *hydromagnetic dynamo theory*, in which both the velocity and the magnetic fields are obtained as a solution of the MHD equations (induction equations and dynamical equations) .

These theories are based on the fact that moving conductors generate electric currents due to electromagnetic induction. It is therefore expected that in the Sun the flows like rotation and convection could provide dynamo action through electromagnetic induction.

However, all the velocity fields cannot maintain the dynamo. For example, according to Cowling's (1934) theorem, steady axisymmetric magnetic fields cannot be maintained by axisymmetric flows. Thus the dynamos for sun-like stars ought to be either non-axisymmetric or non-stationary (or both) .

The 'Turbulent Dynamo Mechanism' (Mean Field Electrodynamics)

In the theory of turbulent dynamo mechanism, the dynamo effect is statistically averaged over the turbulent flows . In the basic treatment of this mechanism, called 'mean field electrodynamics' , the velocity u and magnetic field B are expressed as sums of mean part (which is large-scale and slowly varying) and fluctuating parts (small scale and rapidly varying) as follows :

$$u = \langle u \rangle + u' \tag{1}$$

$$B = \langle B \rangle + B'$$

where $\langle u \rangle$ and $\langle B \rangle$ are representing the 'mean' parts of u and B .

The turbulent motion u' is assumed to have a correlation time τ and correlation length ' l ' small compared with the time scale ' t ' and length ' L ' of variation of $\langle u \rangle$ and $\langle B \rangle$. Using these expressions for u and B in the induction equation give two equations : one for the variation of mean field $\langle B \rangle$ and the other for that of the fluctuating field B' . These two equations are highly non linear and difficult to solve, and are linearized with the following assumptions.

(a) It is supposed that the mean field $\langle B \rangle$ varies very slowly with time.

(b) The turbulent velocity field u' is assumed to have zero mean (i.e., $\overline{u'} = 0$).

(c) The correlation time τ is assumed to be small compared with the time scale of electromagnetic diffusion.

(d) In computation of $\langle u' \times B' \rangle$, the terms quadratic in u' are neglected. This means that turbulent velocities are assumed to be small.

(e) The fluctuating magnetic fields B' are assumed to have small magnitudes compared to the mean magnetic field $\langle B \rangle$. This assumption enables one to neglect the term $(u' \times B' - \langle u' \times B' \rangle)$ in the fluctuating part of the magnetic induction. (This is the " first order smoothing approximation " : FOSA) .

(f) Finally, it is assumed that the turbulent velocity field is assumed to be isotropic.

Finally, the equation governing the average magnetic field takes the form :

$$\frac{\partial \langle \mathbf{B} \rangle}{\partial t} = \text{curl} \left[\alpha \langle \mathbf{B} \rangle + \langle \mathbf{u} \rangle \times \langle \mathbf{B} \rangle \right] - \text{curl} \left[(\eta + \beta) \text{curl} \langle \mathbf{B} \rangle \right] , \quad (2)$$

where α is the helicity , β is diffusivity due to the turbulence, and η is the electromagnetic diffusion. The first bracket in the right hand side represents the effective 'dynamo' action. The first term in the first bracket represents α -effect. The second term represents dissipation and diffusion.

Early Models of Solar Cycle

Initially, a mechanism for the production of sunspots was proposed by Cowling (1953), who suggested that sunspots are eruptions of submerged toroidal fields produced by the differential rotation acting on a weak poloidal field. Subsequently, Parker (1955) proposed that the poloidal field itself is regenerated by the interaction between cyclonic convection and buoyantly rising toroidal flux elements. Incorporating these ideas, Babcock (1961) phenomenologically modeled the solar cycle . Leighton (1964,1969) presented a semi-empirical model of the solar cycle and reproduced the well known butterfly diagram of the sunspots.

Models based on Mean Field Electrodynamics

In these models , the mean field $\langle \mathbf{B} \rangle$ is written in terms of the poloidal component B_p and the toroidal component B_ϕ . This give two equations containing α , β , and η as the free parameters and $\langle \mathbf{u} \rangle = \boldsymbol{\omega} \times \mathbf{r}$ in which $\boldsymbol{\omega}$ is a prescribed form of rotation.

The maintenance of B_p is mainly by α -effect due to the cyclonic turbulence . If the maintenance of B_ϕ is mainly by α -effect , then the model is called α^2 -dynamo model. On the other hand , if it is mainly due to $\langle \mathbf{u} \rangle$ given by rotation then the model is called $\alpha\omega$ -dynamo model. If both are important , the models are called $\alpha^2\omega$ -dynamo model.

By parameterizing the values α , β and assuming the form for $\boldsymbol{\omega}$, one can obtain the periodic solutions. By adopting different assumptions, many properties of the solar cycle and activity phenomena have been reproduced (Parker 1955; Stix 1972; Yoshimura 1978; Krause 1976; Radler 1976).

5.2.2 Difficulties in the Turbulent Dynamo Models

of the Solar Cycle

Though the turbulent dynamo models of the solar cycle reproduced elegantly the properties of the solar cycle phenomenon, these models have the following difficulties.

(i) The ' first order smoothening approximation ' used for the

derivation of the equation (2) is valid only when the fluctuating field is very much smaller than the mean field. This is possible only when (a) the eddy magnetic Reynolds number $R_m \ll 1$, and (b) the correlation time τ , the eddy of length λ , and the r.m.s velocity v are related as $\tau \ll \lambda/v$. In reality, neither of these conditions is valid on the sun where $R_m \gg 1$ and $\tau \simeq \lambda/v$.

(ii) According to Piddington (1971, 1972, 1973) : (a) the concept of turbulence of solar fields is unsound; turbulence may mix magnetic elements but does not destroy large-scale magnetic fields, (b) the field created by eddy motions would be mainly turbulent field, unlike the field that is actually observed, (c) the field created during successive cycles would rise successively to higher levels and the whole field would eventually leave the sun.

(iii) The values of parameters α , β and of the rotational shear ($d\omega/dr$) are either arbitrarily chosen or estimated crudely from the statistical properties of observed motions. There is also a doubt whether the ensemble averages in the theory can be applied to study the observed fields which are space-time averages.

(iv) The cyclic variation of small scale activity structures like ephemeral active regions, x-ray bright points (Martin and Harvey, 1979; Goulub et al, 1979) or the intensity of sunspots (Albregtsen and Maltby 1981) cannot be described by the mean field

turbulent dynamo theories (Schüssler 1982).

(v) Within the frame work of kinematic dynamo models, it is impossible to address the question of limiting amplitude of the generated magnetic flux owing to the linearity of the induction equation. This indicate that kinematic models should include non-linear effects also.

Hydromagnetic dynamo models (Gilman 1983; Glatzmaier 1985; Brandenburg et.al 1989) on the other hand, have modeled in the limit of small magnetic Reynolds number and the magnetic back reaction implied by the Lorentz force is ignored.

By taking into account these effects, recently Vainstein and Cattaneo (1992) showed that the back reaction of the resulting magnetic fields on the motions would eventually lead to the saturation of the dynamo process , thus posing a constraint on the amount of magnetic flux that can be generated by dynamo action. They further argued that in the limit of small diffusivity, only a small amount of magnetic flux will be created by dynamo process, many orders of magnitude less than the observed fluxes .

(vi) One of the basic problems in keeping the dynamo in the convection zone is the buoyant rise of all of the flux on time scales very much smaller than the solar cycle period. This difficulty can be avoided if the dynamo process is operating in a stably stratified region beneath the solar convection zone (Van Ballegooijen 1982; Spiegel and Weiss 1980; Durney et.al. 1990 ;

DeLuca and Gilman 1991). However, as pointed out by DeLuca and Gilman (1991), the process of dynamo mechanism operating beneath the solar convection zone could add some other serious difficulties. For example, how the magnetic flux is injected into the convection zone is a question. Even if it is injected, either convection or buoyancy effects push the flux towards the surface. Detailed interactions between rising flux tubes and convection have yet to be worked out. If the buoyancy is only effect on these flux tubes, these will rise through the convection zone along a trajectory parallel to the rotation axis (Choudhuri and Gilman 1987) instead of travelling in a radial direction.

(vii) Lastly, the crucial difficulty faced by the turbulent dynamo theories is that the radial gradient of rotation inferred from the helioseismological data is opposite to what is needed by the turbulent dynamo theory . The kinematic dynamo theories require that the gradient of internal rotation should increase with depth (i.e., $d\Omega/dr < 0$) in order to reproduce the migration of the sunspot belts from middle latitudes towards the equator. On the contrary, the hydromagnetic dynamo computations show that gradient of the internal rotation decreases with the depth (i.e., $d\Omega/dr > 0$) . In this case, sunspot belts in the model move towards the poles. However, helioseismologically determined rotation shows that , at low latitudes $d\Omega/dr > 0$, while at mid latitudes $d\Omega/dr \approx 0$. In fact, calculations with this form of internal rotation indicate

that the generated 'dynamo modes' do not tend to migrate at all (Levy 1992).

So, in view of the aforementioned difficulties in the formulation of turbulent dynamo mechanisms and the suggestion by LF analysis (in chapter II), one has to reconsider the idea that solar activity and magnetic cycles may be due to oscillations in the presence of a 'steady' magnetic field in the interior of the Sun .

5.2.3 MHD Oscillatory Dynamo Theories

The turbulent dynamo models are elegant , mathematically well developed and they also reproduce many of the observed properties of the solar cycle. However, because of the foregoing difficulties in these models it is important to consider alternative theories for the solar magnetic and activity cycles.

The alternative theory of the solar cycle is based on assumed presence of MHD oscillations . Initially, theories based on this assumption were proposed by Alfven (1943) and by Walen (1949). Later their ideas were revived by many authors (Layzer, *et.al.* 1955; Plumpton and Ferraro 1955; Piddington 1976; Layzer *et.al.* 1979; Vandakurov 1989). The essence of the oscillatory dynamo theory is as follows. In these theories, the observed periodic behavior of the large-scale magnetic field of the sun is viewed as a consequence of MHD oscillation(/s) in the presence of a large-scale internal 'steady' magnetic field. These theories

recognize the fact that most of the observed fields at the surface (including those in the polar regions), are in the form of bipolar regions. Thus these theories treat the problem of 'solar magnetic cycle' as a 'cycle' of toroidal field only. Also, the dominant flow in the sun is that of rotation, and hence field is toroidal. Thus the MHD oscillations must be azimuthal perturbations to the ambient 'steady' poloidal field. The amplification of the toroidal field can result from azimuthal perturbations of ambient 'steady' part of the poloidal magnetic field. Any such perturbations of the field lines would eventually lead to MHD waves. The waves travel along the field lines of the steady field and are reflected due to the density gradients near the surface. Superposition of these travelling waves could lead to stationary or standing oscillations. These oscillations could consist of the fast and the slow rotational velocity 'zones' which oscillate about the regions of mean rotational velocity. These oscillations are termed as " MHD torsional oscillations ". The strong fields needed for activity could result from constructive interference of these waves.

5.2.4 Difficulties in the MHD Oscillatory Dynamo Theories

Main difficulties of the oscillatory theories are : (i) Lack of observational evidence for the existence of 'steady' part of the poloidal magnetic field which may sustain MHD oscillations. On the contrary, sun's poloidal magnetic field appears to be

oscillatory in behavior (ii) How to maintain these oscillations , especially in the convection zone ? (iii) Can the 'steady' field admit global MHD oscillations ? (iv) Is there any observational evidence that the large-scale activity phenomena on the surface result from interference of oscillation modes ?

The first two questions will be dealt with in section 5.6 of this chapter. In section 5.4, we investigate the question (iii) and show that our field models do admit global MHD oscillations. Regarding the last question, the results obtained from the magnetic field inferred from sunspot data (chapter II) indeed show that the solar magnetic cycle and the activity phenomena do seem to be given by interference of large-scale global oscillations.

5.3 Theoretical Formulation of Torsional Oscillations

For axi-symmetric magnetic fields, we can write the magnetohydrodynamic equations in the cylindrical coordinates (ζ , ϕ , z) as (Mestel and Weiss 1987) :

$$\frac{\partial B_\phi}{\partial t} = \zeta (B_p \cdot \nabla) \Omega \quad (3)$$

$$4\pi\rho \zeta^2 \frac{\partial \Omega}{\partial t} = (B_p \cdot \nabla) (\zeta B_\phi) \quad (4)$$

Here Ω is the angular velocity, B_p and B_ϕ are the corresponding components of the magnetic field, $\mathbf{B} = B_p \mathbf{1}_p + B_\phi \mathbf{1}_\phi$, where $\mathbf{1}_\phi$ is a unit vector in the azimuthal direction, and ρ is the density.

Let us take $\rho^{(0)}$ and $B_p^{(0)}$ to be the time independent parts of ρ and B_p . Then according to Mestel and Weiss, the equation of torsional oscillations in a plasma with a magnetic field can be derived from equation (3) and (4) as

$$\frac{\partial^2 \Omega}{\partial t^2} = \frac{(B_p^{(0)} \cdot \nabla)(\zeta^2 (B_p^{(0)} \cdot \nabla) \Omega)}{4\pi \rho^{(0)} \zeta^2} \quad (5)$$

Considering a line element $d\Delta$ along $B_p^{(0)}$ which is small compared to the scales of variation of $B_p^{(0)}$ and Ω (WKB approximation), equation (5) can be written as

$$\frac{\partial^2 \Omega}{\partial t^2} = (B_p^2 / 4\pi\rho) \frac{\partial^2 \Omega}{\partial \Delta^2} \quad (6)$$

Thus, equation (6) implies that, the changes in Ω and B_ϕ propagate with the local Alfvén speed $V_A = |B_p| / (4\pi\rho)^{1/2}$, determined by the steady part of the poloidal field. In the next section, we use this equation for the examination of the admissibility of global torsional MHD oscillation in various

'models' of the steady part of the poloidal magnetic field.

5.4 Alfvén Wave Travel Times

This kind of study was initiated by Alfvén (1943). He proposed that the sunspot activity could be due to superposition of standing Alfvén waves which were formed due to the disturbances some where in the radiative core, and reach the surface along the dipole field. For a polytropic density variation, and the dipole field, he computed the travel times of such waves to be ~ 70 years for the field lines near the pole, and ~ 80 years for the field lines near the equator. Since, these periods did not agree with the 22 year period, he concluded that the 22 year period must be the resonance period of some lines of force in the sun's interior. In addition, Alfvén's theory also explained the observed propagation of sunspot zones and the opposite polarities of sunspots in the two hemisphere.

Here we study the range of Alfvén wave travel times in the following five models by taking into account the real density variation in the sun : (i) the uniform field ; (ii) the dipole field ; (iii) the combination of a uniform and a dipole field ; (iv) the ' steady ' part of the field from the preliminary model ; (v) and the ' steady ' field as modeled in chapter IV.

For the sake of comparison ,all the models are assumed to have the same amount of the steady part of the photospheric magnetic flux with a nominal value of $\Phi_* = 1.5 \times 10^{22}$ Mx

corresponding to a uniform field of ~ 1 G.

5.4.1 Model 1 : Uniform Field

Let us take the uniform field of magnitude B_0 , parallel to the rotation axis of the sun. Then equation for a field line corresponding to flux value ϕ is

$$r = k \operatorname{cosec} \theta \quad , \quad (7)$$

where $r = r/R_0$, R_0 is the radius of the sun and unit of length, and $k = (\phi/\phi_*)$. From equation (7), we have computed the geometry of field structure for different flux values and presented in figure 5.1. The velocity ' V_A ' of a Alfvenic disturbance which travels along the field line is

$$V_A = B_0 / (4\pi\rho)^{1/2} \quad , \quad (8)$$

where ρ is the density of the matter. From equation (7), the line element $d\phi$ of the field line corresponding to a flux value ϕ is

$$d\phi = \left(1 + r^2 (d\theta/dr)^2 \right)^{1/2} dr \quad . \quad (9)$$

From equations (7) and (9) we get

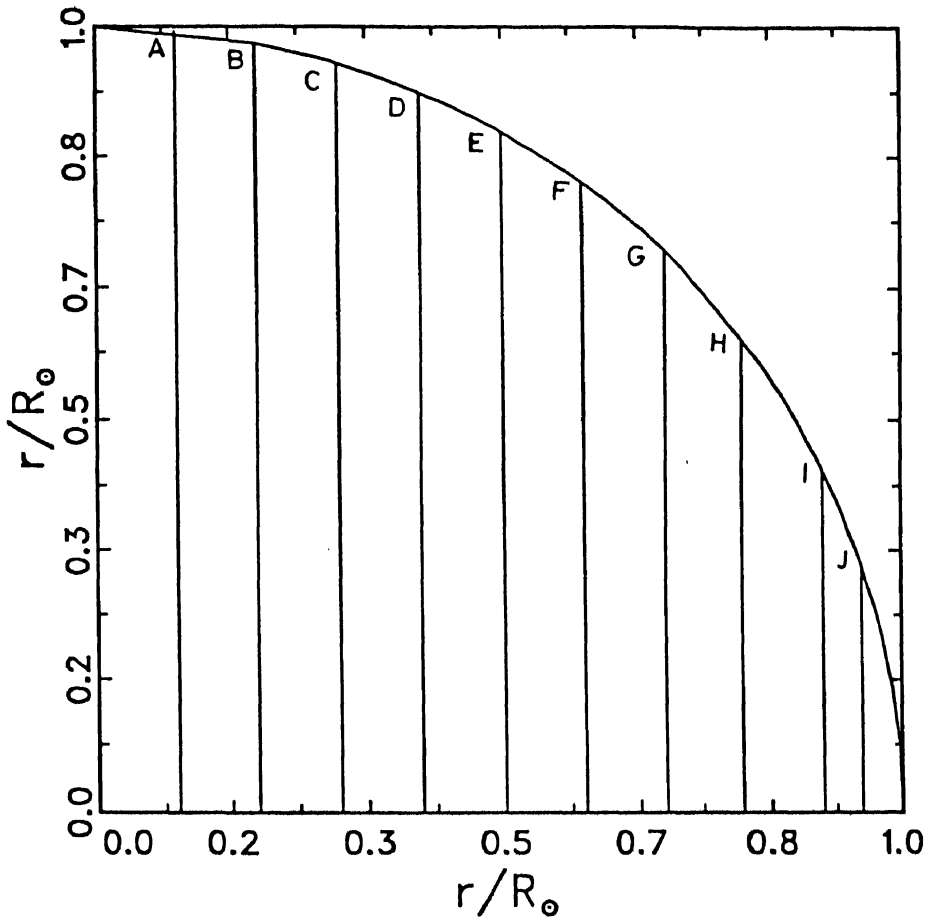


Fig 5.1.- Structure of the uniform magnetic field as given by equation (7) . The field lines correspond to flux (ϕ/ϕ_*) values A : 0.1, B : 0.2, C : 0.3, D : 0.4, E : 0.5, F : 0.6, G : 0.7, H : 0.8, I : 0.9, J : 0.95.

$$d\alpha = \left[1 - (k/r)^2 \right]^{-1/2} dr \quad (10)$$

The time τ taken by the wave to travel along the field line from one of its intersection with surface to the other intersection is

$$\tau = \int d\tau = \int \frac{dS}{V_A} = \frac{2\pi R_0^3}{\Phi_*} \int_k^1 \frac{[4\pi\rho(r)]^{1/2} dr}{\left[1 - (k/r)^2 \right]^{1/2}} \quad (11)$$

5.4.2 Model 2 : Dipole Field

The magnitude of the magnetic field of the dipole field parallel to the rotation axis is

$$B R_0^3 / M_d = \left[B_r^2 + B_\theta^2 \right]^{1/2} \quad (12)$$

where $B_r = 2\cos\theta/r^3$, $B_\theta = \sin\theta/r^3$, and M_d is the magnetic moment of dipole field .

The equation of a field line corresponding to flux value Φ is

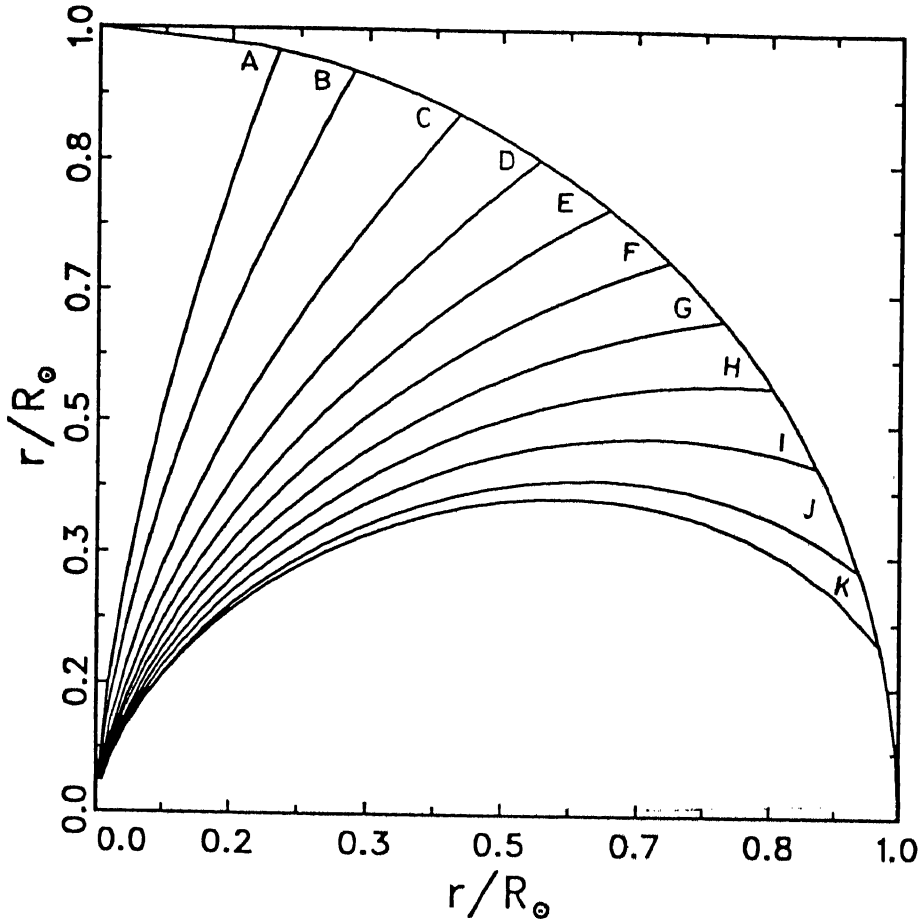


Fig 5.2.- Structure of the dipole field as given by equation (13).
 The field lines correspond to flux (ϕ/ϕ_*) values A : 0.05, B : 0.10, C : 0.20, D : 0.30, E : 0.40, F : 0.50, G : 0.60, H : 0.70, I : 0.80, J : 0.90, K : 0.95.

$$r = k \sin^2 \theta \quad , \quad (13)$$

where $k = (\Phi_*/\Phi)$, $\Phi = 2\pi M_d \sin^2 \theta / r R_0$ and $M_d = \Phi_* R_0 / 2\pi$. Using equation (13), we have given dipole field structure in figure 5.2. The corresponding line element is

$$d\Omega = \left[(1/2) \sec \theta (4 \cos^2 \theta + \sin^2 \theta)^{1/2} \right] dr \quad (14)$$

Hence, the formula for the computation of the Alfvén wave travel time is

$$\tau = \frac{2\pi R_0^3}{\Phi_*} \int_0^1 \frac{r^3 [4\pi\rho(r)]^{1/2} dr}{(1-r/k)^{1/2}} \quad (15)$$

5.4.3 Model 3 : Uniform and Dipole Field

We consider a field obtained by superposing a uniform field B_0 and a dipole field of dipole moment M_d . The magnitude of the magnetic field resulting from the combination of the uniform and the dipole field is

$$B / B_0 = \left[B_r^2 + B_\theta^2 \right]^{1/2} , \quad (16)$$

where

$$B_r = (1 + 2\mu_1 / r^3) \cos\theta ,$$

$$B_\theta = (-1 + \mu_1 / r^3) \sin\theta ,$$

and $\mu_1 = M_d / B_0 R_0^3$.

The flux function is

$$\Phi (r, \theta) = \pi B_0 R_0^2 (r^2 + 2\mu_1 / r) \sin^2\theta . \quad (17)$$

For a given value of μ_1 , B_0 is obtained from the condition $\Phi(1, \pi/2) = \Phi_*$, i.e.

$$\pi B_0 R_0^2 (1 + 2\mu_1) = \Phi_* . \quad (18)$$

From equations (17) and (18), the equation of a field line is

$$(r^2 + \mu_1 / r) \sin^2\theta = \mathcal{K} (\Phi / \Phi_*) , \quad (19)$$

where $\mathcal{K} = (1 + 2\mu_1)$.

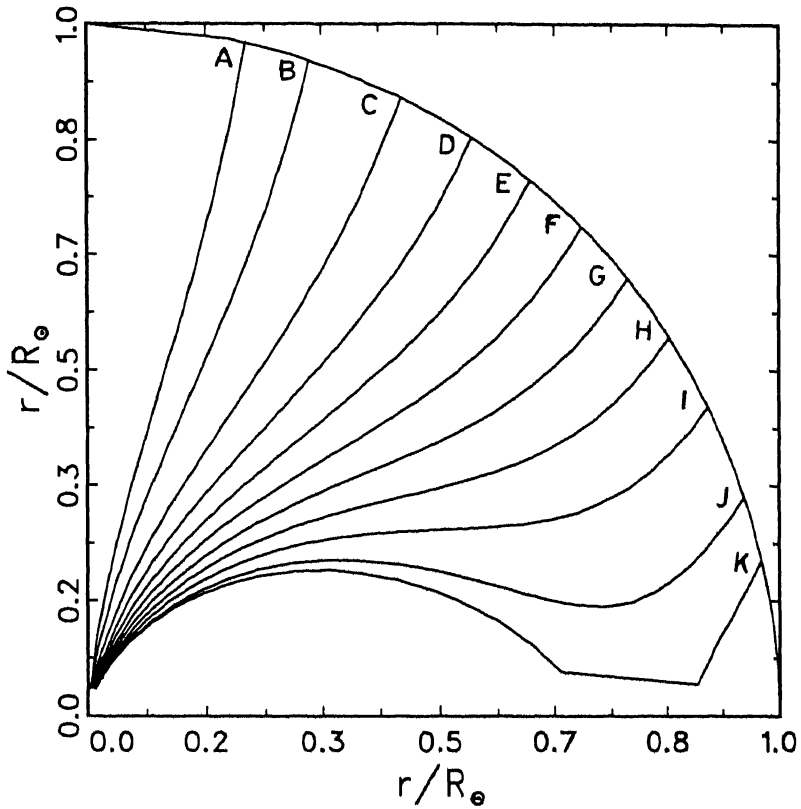


Fig 5.3.- Structure of the magnetic field for the combination of uniform and dipole fields as given by equation (19) and $K = 1.968$. The field lines correspond to flux (ϕ/ϕ_*) values A : 0.05, B : 0.10, C : 0.20, D : 0.30, E : 0.40, F : 0.50, G : 0.60, H : 0.70, I : 0.80, J : 0.90, K : 0.95.

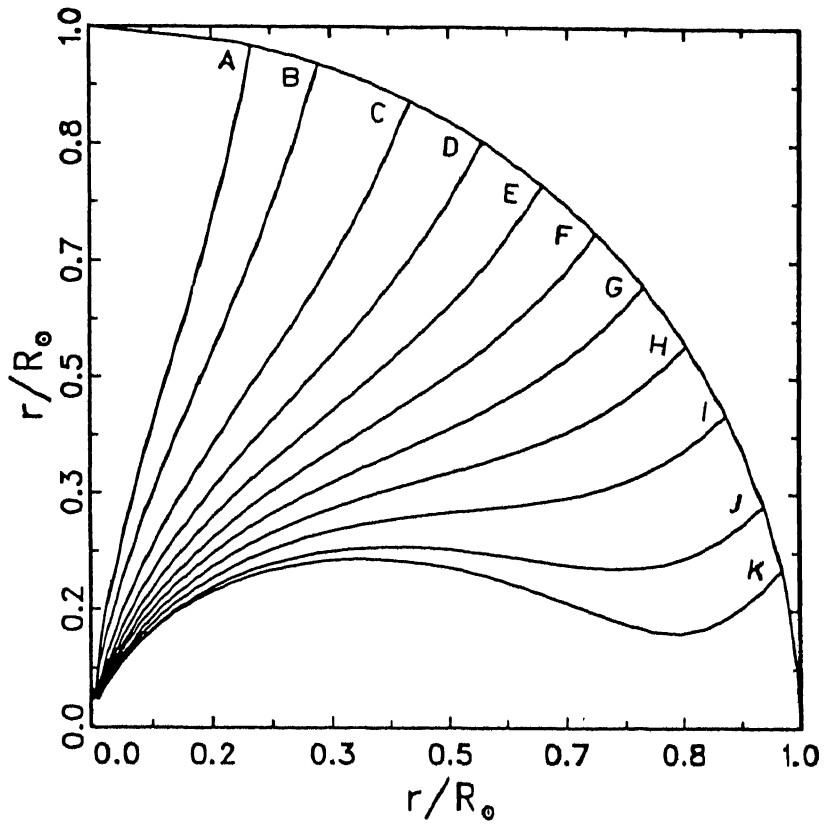


Fig 5.4.- Structure of the magnetic field for the combination of uniform and dipole fields as given by equation (19) and $\mathcal{K} = 2.248$. The field lines correspond to flux (ϕ/ϕ_*) values A : 0.05, B : 0.10, C : 0.20, D : 0.30, E : 0.40, F : 0.50, G : 0.60, H : 0.70, I : 0.80, J : 0.90, K : 0.95.

Hence, the formula for Alfvén wave travel time is

$$\tau = \frac{2 \mathcal{K} \pi R_0^3}{\Phi_*} \int_0^1 \frac{[4\pi\rho(r)]^{1/2}}{B} \left\{ \frac{d\Delta}{dr} \right\} dr, \quad (20)$$

where $d\Delta/dr = \left[1 + (r \, d\theta/dr)^2 \right]^{1/2}$, and $r(d\theta/dr)$ is

$$r \frac{d\theta}{dr} = \frac{-\sin\theta(2r^3 - \mu_1)}{2\cos\theta(r^3 + \mu_1)}. \quad (21)$$

Here we consider two variations of model 3, differing only in the value of μ_1 . In the model 3A the value of μ_1 (= 0.484) is taken from the best two term fit (chapter III, section 3.3.1) of the steady field, whereas in model 3B the value of μ_1 (= 0.624) is taken from the best three term fit (chapter III, section 3.3.1) of the steady field. The corresponding values of \mathcal{K} are :

Model 3A : $\mathcal{K} = 1.968$

Model 3B : $\mathcal{K} = 2.248$

With these values, we have computed the field lines and presented

in figures 5.3 and 5.4 respectively.

*5.4.4 Model 4 : Combination Of Uniform, Dipole,
and Hexapole Fields*

The magnitude of the magnetic field for this combination is

$$B / B_0 = \left[B_r^2 + B_\theta^2 \right]^{1/2}, \quad (22)$$

where

$$B_r = \left[(1 + 2\mu_1/r^3) + (\mu_3/r^5)(10\cos^2\theta - 6) \right] \cos\theta, \quad (23)$$

$$B_\theta = \left[(-1 + \mu_1/r^3) + (\mu_3/r^5)(7.5\cos^2\theta - 1.5) \right] \sin\theta, \quad (24)$$

$\mu_3 = M_3/B_0 R_0^5$, M_3 is the magnetic moment of the hexapole.

The corresponding flux function is

$$\Phi(r, \theta) = \pi B_0 R_0^2 \left[(r^2 + 2\mu_1/r + 4\mu_3/r^3) \sin^2\theta - (5\mu_3/r^3) \sin^4\theta \right] \dots\dots\dots (25)$$

For a given values of μ_1 and μ_3 , B_0 is obtained from the condition $\Phi(1, \pi/2) = \Phi_*$.

Thus the equation of a field line corresponding to flux Φ is

$$\left[(\nu^2 + 2\mu_1/\nu + 4\mu_3/\nu^3) \sin^2\theta - (5\mu_3/\nu^3) \sin^4\theta \right] = 4.29(\Phi/\Phi_*) \dots\dots\dots (26)$$

So, the formula for the Alfvén wave travel times is

$$\tau = \frac{8.58\pi R_0}{\Phi_*} \int_0^1 \frac{[4\pi\rho(\nu)]^{1/2}}{B} \left(\frac{d\theta}{d\nu}\right) d\nu, \quad (27)$$

where $d\theta/d\nu = \left[1 + (\nu \, d\theta/d\nu)^2 \right]^{1/2}$, and $\nu(d\theta/d\nu)$ is

$$\nu \frac{d\theta}{d\nu} = \frac{-\left[(2\nu^5 - 2\mu_1\nu^2 - 12\mu_3) + 15\mu_3 \sin^2\theta \right] \sin\theta}{\left[2(\nu^5 + \mu_1\nu^2 + 4\mu_3) - 20\mu_3 \sin^2\theta \right] \cos\theta} \quad (28)$$

The values of μ_1, μ_3 are taken as those obtained in chapter III from the condition of isorotation with helioseismologically determined internal rotation (see also Fig 3.1).

5.4.5 Model 5 : Travel Times in the Improved Model
of the 'Steady' Field (Model in Chapter IV)

As it is clear from chapter IV that the travel time calculation has to be carried out separately in the convective envelope ($0.7 \leq r \leq 1.0$), and in the radiative core ($0.0 \leq r \leq 0.7$). Thus, the Alfvén travel times have been computed in the following way :

$$\tau = \tau_{CE} + \tau_{RC} \quad , \quad (29)$$

where τ_{CE} is the travel time for the two parts of the field line in the convective envelope, and τ_{RC} is the travel time for part in the radiative core (see also Fig 4.1). For the travel time along the part in the radiative core, we have

$$\tau_{RC} = \frac{8.58\pi R_0^3}{\Phi_*} \int_{r_{min}}^{0.7} \frac{[4\pi\rho(r)]^{1/2}}{B} \left(\frac{d\phi}{dr}\right) dr \quad , \quad (30)$$

where r_{min} is the distance of the field line from the center to the point where it intersects the equatorial plane, in this model $r = r/R_c$, R_c ($= 0.7R_0$) is the radius of the radiative core,

$$B/B_0 = \left[B_r^2 + B_\theta^2 \right]^{1/2}, \quad (31)$$

where B_r and B_θ are given as follows

$$B_r = (1/r^{3/2}) \left[(18.75)J_{3/2}(2.904r) + (1.96)J_{7/2}(5.763r)(12 - 30\sin^2\theta) \right] \cos\theta \quad \dots\dots\dots (32)$$

and

$$B_\theta = -(1/r^{3/2}) \left[(4.69)J_{3/2}(2.904r) + (0.98)J_{7/2}(5.763r)C_2^{3/2}(\mu) + (13.61r) \{ J_{1/2}(2.904r) - J_{5/2}(2.904r) \} + (5.63r)C_2^{3/2}(\mu) \{ J_{5/2}(5.763r) - J_{9/2}(5.763r) \} \right] \sin\theta, \quad \dots\dots\dots (33)$$

where $\mu = \cos\theta$, $C_2^{3/2}(\mu) = 6-7.5\sin^2\theta$.

The flux function in the radiative core is

$$\Phi = 2\pi R_0^2 r^{1/2} \left[A_0 J_{3/2}(\alpha_0 r) + A_2 J_{7/2}(\alpha_2 r) C_2^{3/2}(\mu) \right] \sin^2\theta \quad \dots\dots\dots (34)$$

For a given values of $A_0 = 9.374B_0$, $A_2 = 1.955B_0$, $\alpha_0 = 2.904$, $\alpha_2 = 5.763$; B_0 is obtained from the condition $\Phi(1, \pi/2) = \Phi_*$.

In the radiative core, the equation of a field line is

$$(18.75)r^{1/2} \left[\left\{ J_{3/2}(2.904r) + (1.2526)J_{7/2}(5.763r) \right\} \sin^2 \theta - (1.5645)J_{7/2}(5.763r) \sin^4 \theta \right] = 4.29(\Phi/\Phi_*) \quad (35)$$

In equation (30), $d\delta/dr = \left[1 + (rd\theta/dr)^2 \right]^{1/2}$

where $r \, d\theta/dr = C/D$, (36)

with

$$C = \left\{ J_{3/2}(2.904r) - (2.904r)J_{1/2}(2.904r) - (7.213r)J_{5/2}(5.763r) + 1.2516 J_{7/2}(5.763r) \right\} \sin \theta + \left\{ (9.0162r)J_{5/2}(5.763r) - 1.5645 J_{7/2}(5.763r) \right\} \sin^3 \theta$$

and

$$D = 2\cos \theta \left\{ J_{3/2}(2.904r) + 1.2516 J_{7/2}(5.763r) - 3.129 J_{7/2}(5.763r) \sin^2 \theta \right\}$$

The travel time τ_{CE} along the two parts of the field line in CE is calculated in the same way as in the previous model.

5.4.6 The Results

Using the density values from the standard solar model (Bachal's (1989) model in the radiative core, and Spruit's (1977) model in the convective envelope), we have computed the travel times of Alfvén waves along different field lines in the foregoing five models. The strengths B_0 , M_d , μ_1 , μ_3 , etc are so chosen that in each model, the total flux on the northern solar hemisphere has a fixed value $\Phi_* \sim 1.5 \times 10^{22}$ Mx which corresponds to $B_0 = 1$ G. In the last model we have presented the results for field lines in the radiative core only. The field lines lying fully in the convective envelope are omitted since the Alfvén travel times along them is extremely small. The results are given in Table 5.1. In the first column, the flux values corresponding to each field line are given in the unit of Φ_* (which is same in all the models). In the remaining columns, values of the travel times (in years) from one (photospheric) end of the field line to the other end are presented. At the base of the table, we give for each model the average $\bar{\tau}$ of the travel times, their standard deviation (σ_τ) from the mean, and the percentage of variation from the mean.

The corresponding values of frequency ($1/2\tau$) of its Alfvén mode oscillations given in Table 5.2. These values of the average frequency ($\bar{\nu}$) and standard deviation (σ_ν) from $\bar{\nu}$ and the

Table 5.1 : ALFVEN WAVE TRAVEL TIMES (in years)

FLUX	MODEL 1	MODEL 2	MODEL 3A	MODEL 3B	MODEL 4	MODEL 5
Φ/Φ_*	$B_0=1G$	$M_d =$ ($G \text{ cm}^3$) 1.76×10^{32}	$B_0=0.51G$ $\mu_1=0.484$	$B_0=0.45G$ $\mu_1=0.624$	$B_0=0.12G$ $\mu_1=0.624$ $\mu_3=0.484$	$B_0=0.12 G$ $\mu_1=3.638$ $\mu_3=0.620$ $A_0=1.125$ $A_2=0.235$
0.05	6619	30.60	19.28	17.20	26.10	2.82
0.10	6217	30.90	19.60	17.40	24.59	2.76
0.15	5986	31.30	19.94	17.70	24.19	2.77
0.20	3168	31.70	20.30	18.00	23.84	2.68
0.25	1584	32.10	20.68	18.30	23.62	2.68
0.30	554	32.55	21.09	18.60	23.46	2.81
0.35	345	33.00	21.54	19.00	23.35	2.83
0.40	132	33.50	22.02	19.40	23.30	2.85
0.45	131	34.10	22.54	19.80	23.29	2.88
0.50	110	34.70	23.11	20.20	23.32	2.93
0.55	75	35.30	23.75	20.70	23.40	2.99
0.60	64	36.60	24.46	21.20	23.51	3.10
0.65	54	36.80	25.26	21.80	23.67
0.70	44	37.70	26.18	22.50	23.88
0.75	40	38.80	27.28	23.30	24.14
0.80	36	40.03	28.61	24.20	24.46
MEAN $\bar{\tau}$	1572	34.3	22.85	19.96	23.90	2.84
σ_τ	2395	2.81	2.72	2.09	0.70	0.12
σ_τ/τ	0.152	0.082	0.119	0.105	0.029	0.042

Table 5.2 : ALFVEN FREQUENCIES (in Nano-hertz)

FLUX	MODEL 1	MODEL 2	MODEL 3A	MODEL 3B	MODEL 4	MODEL 5
Φ/Φ_*	$B_0 = 1G$	$M_d =$ (G cm ³) 1.76×10^{32}	$B_0 = 0.51G$ $\mu_1 = 0.484$	$B_0 = 0.45G$ $\mu_1 = 0.624$	$B_0 = 0.12G$ $\mu_1 = 0.624$ $\mu_3 = 0.484$	$B_0 = 0.12G$ $\mu_1 = 3.638$ $\mu_3 = 0.620$ $A_0 = 1.125$ $A = 0.235$
0.05	0.0024	0.5180	0.8169	0.9215	0.6073	5.6206
0.10	0.0026	0.5146	0.8087	0.9190	0.6446	5.7428
0.15	0.0027	0.5064	0.7949	0.8955	0.6552	5.7220
0.20	0.0050	0.5000	0.7808	0.8806	0.6649	5.9142
0.25	0.0100	0.4938	0.7664	0.8661	0.6710	5.9142
0.30	0.0290	0.4869	0.7515	0.8522	0.6756	5.6406
0.35	0.0460	0.4803	0.7198	0.8342	0.7688	5.6007
0.40	0.1200	0.4731	0.7198	0.8170	0.6803	5.5614
0.45	0.1200	0.4648	0.7032	0.8005	0.6805	5.5035
0.50	0.1440	0.4568	0.6859	0.7847	0.6797	5.4096
0.55	0.2110	0.4490	0.6674	0.7657	0.6773	5.3010
0.60	0.2480	0.4331	0.6480	0.7477	0.6742	5.1129
0.65	0.2940	0.4307	0.6275	0.7271	0.6696
0.70	0.3600	0.4204	0.6054	0.7044	0.6637
0.75	0.3940	0.4085	0.5810	0.6803	0.6566
0.80	0.4400	0.3960	0.5540	0.6550	0.6480
MEAN $\bar{\nu}$	0.1518	0.4645	0.7020	0.8032	0.6642	5.5870
σ_{ν}	0.1490	0.0450	0.0800	0.0818	0.0185	0.2249
$\sigma_{\nu}/\bar{\nu}$	0.98	0.097	0.114	0.066	0.028	0.040

percentage of variation of ν from $\bar{\nu}$ are also given.

Models numbers 2,4 and 5 give the values of $\sigma_{\tau}/\bar{\tau} < 0.1$. However, the smallness of $\sigma_{\tau}/\bar{\tau}$ in models 2 and 4 is due to the fact that all the field lines which enter the radiative core have similar arcs passing through similar density structure. This is mainly due to the presence of the central singularity . Hence, we conclude that among models 1 to 5 , model 5 is the only admissible model which sustains global alfvenic mode oscillation with well defined frequency for the fundamental mode.

In the above models, the estimated values of B_0 obtained from the assumed value of Φ_* decreases steadily from model 1 to model 5. However, in order that the travel times may be ~ 22 years, the last model requires that $B_0 \sim 0.01$ G.

5.5 Study of the 'Time-Dependent' Torsional MHD Perturbation (Its Radial and Latitudinal Structure and Time Scale)

5.5.1 'Residual Rotation ' as the Likely Time-Dependent Part of Rotation

Having modeled the 'steady ' parts of the rotation and the magnetic field (chapter IV), we determine the 'residual rotation rates' in ORC and CE as

$$\begin{aligned} \delta\Omega^{\text{ORC}}(r, \theta) &= \Omega_{\text{obs}}^{\text{ORC}}(r, \theta) - \Omega_{\text{mod}}^{\text{ORC}}(r, \theta), \\ \delta\Omega^{\text{CE}}(r, \theta) &= \Omega_{\text{obs}}^{\text{CE}}(r, \theta) - \Omega_{\text{mod}}^{\text{CE}}(r, \theta), \end{aligned} \tag{37}$$

where $\Omega_{\text{mod}}^{\text{ORC}}$ and $\Omega_{\text{mod}}^{\text{CE}}$ are obtained using the equation 25 (in chapter IV) along with equation (17) and (18) with the values of parameters as determined in chapter IV.

If $\Omega_{\text{mod}}^{\text{ORC}}$ and $\Omega_{\text{mod}}^{\text{CE}}$ represent the steady parts of rotation, then the residual rotation will contain mainly time-dependent part of rotation, besides the errors and noise. Here, we study the nature of the time-dependent part neglecting the errors and the noise.

5.5.2 Time-Dependent Parts in CE

To determine whether the residual rotation in CE is time-dependent, we first try to fit it to the form $x^{-5} C_4^{3/2}(\cos\theta)$. Such an attempt gives

$$\hat{\mu}_5 = 0.0125 \pm 0.0335 \quad ,$$

and a very large value of χ^2 . The large value of χ^2 implies that the residual rotation $\delta\Omega$ is not of the form $x^{-5} C_4^{3/2}(\cos\theta)$. On the other hand, if $\delta\Omega^{\text{CE}}$ is of this form, then the large uncertainty in $\hat{\mu}_5$ implies that $\delta\Omega^{\text{CE}}$ contains observational errors which are larger than the real values of the residual rotation.

For further insight, we add a 'third' term of this form with the above value of $\hat{\mu}_5$, to the first two terms already determined in the steady field, and recalculate the χ^2 for the fit between $\Omega_{\text{mod}}(r, \theta)$ and $\Omega_{\text{obs}}(r, \theta)$. The new value of χ^2 is somewhat larger

(43.97) than its two-term value of 42.95. Thus, even if a part of the computed residual rotation constituted a true residual rotation, it would not be of the form $x^{-5}C_4^{3/2}(\cos\theta)$.

This implies that the true residual rotation can not have a corresponding term in the magnetic field to ensure complete isorotation between the field and the plasma. Thus the true residual rotation constitutes a time-dependent part of the sun's rotation.

5.5.3 Time-Dependent Parts in ORC

Fitting the residual rotation to a term $r^{1/2}J_{11/2}(\alpha_4 r)C_4^{3/2}(\cos\theta)$ in ORC yields :

$$\alpha_4 = 8.182$$

and

$$\lambda_4 = 0.0027 \pm 0.0018$$

However, the corresponding χ^2 is large. This may be due to the large ' observational ' errors . The smallness of the uncertainty in λ_4 suggests that the residual rotation may contain a real perturbation of a form similar to $r^{1/2}J_{11/2}(\alpha_4 r)C_4^{3/2}(\cos\theta)$.

Here again, for further insight we add a ' third ' term of this form, with these values of α_4 and λ_4 , to the two terms

already determined from the steady part of the field, and recalculate the χ^2 for the fit of $\Omega_{\text{mod}}(r, \theta)$ with $\Omega_{\text{obs}}(r, \theta)$. The new value of χ^2 (11.56) is in fact slightly smaller than that (11.58) given by the two term fit. At present we do not know a reliable method to determine if lowering of χ^2 is significant or not. However if it is, it would imply presence of a term of the above form in the 'steady' part of rotation in ORC.

One may wonder how the helioseismologically determined rotation $\Omega(r_1, \theta_1)$, which is truncated at $\sin^4 \theta$, can show improvement in the goodness of fit with inclusion of the term $\ell = 5$ which is equivalent to extending the fitting formula up to $\sin^6 \theta$. However, the inclusion of the term $\ell = 5$ also implies inclusion of terms in r^{-5} in the coefficients of $\sin^2 \theta$ and $\sin^4 \theta$. This indicates that at the time of the helioseismological observations there must be (over and above the rotation field represented by the term $\ell = 1$ and $\ell = 3$) a "residual rotation", which is not merely an artifact of noise or errors.

If the real magnetic field does not contain a residual term $\delta B(r, \theta)$ corresponding to the above term in $\delta \Omega$, then $\delta \Omega$ would be time dependent. Even in case such a δB required for the steady state exists in "ORC", the inclusion of the corresponding term in $\Phi(r, \theta)$ in CE (as required by boundary conditions) deteriorates the fit in "CE" (cf. Table 3.1, chapter III) which implies non-isorotation in "CE". Thus, either the residual rotation in "ORC", or the field structure in "CE", or both, would be

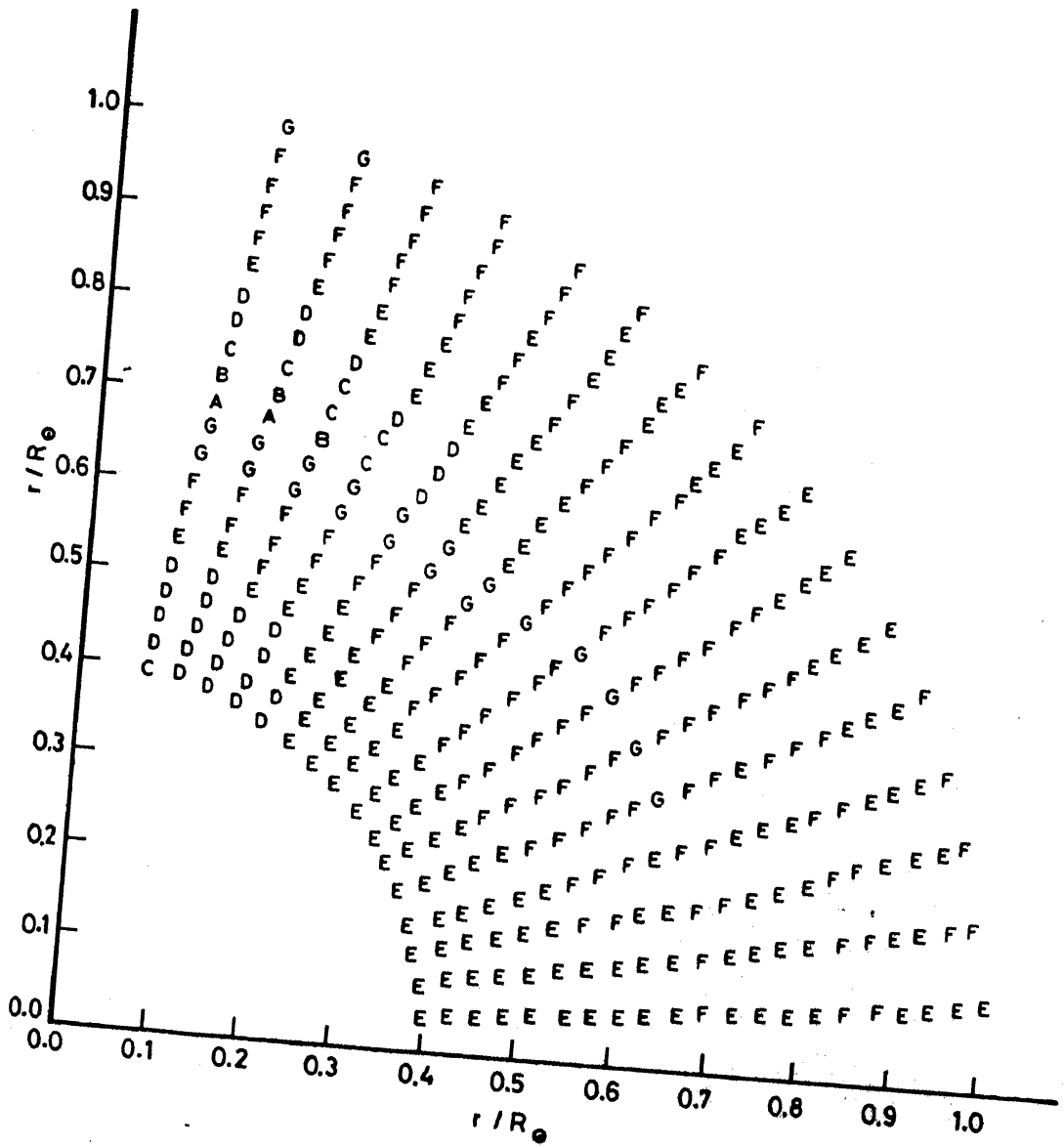


Fig 5.5.- Plot of Sun's internal residual rotation for the epoch 1986 as computed from equation (37). Magnitudes are A : (41 to 50)nHz, B : (31 to 40)nHz, C : (21 to 30)nHz, D : (11 to 20) nHz, E : (0 to 10)nHz, F : (-10 to 0)nHz and G : (-20 to -10)nHz.

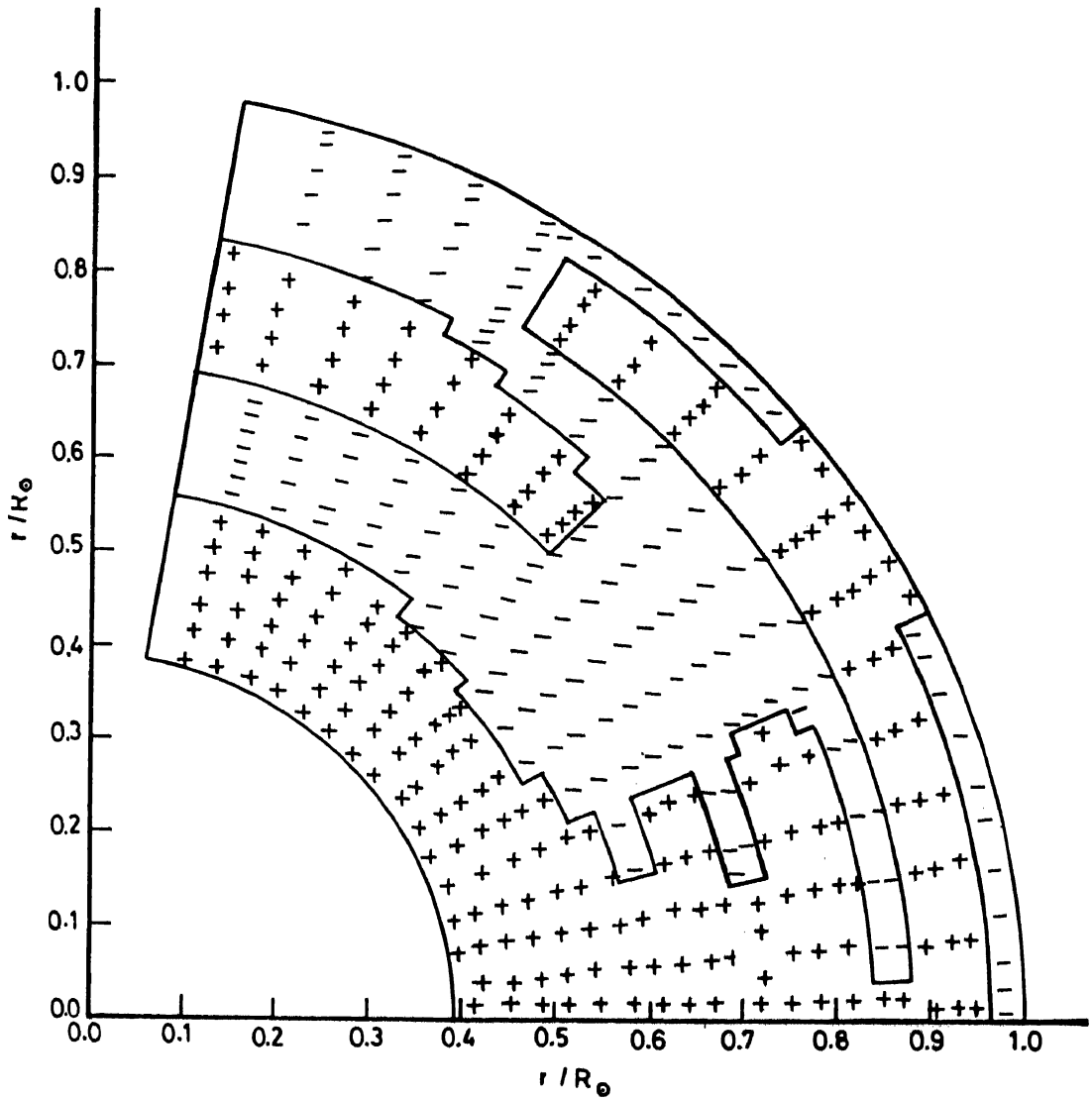


Fig 5.6.- Internal torsional velocity bands . Positive signs represent the 'fast' rotational velocity bands. Negative signs represent the 'slow' rotational velocity bands.

nonsteady. Thus, a time-dependant torsional MHD perturbation seems to exist in the region " ORC + CE ".

5.5.4 Scales of Radial Variations Of the ' Torsional MHD Perturbations '

Assuming that residual rotation (eqn 37) represents the non-steady part of the rotation (i.e. neglecting observational and fitting errors), we have computed $\delta\Omega(r, \vartheta)$ for the epoch of the 1986 helioseismic data. The results are presented in Figures 5.5 and 5.6 . In Fig 5.5, we present the plot of residual rotation with 7 levels of velocity magnitudes. In Fig 5.6, we have given the isocontours of the residual rotation with positive and negative signs. Here positive signs indicate the 'fast rotational' velocity bands whose magnitudes are greater than the modeled rotation. Similarly, negative signs indicate the 'slow rotational' velocity bands whose magnitudes are lesser than the modeled rotation .

From figures 5.5 and 5.6 , it is clear that , there appear to exist large-scale slow and fast rotation bands with the following properties. (i) Radial widths are in the range of $(0.1-0.5)R_{\odot}$. (ii) The magnitudes of rotational perturbation are ~ 50 nHz (i.e 100m/sec). (iii) One latitudinal zone of oscillation at $0.4R_{\odot}$, three at the base of the convection zone, and five on the surface (iv) The latitudinal zones of these oscillations have

their widths in the range $\sim 10^\circ - 180^\circ$. (v) The magnitudes of velocity perturbations are highest near the base of the convection zone (\sim upto 50 nHz), especially near the poles. (vi) The magnitudes are moderate in the outer radiative core.

Thus, the non-steady part of the rotation seems to have global structure. These large-scale perturbations seem to be excited near the base of convection zone.

The afore-mentioned results are based on the data of a single epoch only. However, further analysis is needed for other epochs so that a clear picture of the possible nature of the time-dependent MHD oscillations may emerge in near future.

5.5.5 Time Scales of Variations Of MHD Modes in the Perturbations

It is impossible to determine the time scale of variation from a single epoch observation. However, we show that a time scale comparable to that of solar magnetic cycle is not ruled out. The " frequencies " (ν) of the various MHD modes in these perturbations will be related to the ratio of the toroidal and poloidal magnetic field perturbations δB_T and δB_P as follows : $\nu \sim | \text{curl}(\Omega_0 \times \delta B_P) | / \delta B_T$, where Ω_0 is the " zero-order " flow defined by the approximately " steady " part of the rotation. The order of magnitude of the operator $\text{curl}(\Omega_0 \times \dots)$ has already been estimated crudely in chapter III (equation 13) to be 150 nHz. This

can give the time scales of variations in the range $\sim 2-20$ year, if $\delta B_T / \delta B_P$ is in the range $\sim 10-100$ (similar orders of magnitude for the periods of MHD perturbations have been suggested by Layzer, Rosner and Doyle (1979) using different approach).

Thus, it is not ruled out that the MHD modes in the perturbations detected in section 5.1 and 5.2 have time scales comparable to those of solar magnetic cycle.

5.5.6 Latitudinal Structure of the Perturbations

In order to determine the dominant latitudinal structure of the time-dependent part of the rotation, we integrated the residual rotation with respect to the radial coordinate from $0.4R_\odot$ to $1.0R_\odot$ as follows

$$g(\vartheta) = \int_{0.4R_\odot}^{1.0R_\odot} \delta\Omega(r, \vartheta) dr .$$

The resulting form of $g(\vartheta)$ is shown in Fig.5.7 . Interestingly, this profile is similar to the torsional velocity profile obtained by Howard and LaBonte (1980). However, near the pole , this profile is substantially different from the torsional velocity profile .

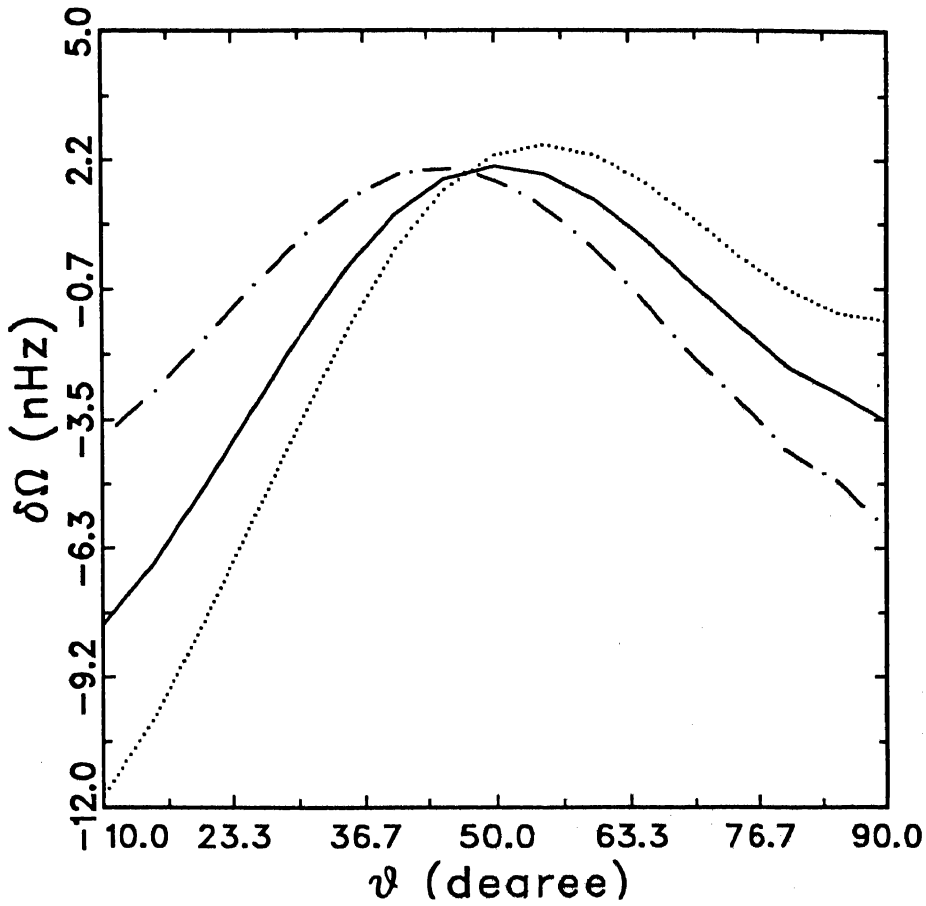


Fig 5.7.- Radial integral of the residual rotation as function of colatitude. Dash dotted line indicates the integral of the residual rotation from $(0.4R_o - 0.7R_o)$. Dotted line indicates integral of the residual rotation from $(0.7R_o - 1.0R_o)$. Solid line indicates the integral of the residual rotation from $(0.4R_o - 1.0R_o)$.

Table 5.3 : RESULTS OF LEAST-SQUARE FIT FOR INTEGRATED PROFILE
OF RESIDUAL ROTATION

TERMS TAKEN	V_0 (nHz)	δV_0 (nHz)	V_2 (nHz)	δV_2 (nHz)	V_4 (nHz)	δV_4 (nHz)	V_6 (nHz)	δV_6 (nHz)	GOODNESS OF FIT
P_0, P_2 & P_4	-0.602	0.281	-4.498	1.628	-7.987	3.204	100 %
P_0, P_2 & P_6	-0.602	0.283	-4.509	1.553	-8.045	3.181	0.022	0.561	100 %

We expand $g(\theta)$ in even degree Legendre polynomial as follows:

$$g(\theta) = V_0 + V_2 P_2(\cos\theta) + V_4 P_4(\cos\theta) + V_6 P_6(\cos\theta) + \dots,$$

and determine coefficients V_0, V_2, V_4, \dots , etc, by least square fit. The results are presented in Table 5.3.

It is interesting to note that, the terms " $\ell = 2$ " and " $\ell = 4$ " are the dominant terms in $g(\theta)$. This is in agreement with the expectation (Gokhale and Javaraiah, 1994) from the dominant terms $\ell = 3$ and $\ell = 5$ in the 'cascade' of the MHD modes.

5.6 Conclusions and Discussion

Main conclusions of this chapter are :

(i) Our ' preliminary ' and ' improved ' models of the steady part of the magnetic field admit global MHD (torsional) oscillations with the smallest relative band width for the frequencies.

(ii) For the period of the fundamental mode to be ~ 22 years , the 'improved' model requires that $B_0 \sim 0.01$ G. This gives for the ' steady ' part of the potospheric magnetic flux a value well within the observational limit of 0.5 G (Stenflo 1993) .

(iii) *Time-dependent torsional MHD perturbations* are likely to be present in the interior of the sun. The radial length scales of these are in the range of $(0.1-0.5)R_0$, and the magnitudes upto ~ 50 nHz. The widths of the latitudinal zones of these oscillations are in the range $\sim 10^\circ - 180^\circ$. The magnitudes are large in the convection zone (upto 50 nHz), with maximum near the base, and are moderate (upto 20 nHz) in the outer radiative core.

(iv) Time scales of these perturbations can be in the range of the periods in the solar magnetic field, if the ratio of the perturbations in the toroidal and poloidal components of the field is in the range $\sim 10-100$.

(v) The terms " $\ell = 2$ " and " $\ell = 4$ " are the dominant terms in the latitudinal profile of the radial integral of the perturbation.

From the conclusions one is tempted to further conclude that *the solar magnetic cycle and hence the solar cycle activity cycle may be due to global torsional MHD oscillations*.

Lack of observational evidence for existence of 'steady' poloidal field (Cowling 1981), and the problem of maintenance of the torsional oscillations (Schussler 1982) seem to be the main difficulties of the oscillatory models.

However, as pointed out by Piddington (1976,1983), the detection of a weak 'steady' field in the presence of strong non-steady fields will require highly accurate measurements. In any case, the absence of evidence of such a field is not the evidence for its absence.

Schussler (1982) estimated the ratio (γ) of the Lorentz force to the viscous force in the convection zone to be very much less than one and hence concluded that the influence of convection on the oscillations cannot be neglected.

However, in his estimates of viscous force he assumed toroidal velocity perturbation $\sim 10^4$ cm/sec. The oscillatory model used need not consist of a single large-scale oscillation. Hence, on large length scales relevant here, the amplitude of any one global toroidal oscillation need not be $\sim 10^4$ G near the base of the convection zone. The strong dissipation will be confined only near the surface and hence the energy needs will be moderate. Thus, viscous forces may not be affecting these large-scale perturbations appreciably. Thus the effect of convective flows will be mainly advective rather than dissipative. In fact at the boundaries of the convective eddies, the field will be amplified.

In the radiative core, the viscous forces are any way negligible.

Thus there seem to be no serious difficulties in the suggestion that *the solar activity including the solar cycle may essentially consists of the internal torsional MHD perturbations.*

CONCLUSIONS AND FUTURE PROSPECTS

Many long periods have been observed in solar activity. In this thesis, we have concentrated mainly on the dominant 22 year magnetic cycle. The conclusions from chapters II to V can be summarized as follows.

Assuming that solar activity results from superposition of sun's global MHD oscillations, we have studied the spectrum of these oscillations and the temporal variations in their amplitudes and phases.

Legendre Fourier analysis of the sun's magnetic field inferred from the data on sunspot groups during 1874-1976 shows that the LF power spectrum has distinct behavior for 'odd' and 'even' degree terms separately. In the amplitude power spectrum, the odd degree terms in the range of $l = 1$ to $l = 21$ have relatively large amplitudes compared to the even degree terms.

The amplitude power spectrum of odd degree terms has a main hump over $l = 1 - 11$, with a high peak at $l = 5, 7$ and a tail for $l \geq 21$. This has been fitted with mathematical forms of the spectra of trapped waves.

The approximate constancy of the relative phases and the relative amplitudes of these LF terms suggests that, these terms

may represent oscillations which have been approximately stationary during last several decades .

Simulation of the butterfly diagram generated from the random data set also showed that the distribution of sunspot activity even with in the " butterfly wings " is not produced by any random process .

The reproduction of solar magnetic behavior at high latitudes by superposition of oscillations, whose amplitudes and phases are obtained from low latitude data, has suggested that the sunspot activity may really be originating in the interference of sun's global oscillations . The dominant contribution seems to come from axisymmetric modes of odd degrees upto $l = 13$ and periods 22 year.

For global oscillations to be possible there must be a steady background field of such a geometry that it allows oscillations of the observed characteristics (e.g. the periods and the wave numbers) . For this purpose we have modeled the 'steady' part of the sun's poloidal magnetic field .

As a first step, we have modeled the ' steady ' part of the sun's magnetic field assuming it to be a current-free field whose field lines ' isorotate ' according to the sun's internal rotation given by helioseismology . This part of the field can be described as that of a central dipole and a central hexapole both parallel to the rotation axis and embedded in a uniform external field .

For such a model the field structure contains a critical surface (running along the base of the convection zone in the low latitudes), where a discontinuity of ~ 7 nHz per unit flux in the

gradient of rotation (with respect to the magnetic flux), may be winding a poloidal field (of $\sim 10^{-4} - 1$ G) into a toroidal field ~ 2 MG in $10^5 - 10^9$ yr .

The current-free field approximation is valid in the convective envelope only , but not so in the radiative core. The least square fit of the magnetic field with the plasma rotation was not good in the radiative core . Moreover, the current-free fields have a singularity near the center . For these reasons, it was necessary to improve the preliminary model.

With reasonable assumptions and approximations it is shown in chapter IV that the 'steady' part of the magnetic field can be modeled as an analytical solution of the equation for magnetic diffusion in an incompressible medium of constant diffusivity with appropriate boundary conditions and that its field lines must iso-rotate with the solar plasma . This analytical solution was then fitted for isorotation to obtain the improved model of the steady part of the field .

In this model the steady field does not have any singularity , separatrix, or closed loop, and yet yields a much better fit with the helioseismologically determined isorotation contours .

The improved model enables us to estimate the ' initial ' relative strengths (i.e. relative strengths at Zero Age Main Sequence) of the two diffusion eigen modes as 4 : 1 . The characteristic diffusion time scales of these modes are estimated to be ~ 10.6 and ~ 2.7 billion year respectively , assuming a mean diffusivity of $\sim 35 \text{ cm}^2 \text{ sec}^{-1}$ in the radiative core .

For determining whether the steady part of the field can sustain global MHD oscillations, as inferred from sunspot data, we have computed in chapter V the Alfvén wave travel times along the field lines in five different models. The last two of which are the 'preliminary' and the 'improved' models given in chapters III and IV respectively.

For these models, the standard deviation from the mean Alfvén wave travel time as well as its ratio to the mean travel time are also calculated. The last two models yield the smallest relative bandwidth for the frequencies of global Alfvénic oscillations. The model number 5 (the 'improved' model) is the only admissible one which can sustain global Alfvénic oscillations with well defined frequency for the fundamental mode.

For the mean Alfvén travel time to give a period ~ 22 yr, we require B_0 in the last model to be ~ 0.01 G. This gives for the steady part of the photospheric magnetic flux in the model a value well within the observational limit (Stenflo 1993).

The following systematic pattern in the 'residual' part of the internal rotation defined in chapter V suggests that there may be presence of global torsional MHD perturbations in the interior of the sun. The widths of the radial ranges defined by the sign of the residual rotation are in the range of $0.1R_0 - 0.5R_0$, and the amplitudes of rotational velocity are $\sim 10 - 100$ m/sec. We find only one latitudinal zone of oscillation at radius of $0.4R_0$, three at the base of convection zone, and five on the surface. The latitudinal zones of these oscillations have their

widths in the range $\sim 10^\circ - 75^\circ$.

Time scales of these perturbations can be in the range $\sim 2-20$ year, if the ratio of perturbations in the toroidal and poloidal components of the magnetic field is in the range of $\sim 10-100$.

By fitting the radial integral of the residual rotation over the radial range ($0.4R_\odot - 1.0R_\odot$) to a linear combination of the first three Legendre polynomial of even degree terms in $\cos\theta$, we find that the terms " $l = 2$ " and " $l = 4$ " are the dominant terms in the time-dependant part of the rotation .

To conclude, the summary of this thesis is as follows .

Assuming that the solar magnetic activity cycle results from global MHD oscillations of the sun, we first presented properties of these oscillations (eg. the amplitude spectrum and the variation of amplitudes and phases) . The approximate constancy of the amplitudes and the phases (and their use in reproducing field behavior in high latitudes) suggests that the mathematical terms represent real global oscillations . We have then modeled the structure and the strength of the steady part of the magnetic field . It is shown that the model allows global MHD oscillations with the frequencies and latitudinal structure similar to those in the magnetic field as inferred from the sunspot data . Finally we studied the 'perturbation' in the internal rotation and showed that the characteristic properties of

this perturbation can be similar to those from magnetic (sunspot) data .

We believe that long period oscillations in the range 0.5 year to 22 year are of similar nature and derive their energy from the " 22 year " oscillations. Periodicities longer than 22 year may be due to the excitation mechanism itself.

A considerable part of this thesis is devoted to the modeling of the ' steady ' part of the sun's internal magnetic field . However, such a modeling is an essential part of studying the long period global oscillations .

Following are the important works to be undertaken in future :

(1) The LF analysis of the sun's magnetic field inferred from sunspot data shows that the spectrum of the odd degree axisymmetric terms are effectively decoupled from the even degree terms. Physics of these long period global oscillations is poorly understood owing to lack of information on the sun's internal magnetic field. Since these oscillations are mainly associated with the magnetic fields , and the periods are much longer than periods of acoustic oscillations , the waves responsible for these oscillations may be slow MHD waves. In analogy with the acoustic branch of helioseismology from which one can infer the sun's internal rotation , etc., one can study also the internal magnetic field structure from the observed properties (

frequencies and phases) of the slow MHD oscillations over very long periods (eg. decades/centuries). This study would constitute another important branch of helioseismology . However such studies will obviously have poor frequency resolutions and (in the sunspot data) poor signal to ratio. As in the acoustic branch , the study of the internal field structure can be by forward method in which the frequencies are computed by choosing suitable internal magnetic field structure . Alternatively inversion methods will have to be developed in which the observed characteristics of the magnetic oscillations will be used to determine the internal structure of the magnetic field .

Using WKB approximation , Brandenburg (1988) has obtained diagnostic diagram for the even degree MHD oscillations modes in the presence of steady toroidal magnetic field. He pointed out that such even degree oscillations would be standing Alfvén waves trapped in a cavity below the convection zone. Further he showed that the estimated eigen frequencies are in rough agreement with the observed frequencies (Stenflo and Vogel 1986).

However, we know from LF analysis of Sun's magnetic field inferred from sunspot data that the typical butterfly diagram is reproduced (Gokhale and Javaraiah, 1992) mainly by the leading odd degree LF terms only (eg. $l \leq 13$). This may require odd parity in the steady toroidal field, i.e. odd parity in the differential rotation. Hence the spectrum of the odd degree LF terms, may be resulting not from the perturbation of the steady part of the toroidal field , but from perturbation of the steady part of the

poloidal field. It will be interesting to examine the dispersion relation for the odd degree modes in the poloidal field.

The diagnostic relations should be obtained for both odd and even degree slow MHD modes of solar oscillations in the presence of the steady poloidal field as modeled in chapter IV, by solving linearized equations with proper boundary conditions .

(2) For modeling the steady part of the poloidal magnetic field, we have used the values of the sun's internal rotational velocities inferred by inversion techniques (Dziembowski , Goode and Libbrecht 1989) from the observed frequency splittings of the acoustic modes (Libbrecht 1989). Rotational velocities have large uncertainties in the high heliographic latitudes and near the center . These uncertainties may be contributed not only by the observational errors but also in the two step fitting to get the parameters of the steady part of the field (μ_1 , μ_3 , etc) and the steady part of the rotation (Ω_0 and Ω_1) . The two steps of fittings are : (i) to get the internal rotation, frequency splittings to be inverted by least square fitting the assumed form of rotation ; (ii) the parameters of magnetic field and rotation to be obtained by fitting the modeled field with the inferred rotation . It is obvious that the uncertainties in μ_1 , μ_3 , Ω_0 , Ω_1 , etc., can be considerably reduced if $\Omega(r, \theta)$ and $\Phi(r, \theta)$ are determined by assuming them to be in the form of equation 25 (Chapter IV) and then fitting this form directly to

the observed frequency splittings . We plan to do this in near future .

(3) In chapter IV, we have presented the model for steady part of the poloidal magnetic field only. However, either the poloidal part of the magnetic field, or the toroidal part of the magnetic field, alone can not satisfy the stability condition . For stability, a combination of the the poloidal and the toroidal magnetic fields of similar orders is necessary (Mestel and Weiss 1987; Spruit 1990). Thus , for the sake of the stability of the Sun's general magnetic field, we expect that the steady part of the toroidal magnetic field may also be present in the interior. In fact, we have already pointed out in chapter IV (section 4.5.5) the corresponding form of the steady part of the toroidal magnetic field. According to this, the steady parts of both the components (poloidal and toroidal) of the field may be diffusive everywhere in the solar interior except near the base of the convection zone, where the winding due to the rotational gradient dominates over the diffusion . However, modeling of the 'steady ' part of the toroidal magnetic field remains to be worked out .

(4) For modeling the steady parts of magnetic field and rotation, we have used the data at a single epoch (1986) only. However, data at different epochs is necessary for studying the time-dependant parts of the solar magnetic field and the rotation

by studying the radial, latitudinal and temporal variations in the residual rotation rates . Better and better understanding of the time-dependent parts of the Sun's internal magnetic field and the rotation will be possible as helioseismological observations continue year after year (for example from the Global Oscillation Network Group - GONG).

(5) Magnetic fields in the stars other than the sun have been known to exist since Babcock's (1947) discovery of a strong field in the peculiar A type star 78 Vir. Presently, a wide range of objects right from the pre-main-sequence phase to the post-main-sequence phase have been detected to have moderate to strong magnetic fields. It may be possible to extend our steady magnetic field model to these stellar objects in the following way . According to Moss (1986), only slow rotators may display the core dynamo fields on the surface . However, most of the early type main sequence stars are rapid rotators . Hence, it may be virtually impossible to have the dynamo generated magnetic fields in them . Thus, the only other possibility is that the early type main sequence stars might have retained most of their fossil fields from the proto star phase (Dudorov , 1987). For example, the magnetic fields of CP stars appear to be globally ordered and have much simpler geometries (Saar 1990). Hence , our model of the field in the radiative core of the Sun may be appropriate also for early type main sequence stars, especially chemically peculiar (CP) stars .

(6) Studying of internal rotation of the Sun (especially core rotation) has wide astrophysical implications. Stellar rotational velocities indicate that (Skumanich 1972; Stauffer 1991) when the Sun was a young star, its surface rotation rate was much larger than that observed today. This possibly (Libbrecht and Morrow 1990) represents the rotation of the convective envelope which could have been reduced through magnetic braking, while the massive core may be still rotating faster. The speculation that the solar core may be rotating faster can be confirmed by helioseismic inversion of either low degree acoustic rotational splittings or from rotational splittings of 'g' modes . Presently, it is not possible to detect ' g ' modes with sufficient accuracy , because of their low amplitudes near the surface. On the other hand, though the measurements of rotational splittings of low l 'p' modes is quite feasible , they are based on poor signal to noise ratio. Moreover, the maximum splitting 'm' of the low degree modes depends upon $\pm l$ and the order of the line width. In fact the line width is decreasing with decreasing frequency and l also. Thus it is extremely difficult to resolve the lines of low degree acoustic modes with adequate accuracy (Palle et.al. 1990; Toutain and Frolich 1992; Hill et.al. 1990). This may lead to uncertainties in the determination of the angular velocity near the Sun's interior. The eigen functions of low degree acoustic modes have low amplitudes near the core and thus rotational splittings are less sensitive to the core rotation. Yet, the accurate determination of low degree rotational

splittings is clearly necessary for measuring the solar core rotation . Our present study could be useful in this context.

The rotational splitting for $\ell = 1$ (which is sensitive to the core rotation) mode will be simply a linear function of the core's rotation and the differential rotation of the convective envelope. If one has the model of the rotation of solar core and the convective envelope (such as the rotation modeled in Chapter IV) one can predict the rotational splitting for ' $\ell = 1$ ' degree mode so that this can be used as preliminary input in the inversions of the observed frequency splittings .

REFERENCES

- Ananthakrishnan, R. & Nayar, P.M., 1953, Kodaikanal Observatory
Bulletin, No. 137, 194
- Ando, H. & Osaki, Y., 1975, Pub. Astron. Soc. Japan, 27, 581
- Attolini, M.R ; Secchini, S ; Galli, M ; Nanni, T, 1990, Sol. Phys ,
125, 389
- Apostolov, E.M. & Letfus, V., 1985, Bull. Astron. Inst. Czech, 36,
199
- Albregtsen, F. & Maltby, P., 1981, Sol. Phys, 71, 269
- Alfven, H. 1943, Arkiv. Math. Astr. Fys., 29A, No. 12
- Babcock, H.W., 1947, ApJ, 105, 105
- Babcock, H.W., 1961, ApJ, 133, 572
- Bachal, J.N. & Ulrich, R.K., 1971, ApJ, 170, 593
- Bachal, J.N., 1989, in " Neutrino Astrophysics ", p.90
- Bai, T., 1987, ApJ , 318, L85
- Balthasar, H. & Wohl, H., 1980, Astron. Astrophys, 92, 111
- Balthasar, H; Wiehr, E., Schleicher, H; & Wohl, H. 1993, Astron.
Astrophys, 277, 635
- Beckers, J.M. & Schultz, R.B., 1972, Sol. Phys, 27, 61
- Becker, U., 1955, Z. Astrophys., 37, 47
- Bigelow , 1889, in The Solar Corona, Smithsonian. Inst. Washington
.D.C.
- Biermann, L., 1951, Zs.f. Ap., 28, 304
- Biermann, L., 1958 , Trans. IAU., 6 , 248

- Brandenburg, A., 1988, in " Proceedings of the Sixth Soviet-Finnish Astronomical Meeting ", eds. Hanni, U. & Tuominen, I., p. 34
- Brandenburg, A., Krause, F., Meinel, R., Moss, D., & Tuominen, I., 1989, *Astron. Astrophys.*, 213, 411
- Bretz, M.C. & Billings, D.E., 1959, *ApJ*, 129, 134
- Brookes, J.R., Isaak, G.R. & van der Raay, H., 1976, *Nature*, 259, 92
- Carrington, R.C., 1863, in " Observations Of the Spots On the Sun" , London, Williams & Norgate, p. 412
- Chandrasekhar, S., 1956 a, *ApJ*, 124, 232
- Chandrasekhar, S., 1956 b, *ApJ*, 124, 244
- Charbonneau, P., & Macgregor, K.B., 1993, *ApJ*, 417, 762
- Choudhuri, A.R. & Gilman, P.A., 1987, *ApJ*, 316, 788
- Christensen-Dalsgaard, J. & Schou, J., 1988, in " Seismology of the Sun & Sun-like Stars " ed. V. Domingo & Rolfe, E.J., ESA (sp-286) p. 149
- Christensen-Dalsgaard, J., 1992, in " The Sun A Laboratory for Astrophysics ", eds. Schmelz, J.T. & Brown, J.C., p. 29
- Chitre, S.M., Ezer, E., & Stothers, R., 1973, *ApJ.Let.*, 14, 37
- Cohen, T.J. & Lintz, P.R., 1974, *Nature*, 250, 398
- Cole, T.W., 1973, *Sol. Phys.*, 30, 103
- Cowling, T.G., 1934, *MNRAS*, 94, 39
- Cowling, T.G., 1953, in " The Sun ", ed. G.P. Kuiper (Chicago : Univ Chicago Press), p. 532
- Cowling, T.G., 1981, *Ann. Rev. Astron. Astrophys.*, 19, 115
- Cram, L.E. & Dame, L., 1983, *ApJ*, 272, 355

- Csada, I.K., 1974, Sol.Phys., 35, 325
- Delache, P., Lachare, F., & Sadsoud, H., 1985, Nature, 317, 416
- Deland, M.T. & Cebula, R.P., 1992, in " Proceedings of the Workshop on the Solar Electromagnetic Radiation on Study for the Solar Cycle 22 ", ed. Donnelly, R.F. p. 150
- De Luca, E.E. & Gilman, P.A., 1991, in " Solar Interior and Atmosphere ", eds., Cox, A.N. ; Livingston, W.C. and Mathews, M.S., The University of Arizona Press, Tucson ; p. 275
- Deubner, F.L., 1975, Astron.Astrophys, 44, 371
- Dicke, R.H., 1977, ApJ, 218, 547
- Dicke, R.H., 1978, Nature, 276, 676
- Dicke, R.H., 1979, ApJ, 228, 898
- Dicke, R.H., 1979, ApJ, 229, 89
- Dicke, R.H., 1988, Sol.Phys., 33, 281
- Droge, W., Gibbs, K., Grunsfeld, J.M., Meyer, P., Newport, B.J., Evenson, P., & Mosses, O., 1990, ApJ, Supp, 73, 279
- Dudorov, A.E., 1987, in " Magnetic Stars, problem of physics and evolution of Stars ", eds. Glagolevsky, Y.V. & Kopylov, I.M., p. 226
- Dudorov, A.E., Krinotubski, V.N., Ruzmaikina, T.V. & Ruzmaikina, A. A., 1989, Sov.Astr., 33, 4, 420
- Dunn, R.B. & Zirker, J.B., 1973, Sol.Phys., 33, 281
- Durney, B.R., De Young, D.S. & Passot, T.P., 1990, ApJ, 362, 709
- Duvall, T.L. Jr., 1982, Sol.Phys., 76, 137
- Dziembowski, W.A., Goode, P.R. & Libbrecht, K.G., 1989, ApJ, L53
- Dziembowski, W.A., & Goode, P.R., 1991, ApJ, 376, 782

- Eddy, J.A., 1976, *Science*, 192, 1189
- Frohlich, C., Foukal, P.V., Hickey, J.R., Hudson, H.S & Wilson, R.C., 1991, in " The Sun in Time " , eds : Sonet, C.P., Giampapa, M.S & Mathews, M.S., The University Arizona, Tuscon p. 11
- Ferraro, V.C.A., 1937, *MNRAS* , 97, 457
- Gilman, P.A., 1974, *Ann.Rev.Astron.Astrophys.*, 12, 47
- Gilman, P.A., 1983, *ApJS*, 53, 243
- Gilman, P.A. & Howard, R., 1984, *ApJ*, 283, 385
- Glatzmaier, G.A., 1985, *ApJ*, 291, 300
- Godoli, G. & Mazzucconi, F., 1979, *Sol.Phys.*, 64, 247
- Gokhale, M.H. & Zwaan, C., 1972, *Sol.Phys.*, 26, 52
- Gokhale, M.H., 1977, *Kodaikanal.Obs.Bull.*, A2, 19
- Gokhale, M.H., 1984, *Kodaikanal.Obs.Bull.*, A4, 25
- Gokhale, M.H., Javaraiah, J., & Hiremath, K.M., 1990, in " Structure, Convection and Magnetic Fields " , ed. Stenflo , J.O., *IAU Symp*, p 375
- Gokhale, M.H., Javaraiah, J., Kutty, K.N. & Verghese, B.A., 1992, *Sol.Phys.*, 138, 35
- Gokhale, M.H. & Javaraiah, J., 1992a, *Sol.Phys.*, 138, 399
- Gokhale, M.H. & Javaraiah, J., 1992b, private communication
- Gokhale, M.H. & Hiremath, K.M., 1993, *ApJ*, 407, 359
- Gokhale, M.H. & Javaraiah, J., 1994, private communication
- Goode, P.R. & Dziembowski, W.A., 1991, *Nature*, 349, 223
- Gough, D.O., 1986, *Nature*, 314, 14
- Gough, D.O., 1988, in " Solar-terrestrial relationships and the

- Earth environment in the last millenia " , ed.G.Castagnoli.Cini,
International Sch.Phys.Enrico Fermi., Corso, 95 , p. 90
- Gough, D.O., 1990., Phil.Trans.R.Soc.Lond ., A., 330, 627
- Gough, D.O. & Stark,P.B., 1993, ApJ, 415, 376
- Goulub, L., Davis, J.M. & Krieger, A.S., 1979, ApJ, 229, L145
- Goulub, L ., Harvey, K.L., Herant, M. & Webb, D.F., 1989,
Sol.Phys., 124, 211
- Hale, G.E., 1908, ApJ, 28, 315
- Hale, G.E., 1913, ApJ, 38, 27
- Hale, G.E., Sears, F.H., Van Maanen, A. & Ellerman, F., 1918, ApJ,
47, 206
- Harvey, K.L., 1992, in " Proceedings of the Workshop on the Solar
Electromagnetic Radiation Study for the Solar Cycle 22 " , ed.
Donnelly, R.F., p. 113
- Harvey, K.L. & Harvey, J.W., 1973, Sol.Phys., 28, 61
- Hasan, S.S., 1985, Astron.Astrophys., 143, 39
- Hasan, S.S., 1986, MNRAS, 219, 357
- Hill,F., Deubner, F.L. & Isaak, G., 1990, in " Solar Interior and
Atmosphere ", eds. Cox, A.N ; Livingston, W.C. & Mathews, M.S.
p. 329
- Hiremath, K.M. & Gokhale, M.H., 1994, Submitted to ApJ
- Hogenson, E.A., 1992, J. Undergrad.Res.in.Phys., 1992, 10, 57
- Howard, R., 1967, Ann.Rev.Ast.Astrophys., 5, 1
- Howard, R. & Harvey, J., 1970, Sol.Phys., 12, 23
- Howard, R. & Stenflo, J.O., 1972, 22, 402
- Howard, R., 1974., Sol.Phys., 38, 59

- Howard, R. & LaBonte, B.J., 1980, ApJ., 239, L33
- Hufbauer, K., 1991, in " Exploring the Sun-Solar Science since Galileo ", p.14
- Hughes, V.A. & Kesteven, M.J.L., 1981, Sol.Phys., 71, 259
- Ichimota, K., Kubota, J., Suzuki ., Tohmura, I. & Kurokawa, H., 1985, Nature, 316, 422
- Javaraiah, J. & Gokhale, M.H., 1994, Submitted to Sol.Phys
- Kariyappa, R., 1992, Ph.D. Thesis
- Kippenhan, R., 1963, ApJ, 137, 664
- Krause. F., 1976, in " Basic Mechanisms of Solar Activity ", eds. Bumba, V. & Kleczek, J., IAU Symp, 71, (Dordrecht : Reidel), p. 305
- Kuhn, J.R., 1988, ApJ, 331, L131
- Kurtus, J., & Ruzmaikin, A.A., 1990, Sol.Phys., 126, 407
- Lamb, H., 1881, Proc.Lond.Math.Soc., 13, 51
- Layzer, D., Krook, M. & Menzel, D.H., 1955, Proc.Roy.Soc., A223, 302
- Layzer, D., Rosner, R. & Doyle, H.T., 1979, ApJ, 229, 1126
- Lean , J.L. & Brueckner, G.E., 1989, ApJ, 337, 568
- Lean, J.L., 1990, ApJ, 363, 718
- Lean, J., 1991, Rev.Geophys., 29, 4, 505
- Leibacher, J.W. & Stein, R.F., 1971, ApJ, 7, L191
- Leighton, R.B., 1960, Proc. IAU. Symp., 12, 321
- Leighton, R.B., Noyes, R.W., & Simon, G.W., 1962, ApJ, 135, 474
- Leighton, R.B., 1964, ApJ, 140, 1547
- Leighton, R.B., 1969, ApJ, 156, 1

- Leroy, J.L. & Neons, J.C., 1983, Astr.Astrophys., 120, L1
- Levy, E.H., 1992, in " The Solar Cycle ASP Confer.Ser. vol 27, p.139
- Libbrecht, K.G., 1988, in " Seismology of the Sun & Sun-Like Stars " , ed. V. Domingo & Rolfe, E.J., ESA (SP-286) , p. 131
- Libbrecht, K.G., 1989, ApJ, 336, 1092
- Libbrecht, K.G., & Morrow , C.A., 1990, in " Solar Interior and Atmosphere ", eds. Cox, A.N ; Livingston, W.C. & Mathews, M.S. p. 479
- Lites, B.W., 1986, ApJ, 301, 939
- Liu, S.Y., 1974, ApJ, 189, 359
- Livingston, W.C. & Duvall, T.L.Jr., 1979, Sol>phys., 61, 219
- Loudagh, S., Provost, J., Berthomieu, G., Ehgamberdiev, S., Fossat, E ., Gelly, B., Grec, G., Khalikov, S., Lazreck, M., Palle, P., Regulo, C., Sanchez, L. & Schmider, F.X., 1993, Astron.Astrophys., 275, L25
- Makarov, V.I., Stayanova, M.N. & Sivaraman, K.R., 1982, J.Astrophys. Astr., 3, 379
- Makarov, V.I. & Sivaraman, K.R., 1986, Bull.of. Astr.Soc.India, 14, 3, 163
- Makarov, V.I., Makarova, V.V., Koutchmy, S. & Sivaraman, K.R., 1988, in " Solar & Stellar Coronal Structure & Dynamics " , Proc.of.the 9th Sacramento Peak Summer Symp, p. 362
- Makarov, V.I. & Sivaraman, K.R., 1988, Sol.Phys., 123, 367
- Martin, S.F. & Harvey, K.L., 1979, Sol.Phys., 64, 93
- Maunder, E.W., 1890, MNRAS, 1, 251

- Maunder, E.W., 1922, J.Brit.Astron.Assoc., 32, 140
- Maunder, E.W., 1922, MNRAS, 82, 534
- Mehlretter, J.P., 1974, Sol.Phys., 38, 43
- Mestel, L., 1965, in " Stellar Structure ", eds. Aller, L.H. & McLaglin, D.B., Univ.Of.Chicago.Press., p. 465
- Mestel, L. & Thakar, H.S., 1972, MNRAS, 156, 419
- Mestel, L. & Weiss, N.O., 1987, MNRAS, 226, 123
- Morfill, G.E., Scheigraber, H. & Sonnet, C.P., in " The Sun in Time ", 1991, eds. Sonnet, C.P., Giampapa, M.S. & Mathews, M.S., p. 30
- Moss, D., 1986, Phys Reports., 140, 1
- Moss, D., 1987, MNRAS, 224, 1019
- Nakagawa, Y & Trehan, S.K., 1968, ApJ, 151, 1111
- Nakagawa, Y., 1969, ApJ, 157, 881
- Newton, H.W. & Nunn, M.L., 1951, MNRAS, 111, 413
- Nicolini, T., 1977, in " Sky & Telescope ", Aug, 106
- Oliver, R., Carbonell, M. & Ballester, L., 1992, Sol.Phys., 137, 141
- Orall, F.Q., 1966, ApJ, 143, 917
- Palle, P., Regulo, C. & Roca Cortes T., 1990, in " Progress of Seismology of the Sun and Stars, Lecture notes in physics ", eds. Osaki, Y., Shibahashi, H., Springer Verlag., p. 189
- Pap, J., Tobiska, W.K. & Bouwer, S.D., 1990, Sol.Phys., 129, 165
- Parker, E.N., 1955, ApJ, 122, 293
- Parker, E.N., 1978, ApJ, 221, 368
- Parker, E.N., 1984, ApJ, 286, 666

- Pearce, G., Harrison, R.A., Bromage, B.J.I. & Pickering, A.G.M.,
1992, in " Proceedings of the Workshop On the Solar
Electromagnetic Radiation Study for the Solar 22 ", ed.
Donnelly, R.F., p. 250
- Piddington, J.H., 1971, Proc.Astron.Soc.Australia, 2, 7
- Piddington, J.H., 1972, Sol.Phys., 22, 3
- Piddington, J.H., 1973, Astrophys.Space.Sci, 24, 259
- Piddington, J.H., 1976, in " Basic Mechanisms of Solar Activity ",
eds. Bumba, V. & Kleczek, J., IAU Symp, 71, (Dordrecht: Reidel)
p. 389
- Piddington, J.H., 1983, Astrophys.Space.Sci., 90, 217
- Plumpton, C. & Ferraro, V.C.A., 1955, ApJ, 121, 168
- Price, C.P., Prichard, D. & Hogenson, E.A., 1993, JGR, 97, No A12,
19113
- Punetha, L.M., 1974, Bull.Astron.Inst.Czechoslovakia, 25, 207
- Radler, K.H., 1976, in " Basic Mechanisms of Solar Activity ",
eds. Bumba, V. & Kleczek, J., IAU Symp, 71, (Dordrecht: Reidel)
p.323
- Rieger, E., Share, G.H., Forrest, D.J., Kanbach, G., Reppin,
C. & Chupp, E.L., 1984, Nature, 312, 623
- Rosner, R. & Weiss, N.O., 1985, Nature, 317, 790
- Rusin, V., Rybansky, M. & Zuerko, J., 1987,
Bull.Astron.Inst.Czech, 38, 181
- Rusin, V. & Rybansky, M., 1992, in " Proceedings of the Workshop
On the Solar Electromagnetic Radiation: Study for the Solar
cycle 22 " , ed. Donnelly, R.F. p. 15

- Rutten, J.R. & Uitenbrock., 1991, Sol.Phys., 134, 15
- Ruzmaikin, A.A., 1989, in " Solar Photosphere, Convection, and Magnetic Fields " , ed. Stenflo, J.O., IAU. Symp. 138, 343
- Saar, H., 1990, in " Solar Photosphere : Structure, Convection and Magnetic Fields ", ed. Stenflo, J.O., Kluwer: Dordrecht, p. 427
- Sakurai, K., 1979, Nature, 278, 146
- Schou, J., Christense-Dalsgard, J. & Thomson, M.J., 1992, ApJ, 385, L59
- Schussler, M., 1982, in " Solar and Stellar Magnetic Fields : Origins and Coronal Effects ", ed. Stenflo, J.O., p. 213
- Schussler, M., 1992, in " The Sun, A Laboratory for Astrophysics " , eds. Schmelz, J.T. & Brown, J.C., p. 191
- Schwabe, H., 1843, in " Solar Observations during 1843 " , Reprinted in Early Solar Physics , ed. Meadows, A.J., 1970, Pergamon, Newyork, p. 95
- Sekii, T., 1989, in " Progress of Seismology of the Sun & Stars " , eds. Osaki, Y. & Shibabhashi, H., (Berlin : Springer-Verlag), p. 337
- Severney, A.B., Kotov, V.A. & Tsap, T.T., 1976, Nature, 259, 87
- Shapiro, R. & Ward, F., 1962, J.Atmos.Sci., 19, 506
- Singh, J. & Prabhu, T.P., 1985, Sol.Phys. 97, 203
- Skumanich, A., 1972, ApJ, 171, 265
- Snodgrass, H.B., 1983, ApJ, 270, 288
- Snodgrass, H.B., 1987, Sol.Phys., 110, 35
- Snodgrass, H.B., 1992, in " The Solar Cycle " , ed. Harvey, K.L., ASP Conf.Ser, Vol, 27, p.220

- Speigel, E. A. & Weiss, N. O., 1980, *Nature*, 287, 616
- Spitzer, L. J., 1956, *ApJ*, 124, 525
- Spruit, H. C., 1977, Ph.D. Thesis
 , University of Utrecht, 2
- Spruit, H. C. & Zweibel, E. G., 1979, *Sol. Phys.*, 62, 15
- Spruit, H. C., 1990, in " Inside the Sun " , eds. Gabrielle, B. &
 Cribier, M., Kluwer Academic Publishers, p. 415
- Stauffer, J. R., 1991, in " Angular Momentum Evolution of Young
 Stars " , eds. Catalano . & Stauffer, J. R., Kluwer Academic
 Publishers , p. 117
- Steenbeck, M. & Krause, F., 1969, *Astron. Nachr*, 291, 49
- Stenflo, J. O., 1974, *Sol. Phys.*, 36, 495
- Stenflo, J. O., 1976, in " Basic Mechanisms of Solar Activity " ,
 IAU. Symp , eds. Bumba, V. & Kleczek, J., 71, 69
- Stenflo, J. O., 1977, *Astron. Astrophys.*, 61, 797
- Stenflo, J. O. & Vogel, M., 1986, *Nature*, 319, 285
- Stenflo, J. O., 1988, *Ap & SS* , 144, 321
- Stenflo, J. O., 1989, *Astron. Astrophys. Rev.*, 1, 3
- Stenflo, J. O., 1993, in " Solar Surface Magnetism " , eds. Rutten,
 R. J. & Shrijver, C. J., (kluwer) Proc. NATO Advanced Research
 Workshop , Socsterberg, The Netherlands
- Stix, M., 1972, *Astron. Astrophys.*, 20, 9
- Stormer, K., 1911, *Compt. Rend.*, 152, 425
- Sykora, J., 1980, in " Solar and Interplanetary Dynamics " , eds.
 Dryer, M & Tanberg-Hanssen, E., Riedel, Dordrecht
- Tayler, R. J., 1980, *MNRAS*, 191, 151
- Thomas, J. H., Cram, L. E. & Nye, A. H., 1982, *Nature*, 297, 485

- Thompson, W.T. & Schmieder, B., 1991, *Astron.Astrophys.*, 243, 501
- Toutain, Th. & Frohlich, C., 1992, *Astron.Astrophys.*, 257, 287
- Toutain, T. & Kosovichev, A.G., 1994, 284, 265
- Tsubaki, T., 1988, in " Solar and Stellar Coronal Structure & Dynamics ", Sac Peak Workshop., ed. Altruck, R.C., p. 140
- Ulrich, R.K., 1970, *ApJ*, 162, 933
- Unno, W. & Ando, H., 1979, *Geophys.Astrophys.Fluid.Dyn.*, 12, 107
- Van Ballegooijen, A.A., 1982, *Astron.Astrophys.*, 113, 99
- Vandakurov, Y.V., 1989, in " Solar Photosphere : Structure, Convection, and Magnetic Fields ", ed. Stenflo, J.O., p. 333
- Vainstein, S.I. & Cattaneo, F., 1992, *ApJ*, 393, 165
- Venkatakrisnan , P., 1985, *J.Astron.Astrophys.*, 6, 21
- Venkatakrisnan, P., 1986, *Nature*, 322, 156
- Walén, 1949, in " On the Vibratory Rotation of the Sun ", Henrik Lindstahls, Bokhandel, Stockholm
- Wallenharst, S.G., 1982, *Sol.Phys.*, 80, 379
- Wang, H., 1988, *Sol.Phys.*, 116, 1
- Ward, F., 1966, *ApJ*, 145, 416
- Wier, E., Stellmacher, G. & Balthasar, H., 1984, *Sol.Phys.*, 94, 285
- Wilcox, J.M. & Howard, R., 1970, *Sol.Phys.*, 13, 251
- Wilson, P.R., Altruck, R.C., Harvey, K.L., Martin, S.F. & Snodgrass , H.B., 1988, *Nature*, 333, 748
- Wolf, R., 1856 , *Astron.Mitt.Zurich*, 1, 5
- Wolf, R., 1868 , *Astron.Mitt.Zurich*, 24, 103
- Wolf, C.L., 1983, *ApJ*, 264, 667

Yallop, B.D., 1980, Sol.Phys., 68, 303

Yoshimura, H., 1972, ApJ, 178, 863

Yoshimura, H., 1978, ApJ, 22, 706

Zang 1991, Sol.Phys., 132, 1, 63

Zappala, R.R., 1972, ApJ, 172, 57

Zwaan, C., 1981, in " The Sun as a Star " , ed. Jordan, S., NASA

SP-450, p. 163